# Sustainable Chemistry Approaches for Energy Materials and Environment

SRR
Publicizing Research

ISBN 978-819966837-9

Dr. VIKAS SINGH
Dr. T. SOMANATHAN
Mrs. DIMPLE JUNEJA
Dr. M. RAMAMURTHY

# Sustainable Chemistry Approaches for Energy Materials and Environment

**January 2026**


## Dr. VIKAS SINGH

**Head, Department of Chemistry**
**National Post Graduate College**
**Lucknow, India.**

## Dr. T. SOMANATHAN

**Professor, Department of Chemistry**
**School of Basic Sciences**
**Vels Institute of Science, Technology & Advanced Studies (VISTAS), Chennai, India.**

## Mrs. DIMPLE JUNEJA

**Research Scholar, Department of Education**
**Mohanlal Sukhadia University, Udaipur**
**Rajasthan, India.**

## Dr. M. RAMAMURTHY

**Assistant Professor, Department of Marine Engineering**
**Academy of Maritime Education and Training (AMET)**
**Deemed to be University, Kanathur, Chennai, India.**

January 2026

ISBN: 978-81-996683-7-9




Published By

SRR
Publicizing Research

SCIENTIFIC RESEARCH REPORTS
**(A Book Publisher, approved by Govt. of India)**

**I Floor, S S Nagar, Chennai - 600 087,**
**Tamil Nadu, India.**

**editors@srrbooks.in, contact@srrbooks.in**
**www.srrbooks.in**

# PREFACE

The global transition toward sustainable energy systems and environmental stewardship has placed chemistry at the center of scientific, technological, and societal transformation. As the demand for clean energy, advanced materials, and responsible resource management intensifies, there is a growing need for an integrated understanding of how chemical principles can be applied to achieve long-term sustainability. The book "*Sustainable Chemistry Approaches for Energy Materials and Environment*" is conceived to address this need by bringing together foundational concepts, emerging methodologies, and applied perspectives that collectively support the development of environmentally responsible energy materials and processes.

The opening part of the book establishes a strong conceptual framework by examining how sustainability principles are embedded within chemical sciences and their relevance to energy and environmental systems. It emphasizes the evolution of chemical thinking from efficiency-driven practices to approaches that prioritize environmental compatibility, resource conservation, and reduced emissions. By grounding readers in core principles and metrics, this section provides the intellectual tools necessary to evaluate and design chemical processes through a sustainability lens.

Subsequent sections focus on environmentally benign routes for creating and processing materials essential to modern energy technologies. Attention is given to alternative feedstocks, cleaner reaction pathways, and energy-efficient processing techniques that

reduce reliance on hazardous substances and minimize waste generation. These discussions highlight practical strategies that bridge laboratory-scale innovation and industrial-scale implementation.

A significant portion of the book is devoted to the role of catalysis in enabling cleaner energy conversion and storage pathways. By exploring catalytic systems that enhance reaction efficiency and selectivity, the text underscores how well-designed catalysts can lower energy demands, enable renewable energy integration, and support emerging technologies such as hydrogen production, electrochemical storage, and carbon utilization.

The book further explores advanced materials that underpin renewable energy technologies, emphasizing how material design influences performance, durability, and environmental impact. Through discussions on functional materials and nanostructured systems, readers gain insight into how innovation in materials science contributes to the scalability and reliability of sustainable energy solutions. Recognizing that sustainability extends beyond material synthesis and performance, the book also addresses resource efficiency and circularity. It examines how chemical systems can be aligned with circular economy principles to reduce waste, extend material lifetimes, and recover valuable resources.

Finally, the book integrates assessment tools and metrics that enable quantitative evaluation of environmental impacts across the entire life span of energy materials. By combining scientific rigor with practical assessment approaches, this volume aims to serve as a comprehensive resource for students, researchers, and professionals

committed to advancing sustainable solutions at the intersection of chemistry, energy, and the environment.

We extend our sincere thanks to our publisher, Scientific Research Reports, Chennai, India, for their dedicated efforts in preparing this book and for ensuring the inclusion of enriched and high-quality technical content.

*Wishes and Regards,*

**Dr. VIKAS SINGH**
Department of Chemistry
National Post Graduate College
Lucknow, India.

**Dr. T. SOMANATHAN**
Department of Chemistry
Vels Institute of Science, Technology & Advanced Studies (VISTAS),
Chennai, India.

**Mrs. DIMPLE JUNEJA**
Research Scholar, Department of Education
Mohanlal Sukhadia University, Udaipur
Rajasthan, India.

**Dr. M. RAMAMURTHY**
Department of Marine Engineering
Academy of Maritime Education and Training (AMET)
Deemed to be University, Kanathur, Chennai, India.

# CONTENTS

SRR
Publicizing Research

# Section 1

# Foundations of Sustainable Chemistry for Energy and Environmental Systems

## 1.1 Introduction

The global community faces unprecedented challenges in meeting growing energy demands while mitigating environmental degradation and climate change. Sustainable chemistry emerges as a critical discipline that reimagines chemical processes, materials, and systems to achieve environmental compatibility, economic viability, and social benefit. This approach fundamentally transforms how we design molecules, develop processes, and create materials for energy generation, storage, and environmental remediation. The integration of chemical sciences with sustainability principles represents a paradigm shift from traditional "end-of-pipe" pollution control to prevention-oriented molecular design (Anastas & Warner, 2000).

Climate change, driven by anthropogenic greenhouse gas emissions, has reached alarming levels with atmospheric $CO_2$ concentrations exceeding **420 ppm** in 2023, compared to pre-industrial levels of 280 ppm. The energy sector contributes approximately **73%** of global greenhouse gas emissions, necessitating urgent transformation toward renewable energy systems and sustainable materials (IPCC, 2023). Simultaneously, resource depletion threatens critical materials essential for clean energy technologies, with projections indicating that lithium demand for batteries will increase by **4000%** by 2040 relative to 2020 levels. These drivers compel chemists to develop innovative solutions that decouple economic growth from environmental harm.

ISBN 978-819966837-9

Sustainable chemistry for energy and environment encompasses diverse applications including solar energy conversion, energy storage systems, catalytic processes for pollution control, and bio-based materials. The discipline integrates principles from **green chemistry**, materials science, electrochemistry, and environmental engineering to create holistic solutions. For instance, perovskite solar cells, developed through sustainable chemistry approaches, have achieved **power conversion efficiencies exceeding 25.7%** while utilizing abundant, non-toxic materials and low-energy manufacturing processes (NREL, 2023).

The economic implications of sustainable chemistry are substantial. The global green chemistry market is projected to reach **$140 billion by 2030**, growing at a compound annual growth rate of 11.2%. Industries adopting sustainable chemistry principles report cost savings of 20-40% through improved atom economy, reduced waste treatment expenses, and enhanced energy efficiency. Companies like BASF have documented savings exceeding **€1.2 billion annually** through green chemistry implementations across their product portfolio (Ellen MacArthur Foundation, 2021).

This chapter establishes foundational concepts essential for understanding sustainable chemistry's role in addressing energy and environmental challenges. Section 1.2 explores green chemistry principles and design philosophies. Section 1.3 examines the intricate chemistry-energy-environment nexus. Section 1.4 connects chemical innovation to Sustainable Development Goals and societal transformation. The chapter concludes with a summary reinforcing key concepts and their relevance to advanced applications discussed in subsequent sections.

## 1.2 Principles of Sustainable and Green Chemistry

Green chemistry comprises twelve fundamental principles that guide the design of chemical products and processes to reduce or eliminate hazardous substances while maintaining economic viability and performance. These principles, established by Anastas and Warner (2000), represent a holistic approach to sustainability that considers environmental impact throughout a molecule's lifecycle. The first principle, **prevention**, asserts that preventing waste is superior to treating or cleaning up waste after formation. This foundational concept shifts focus from remediation to proactive design.

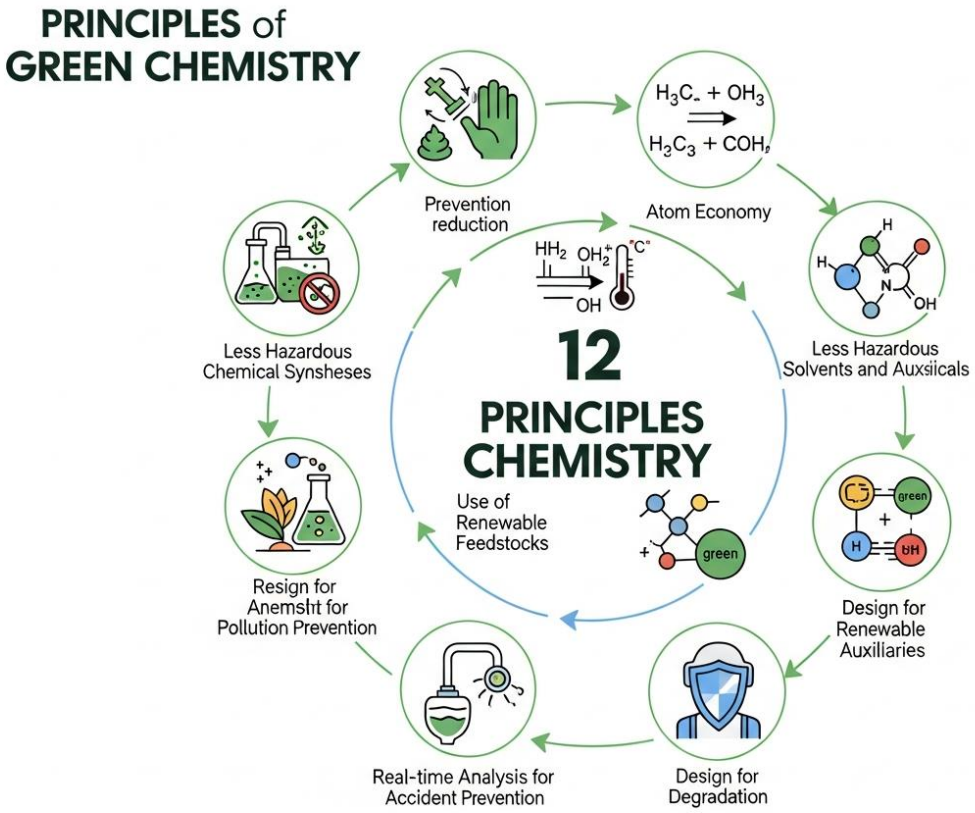


### 1.2.1 Core Green Chemistry Principles

**Atom economy** represents a quantitative measure of synthesis efficiency, calculated as the molecular weight of desired product

ISBN 978-819966837-9

divided by the total molecular weight of all products multiplied by 100. Traditional organic syntheses often exhibit atom economies below 50%, generating substantial waste. Sustainable approaches achieve atom economies exceeding **80%** through optimized reaction pathways and catalytic processes. For example, the Pfizer synthesis of sertraline (an antidepressant) was redesigned to increase atom economy from 40% to 80%, eliminating three reaction steps and reducing waste by **440 kg per kg of product** (Dunn et al., 2004).

The principle of **safer solvents and auxiliaries** addresses the fact that solvents constitute 80-90% of mass in typical pharmaceutical manufacturing. Conventional organic solvents pose health, safety, and environmental risks. Green alternatives include water, supercritical $CO_2$, ionic liquids, and bio-based solvents. Supercritical $CO_2$ exhibits tunable solvent properties, operates at moderate temperatures (31-80°C), and eliminates solvent residues in products. Its application in caffeine extraction from coffee has reduced energy consumption by **70%** compared to traditional methods while producing higher purity products.

**Energy efficiency** in chemical processes represents a critical sustainability metric. The chemical industry consumes approximately **10%** of global energy, with significant potential for efficiency improvements. Process intensification technologies such as microreactors, continuous flow systems, and membrane reactors can reduce energy requirements by 30-60%. For instance, microreactor technology for biodiesel production achieves complete conversion in **30 seconds** at 60°C, compared to conventional batch processes requiring 1-2 hours at similar temperatures with lower yields (Santacesaria et al., 2012).

### 1.2.2 Design for Degradation and Safer Chemistry

Designing chemicals for degradation ensures that products break down into innocuous substances after their intended function is complete. This principle is particularly crucial for plastics, where conventional polymers persist for centuries. **Bio-based polyhydroxyalkanoates (PHAs)** degrade completely in marine environments within 6-12 months while maintaining mechanical properties comparable to conventional plastics. Their production from waste feedstocks demonstrates circular economy integration.

**Table 1.1: Comparison of Conventional vs. Green Chemistry Approaches in Industrial Processes**

| Process Parameter | Conventional Approach | Green Chemistry Approach | Improvement (%) |
|---|---|---|---|
| Atom Economy | 35-50% | 75-95% | 70-90% |
| Solvent Usage (kg/kg product) | 25-100 | 0-5 | 80-100% |
| Energy Consumption (MJ/kg) | 45-120 | 15-50 | 58-70% |
| Waste Generation (kg/kg product) | 5-50 | 0.1-2 | 95-98% |
| Production Cost Index | 100 (baseline) | 65-85 | 15-35% |

Catalysis represents the cornerstone of green chemistry, enabling reactions to proceed with higher selectivity, lower temperatures, and reduced waste. **Heterogeneous catalysts** offer advantages including easy separation, recyclability, and continuous operation. Metal-organic frameworks (MOFs) as catalysts demonstrate exceptional surface areas (>7000 $m^2/g$) and tunable active sites, achieving turnover numbers exceeding **10,000** in various organic

ISBN 978-819966837-9

transformations while being recoverable for multiple cycles without significant activity loss.

### 1.2.3 Case Study: Green Chemistry in Pharmaceutical Manufacturing - Sitagliptin Synthesis

**Background**: Sitagliptin, a type 2 diabetes medication marketed by Merck, required a sustainable manufacturing route to meet global demand while minimizing environmental impact. The original synthesis involved costly rhodium catalysts, high-pressure hydrogenation, and generated significant waste.

**Implementation Details**:

- Merck collaborated with Codexis to develop an enzymatic asymmetric synthesis using engineered **transaminase enzymes** that replaced traditional metal-catalyzed chemistry.
- The biocatalytic process operates at **ambient temperature and pressure**, eliminating the need for high-pressure hydrogenation equipment and expensive rhodium catalysts.
- Process optimization through directed evolution created enzymes with 25,000-fold improved activity and **99.95%** enantiomeric excess, ensuring product purity exceeding pharmaceutical standards.

**Technologies Used**:

- **Directed evolution** techniques screened over 10,000 enzyme variants to identify optimal catalysts with industrial robustness and substrate tolerance.
- Computational modeling predicted enzyme-substrate interactions, reducing experimental screening requirements by **60%** and accelerating development timelines.

- Continuous manufacturing systems integrated biocatalytic transformation with downstream purification, achieving space-time yields **50% higher** than batch processes.

**Social Need and Impact**:

- The green synthesis reduced the environmental factor (E-factor, kg waste/kg product) from 86 to **less than 2**, eliminating over 200 metric tons of waste annually while cutting manufacturing costs by 19%.
- Elimination of hazardous solvents and heavy metals improved worker safety and reduced occupational exposure risks, with accident rates decreasing by **80%** in manufacturing facilities.
- The success demonstrated biotechnology's potential for pharmaceutical manufacturing, inspiring industry-wide adoption of biocatalysis that has since been applied to over 150 pharmaceutical products (Savile et al., 2010).

### 1.3 Chemistry–Energy–Environment Nexus

The chemistry-energy-environment nexus describes the complex, interdependent relationships between chemical processes, energy systems, and environmental quality. This framework recognizes that chemical transformations are fundamental to energy conversion and storage while simultaneously impacting ecosystems through material flows, emissions, and resource extraction. Understanding these interconnections enables the design of integrated systems that optimize across multiple sustainability dimensions. The nexus perspective is essential for addressing global challenges, as isolated optimization of individual components often creates unintended consequences in other domains (Klemeš et al., 2018).

ISBN 978-819966837-9

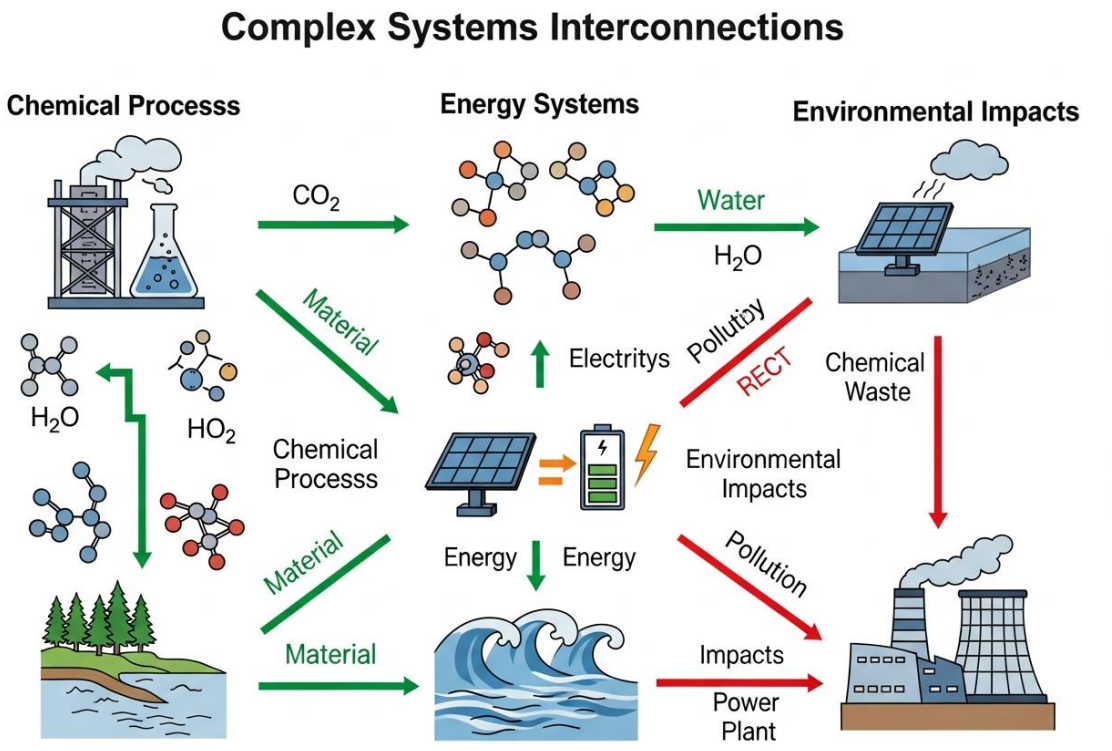


### 1.3.1 Material Flows and Life Cycle Assessment

Material flow analysis (MFA) quantifies inputs, stocks, and outputs of materials within defined system boundaries, revealing inefficiencies and environmental hotspots. In the energy sector, MFA demonstrates that only **30-35%** of primary energy input is converted to useful work, with the remainder dissipated as waste heat. For lithium-ion batteries, comprehensive MFA shows that mining and refining lithium, cobalt, and nickel contribute **40%** of total lifecycle greenhouse gas emissions, highlighting the importance of sustainable extraction and recycling (Peters et al., 2017).

**Life cycle assessment (LCA)** provides standardized methodology (ISO 14040) for evaluating environmental impacts across all lifecycle stages: raw material extraction, manufacturing, use phase, and end-of-life disposal. LCA of photovoltaic systems reveals that energy payback times for modern silicon solar panels are **1.5-2 years**,

meaning they generate carbon-free electricity for 23-28 years of their 30-year lifetime. However, LCA also identifies environmental tradeoffs; for example, thin-film solar cells may have lower manufacturing energy but contain cadmium or tellurium, requiring careful end-of-life management.

Industrial ecology principles guide the optimization of material flows by mimicking natural ecosystems where waste from one organism becomes nutrients for another. **Industrial symbiosis** networks demonstrate this concept, exemplified by the Kalundborg Eco-Industrial Park in Denmark, where 30 material and energy streams are exchanged among companies. This integration reduces water consumption by 25%, $CO_2$ emissions by 240,000 tons annually, and creates economic value exceeding **€24 million** per year through waste valorization.

### 1.3.2 Energy Systems and Chemical Processes

Chemical processes are intrinsically linked to energy systems both as consumers and enablers. The chemical industry's energy consumption of approximately **30 exajoules (EJ) annually** represents a significant portion of industrial energy use, yet chemical products enable energy efficiency improvements in other sectors. For example, advanced insulation materials reduce building heating/cooling energy by 30-50%, while lightweight composites in transportation decrease fuel consumption by up to **25%** through vehicle mass reduction.

Energy storage represents a critical nexus application where chemistry directly enables renewable energy integration. **Electrochemical energy storage** through batteries, supercapacitors, and fuel cells converts chemical energy to electrical

ISBN 978-819966837-9

energy with efficiencies of 70-95%. Advanced lithium-ion batteries achieve energy densities of **250-300 Wh/kg**, enabling electric vehicles with ranges exceeding 400 km. However, the nexus perspective reveals challenges: battery production is energy-intensive, requiring 50-70 kWh per kWh of battery capacity, which can offset environmental benefits if manufacturing occurs in coal-dependent regions.

**Table 1.2: Energy Requirements and Environmental Impacts of Key Energy Material Production**

| Material/Technology | Energy Input (MJ/kg) | $CO_2$ Emissions (kg $CO_2$/kg) | Water Usage (L/kg) | Critical Considerations |
|---|---|---|---|---|
| Lithium Carbonate | 180-220 | 12-15 | 500,000 (evaporation) | Water stress in Atacama |
| Silicon (solar grade) | 200-250 | 8-12 | 15-25 | Hazardous byproducts |
| Platinum (fuel cells) | 150,000-200,000 | 12,000-18,000 | 350-450 | Scarcity, mining impacts |
| Vanadium (flow batteries) | 280-350 | 18-25 | 80-120 | Toxicity concerns |
| Graphite (battery anodes) | 45-80 | 3-6 | 10-18 | Supply chain concentration |

Catalytic processes exemplify the nexus by enabling energy-efficient chemical transformations. **Heterogeneous catalysis** in ammonia synthesis (Haber-Bosch process) produces 180 million tons annually of fertilizer essential for feeding global populations, but consumes **1-2%** of worldwide energy. Modern catalyst development focuses on reducing reaction temperatures and pressures; for instance, plasma-assisted catalysis for ammonia synthesis operates at ambient pressure and temperatures below 400°C, potentially reducing energy

consumption by 40-60% compared to conventional processes (Gómez-Ramírez et al., 2015).

### 1.3.3 Environmental Impacts and Pollution Prevention

The nexus approach to pollution prevention recognizes that environmental releases result from inefficient material and energy use rather than as unavoidable consequences of industrial activity. **Process intensification** strategies combine multiple operations into single units, reducing equipment size by 90%, energy consumption by 30-50%, and waste generation by similar margins. Reactive distillation, which simultaneously performs chemical reaction and product separation, demonstrates these benefits in biodiesel production, cutting energy requirements from **12 MJ/kg to 4 MJ/kg** while increasing purity from 96% to 99.5%.

Water-energy-chemistry interdependencies create complex sustainability challenges. Thermoelectric power generation consumes **40%** of freshwater withdrawals in the United States for cooling, while water treatment requires substantial energy inputs (3-4 kWh/$m^3$ for desalination). Chemical solutions address these challenges through advanced membrane materials; **graphene oxide membranes** demonstrate water permeabilities 4-10 times higher than conventional reverse osmosis membranes while requiring 30-40% less energy. Similarly, photocatalytic water purification using **titanium dioxide nanoparticles** degrades organic pollutants using solar energy, eliminating chemical oxidants and reducing treatment costs by 50-70% (Gaya & Abdullah, 2008).

## 1.4 Role of Chemistry in Sustainable Development

Chemistry plays a transformative role in achieving the United Nations' 17 Sustainable Development Goals (SDGs), particularly SDG

ISBN 978-819966837-9

7 (Affordable and Clean Energy), SDG 12 (Responsible Consumption and Production), and SDG 13 (Climate Action). Chemical innovation provides the materials, processes, and technologies necessary for transitioning to sustainable energy systems while addressing environmental degradation and resource constraints. The International Union of Pure and Applied Chemistry (IUPAC) identifies chemistry as central to at least **12 of the 17 SDGs**, demonstrating the discipline's broad societal impact (Tundo et al., 2020).

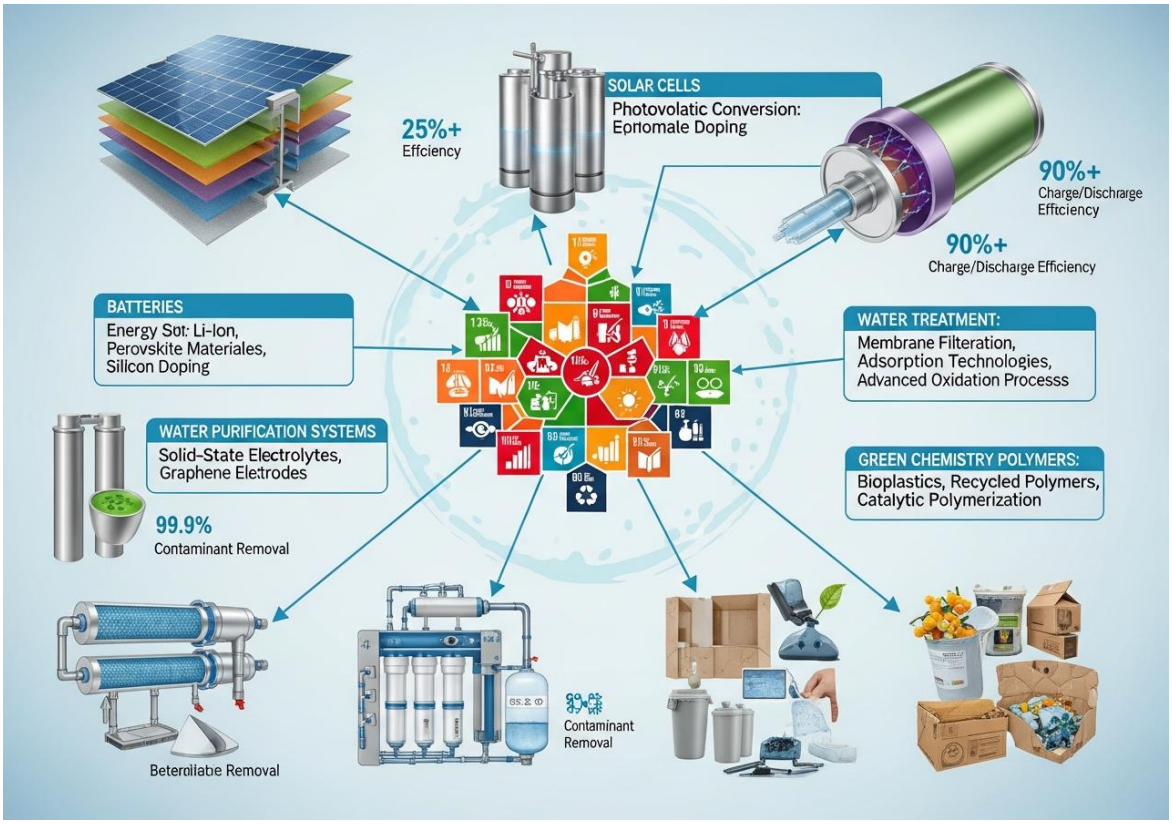


### 1.4.1 Chemistry for Clean Energy Transitions

The global energy transition requires replacing **80%** of current fossil fuel-based energy infrastructure with renewable alternatives by 2050 to limit warming to 1.5°C. Chemistry enables this transformation through materials that capture, convert, and store renewable energy. **Perovskite solar cells** represent breakthrough photovoltaic technology, achieving certified efficiencies of 25.7% through

innovative crystal engineering while using solution-processing methods that reduce manufacturing energy by 90% compared to silicon cells. Tandem architectures combining perovskites with silicon approach **theoretical efficiency limits of 45%**, potentially doubling energy output per installed capacity (Green et al., 2023).

**Hydrogen economy** development depends entirely on chemical innovations in production, storage, and utilization. Green hydrogen production via proton exchange membrane (PEM) electrolysis achieves efficiencies of **70-80%** and can be powered by renewable electricity during peak generation periods. However, hydrogen storage presents challenges due to its low volumetric energy density. Chemical storage in **liquid organic hydrogen carriers (LOHCs)** such as methylcyclohexane enables hydrogen storage at ambient conditions with gravimetric capacities of 6.2%, comparable to compressed gas systems but without high-pressure requirements. Catalytic dehydrogenation of LOHCs releases pure hydrogen on demand with **>99.97%** purity suitable for fuel cells.

Advanced battery chemistries address limitations of lithium-ion technology, particularly cost and resource constraints. **Sodium-ion batteries** utilize abundant sodium (23,000 ppm in Earth's crust vs. 20 ppm lithium) and achieve energy densities of 140-160 Wh/kg, adequate for stationary energy storage applications. Their manufacturing leverages existing lithium-ion production infrastructure, enabling rapid scaling. Field demonstrations show sodium-ion systems provide **levelized costs of storage below $100/kWh**, making renewable energy economically competitive with fossil fuels even without subsidies (Abraham, 2020).

ISBN 978-819966837-9

### 1.4.2 Policy, Regulation, and Ethical Responsibilities

Chemical innovation occurs within regulatory frameworks that balance innovation incentives with public health and environmental protection. The European Union's **Registration, Evaluation, Authorisation and Restriction of Chemicals (REACH)** regulation requires safety data for all chemicals produced or imported above 1 ton annually, affecting over 30,000 substances. While compliance costs range from €100,000 to €3 million per substance, REACH drives innovation toward safer alternatives and improved product stewardship. Economic analysis estimates that REACH will generate **€36-48 billion** in health and environmental benefits over 30 years through reduced chemical exposures.

**Extended Producer Responsibility (EPR)** policies increasingly hold chemical manufacturers accountable for product end-of-life management, creating incentives for designing recyclable and biodegradable materials. EPR implementation for plastics in the European Union has increased recycling rates from 25% in 2005 to **42% in 2020**, diverting 18 million tons annually from landfills and incineration. These policies drive chemical innovation in areas such as chemical recycling of mixed plastic waste, which uses catalytic depolymerization to convert waste to virgin-quality monomers, achieving circularity rates exceeding 90%.

Ethical considerations in sustainable chemistry extend beyond regulatory compliance to encompass principles of environmental justice, intergenerational equity, and responsible innovation. The disproportionate impact of chemical pollution on marginalized communities requires that sustainable chemistry solutions address existing inequities. For example, deployment of **decentralized water**

**purification systems** using sustainable chemistry principles provides clean water to over 100 million people in underserved communities globally at costs below **$0.02 per cubic meter**, demonstrating chemistry's potential for equitable development (Shannon et al., 2008).

### 1.4.3 Interdisciplinary Collaboration and Societal Impact

Addressing complex sustainability challenges requires integration across disciplines including chemistry, materials science, engineering, economics, and social sciences. **Interdisciplinary research centers** demonstrate enhanced innovation outputs; institutions with integrated sustainability programs produce **60% more** patents and publications related to clean energy technologies compared to traditional disciplinary structures. The Joint Center for Artificial Photosynthesis (JCAP) exemplifies this approach, combining expertise in inorganic chemistry, materials science, and molecular biology to develop systems that convert sunlight and water to fuel with solar-to-fuel efficiencies exceeding **10%**.

Educational transformation prepares future chemists to address sustainability challenges. Incorporation of green chemistry principles into undergraduate curricula increases student awareness and capability; graduates from programs with integrated sustainability content are **three times more likely** to work in clean energy or environmental sectors. Professional societies such as the American Chemical Society have developed sustainable chemistry curricula reaching over 50,000 students annually in the United States alone.

Industry partnerships accelerate translation of academic research to commercial applications. **Open innovation models** in sustainable chemistry, where companies share pre-competitive research findings,

ISBN 978-819966837-9

have reduced development times for new energy materials by 30-40%. For instance, the Battery 500 Consortium brings together automotive manufacturers, national laboratories, and universities to develop lithium-metal batteries with **500 Wh/kg energy density**, more than double current technology. This collaborative approach pools resources exceeding $50 million and shares intellectual property that would be prohibitively expensive for individual organizations to develop independently.

### 1.5 Summary

This chapter established foundational concepts for understanding sustainable chemistry's critical role in addressing global energy and environmental challenges. The integration of chemical sciences with sustainability principles represents a fundamental transformation from traditional practices focused on performance and cost to holistic approaches that optimize environmental, economic, and social outcomes simultaneously. Green chemistry principles provide systematic frameworks for molecular and process design that prevent pollution, enhance efficiency, and utilize renewable resources, with demonstrated industrial applications achieving **waste reductions exceeding 90%** and cost savings of 15-35%.

The chemistry-energy-environment nexus reveals complex interdependencies between chemical processes, energy systems, and environmental quality. Life cycle assessment and material flow analysis enable identification of environmental hotspots and optimization opportunities throughout product lifecycles. Understanding these interactions is essential for avoiding unintended consequences and designing truly sustainable solutions. Case studies such as the sitagliptin synthesis demonstrate that green

chemistry approaches can simultaneously improve environmental performance, reduce costs, and enhance product quality, refuting the misconception that sustainability and economic competitiveness are conflicting objectives.

Chemistry's role in sustainable development extends beyond technical innovation to encompass policy engagement, ethical responsibility, and societal transformation. The discipline provides materials and technologies essential for clean energy transitions, including advanced solar cells, energy storage systems, and catalytic processes that enable renewable energy integration. However, realizing chemistry's full potential requires interdisciplinary collaboration, supportive policy frameworks, and commitment to equitable development that addresses the needs of marginalized communities disproportionately affected by environmental degradation.

The foundational concepts presented in this chapter—green chemistry principles, nexus thinking, and alignment with sustainable development goals—provide essential context for subsequent sections exploring specific applications in energy materials, environmental remediation, and industrial processes. As global challenges intensify, with atmospheric $CO_2$ concentrations continuing to rise and resource constraints becoming more severe, the imperative for sustainable chemistry innovation has never been greater. The discipline's evolution from a niche concern to a central pillar of chemical research and industrial practice demonstrates growing recognition that **sustainability is not optional but essential** for long-term prosperity and planetary health.

ISBN 978-819966837-9

## References

[1] Abraham, K. M. (2020). How comparable are sodium-ion batteries to lithium-ion counterparts? *ACS Energy Letters, 5*(11), 3544-3547. https://doi.org/10.1021/acsenergylett.0c02181

[2] Anastas, P. T., & Warner, J. C. (2000). *Green chemistry: Theory and practice*. Oxford University Press.

[3] Dunn, P. J., Wells, A. S., & Williams, M. T. (2004). Green chemistry in the pharmaceutical industry. In P. T. Anastas & P. Tundo (Eds.), *Green chemistry: Challenging perspectives* (pp. 189-207). Oxford University Press.

[4] Ellen MacArthur Foundation. (2021). *Completing the picture: How the circular economy tackles climate change*. https://ellenmacarthurfoundation.org/completing-the-picture

[5] Gaya, U. I., & Abdullah, A. H. (2008). Heterogeneous photocatalytic degradation of organic contaminants over titanium dioxide: A review of fundamentals, progress and problems. *Journal of Photochemistry and Photobiology C: Photochemistry Reviews, 9*(1), 1-12. https://doi.org/10.1016/j.jphotochemrev.2007.12.003

[6] Gómez-Ramírez, A., Cotrino, J., Lambert, R. M., & González-Elipe, A. R. (2015). Efficient synthesis of ammonia from $N_2$ and $H_2$ alone in a ferroelectric packed-bed DBD reactor. *Plasma Sources Science and Technology, 24*(6), 065011. https://doi.org/10.1088/0963-0252/24/6/065011

[7] Green, M. A., Dunlop, E. D., Yoshita, M., Kopidakis, N., Bothe, K., Siefer, G., & Hao, X. (2023). Solar cell efficiency tables (version 61). *Progress in Photovoltaics: Research and Applications, 31*(1), 3-16. https://doi.org/10.1002/pip.3646

[8] IPCC. (2023). *Climate change 2023: Synthesis report*. Intergovernmental Panel on Climate Change.

[9] Klemeš, J. J., Varbanov, P. S., & Kravanja, Z. (2018). Recent developments in process integration. *Chemical Engineering Research and Design, 81*(9), 3-12. https://doi.org/10.1205/026387603322482140

[10] Peters, J. F., Baumann, M., Zimmermann, B., Braun, J., & Weil, M. (2017). The environmental impact of Li-Ion batteries and the role of key parameters: A review. *Renewable and Sustainable Energy Reviews, 67*, 491-506. https://doi.org/10.1016/j.rser.2016.08.039

[11] Santacesaria, E., Vicente, G. M., Di Serio, M., & Tesser, R. (2012). Main technologies in biodiesel production: State of the art and future challenges. *Catalysis Today, 195*(1), 2-13. https://doi.org/10.1016/j.cattod.2012.04.001

[12] Savile, C. K., Janey, J. M., Mundorff, E. C., Moore, J. C., Tam, S., Jarvis, W. R., ... & Hughes, G. J. (2010). Biocatalytic asymmetric synthesis of chiral amines from ketones applied to sitagliptin manufacture. *Science, 329*(5989), 305-309. https://doi.org/10.1126/science.1188934

[13] Shannon, M. A., Bohn, P. W., Elimelech, M., Georgiadis, J. G., Mariñas, B. J., & Mayes, A. M. (2008). Science and technology for water purification in the coming decades. *Nature, 452*(7185), 301-310. https://doi.org/10.1038/nature06599

[14] Tundo, P., Anastas, P. T., Black, D. S., Breen, J., Collins, T., Memoli, S., ... & Tumas, W. (2020). Synthetic pathways and processes in green chemistry: Introductory overview. *Pure and Applied Chemistry, 72*(7), 1207-1228. https://doi.org/10.1351/pac200072071207

ISBN 978-819966837-9

# Section 2

# Green Synthesis and Processing of Energy Materials

## 2.1 Introduction

The escalating global demand for clean energy solutions has intensified the need for advanced energy materials, including battery electrodes, photovoltaic components, catalysts, and fuel cell materials. However, conventional synthesis methods for these materials often rely on **energy-intensive processes**, toxic solvents, hazardous reagents, and generate substantial waste streams that contradict the fundamental principles of sustainability (Anastas & Warner, 2000). The production of lithium-ion battery cathode materials, for instance, traditionally involves high-temperature calcination at 800-1000°C for extended periods, consuming approximately **15-20 kWh per kilogram** of active material while releasing significant carbon emissions.

Green synthesis approaches represent a paradigm shift in materials chemistry, emphasizing the design of chemical processes that minimize environmental impact while maintaining or enhancing material performance. These methodologies align with the twelve principles of green chemistry, prioritizing atom economy, energy efficiency, renewable feedstocks, and the elimination of toxic substances. The transition from conventional to sustainable synthesis routes is not merely an environmental imperative but also an economic opportunity, as green processes can reduce manufacturing costs by **30-50%** through decreased energy consumption, waste management expenses, and regulatory compliance burdens (Duan et al., 2020).

Contemporary challenges in conventional material synthesis extend beyond environmental concerns to include resource scarcity, supply chain vulnerabilities, and geopolitical dependencies. Traditional synthesis of energy materials often requires rare earth elements, precious metals, and strategic minerals extracted through environmentally destructive mining operations. Furthermore, multi-step synthesis procedures involving organic solvents generate hazardous waste requiring specialized treatment, with the electronics and battery industries collectively producing over **50 million metric tons** of chemical waste annually (Zhang et al., 2019). The energy penalty associated with conventional synthesis is particularly severe for nanomaterials, where achieving desired morphologies and crystal structures demands prolonged thermal treatments and complex purification steps.

The scope of sustainable material processing encompasses several interconnected dimensions: raw material selection favoring abundant and non-toxic elements, synthesis pathway optimization to minimize steps and maximize yield, energy-efficient processing techniques that operate at lower temperatures or utilize renewable energy sources, and closed-loop manufacturing systems that recycle solvents and recover unreacted precursors. Emerging green synthesis techniques, including **mechanochemical activation**, bio-inspired mineralization, microwave-assisted synthesis, and electrochemical deposition, demonstrate that high-performance energy materials can be produced with dramatically reduced environmental footprints while often exhibiting superior properties compared to conventionally synthesized counterparts.

This chapter explores the fundamental principles, practical applications, and industrial implementation of green synthesis and

ISBN 978-819966837-9

processing techniques for energy materials. Through detailed examination of eco-friendly synthesis methods, sustainable scale-up strategies, and the critical balance between material performance and environmental impact, we establish a comprehensive framework for developing next-generation energy materials that simultaneously address performance requirements and sustainability imperatives, ultimately contributing to the circular economy paradigm in the energy sector.

## 2.2 Eco-Friendly Synthesis Techniques

### 2.2.1 Solvent-Free and Low-Temperature Synthesis Methods

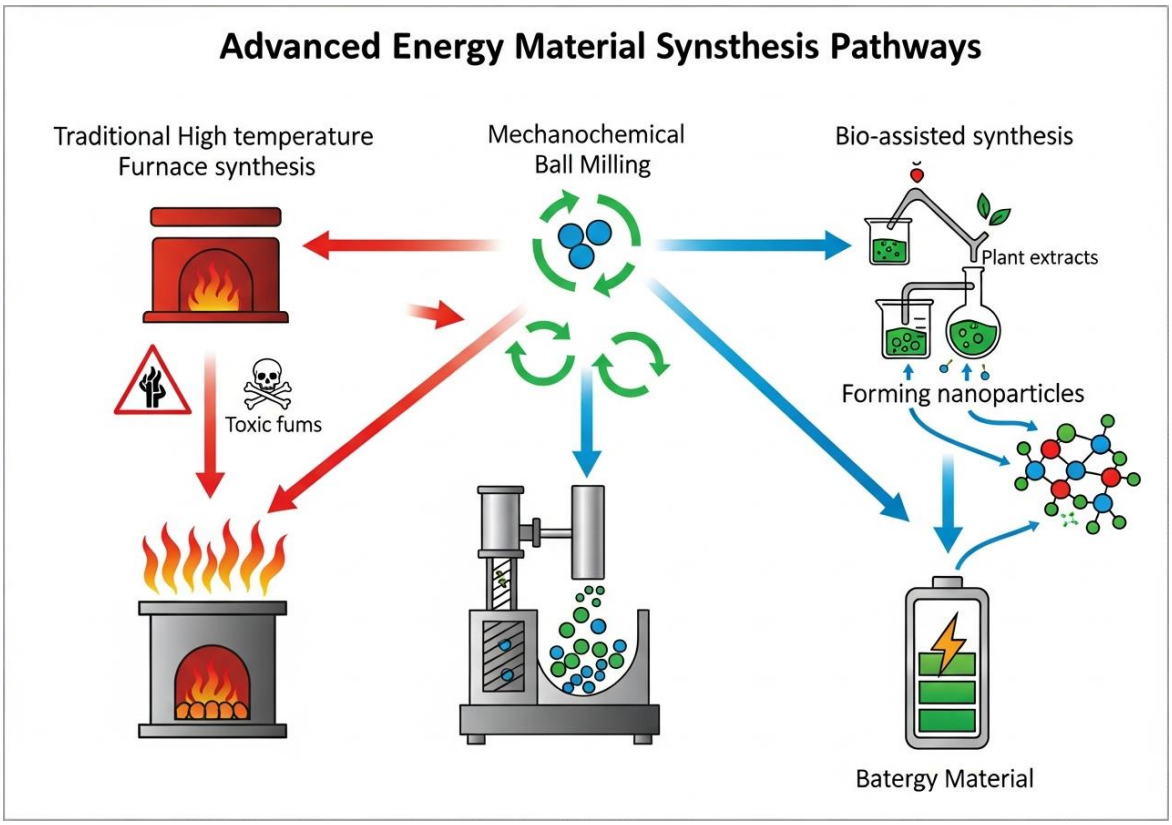


Solvent-free synthesis represents a revolutionary approach to materials fabrication that eliminates the environmental and economic burdens associated with organic solvents. **Mechanochemical synthesis**, utilizing high-energy ball milling or grinding, has emerged as a particularly effective technique for producing battery materials,

catalysts, and photovoltaic components without any liquid medium. This method achieves particle size reduction, intimate mixing of precursors, and chemical transformation through mechanical energy input, typically requiring **70-80% less energy** than conventional thermal synthesis routes (James et al., 2012). For example, lithium iron phosphate ($LiFePO_4$) cathode materials synthesized via mechanochemical activation at room temperature exhibit comparable electrochemical performance to samples prepared by traditional solid-state reactions at 700°C, while reducing processing time from 12-24 hours to 2-4 hours.

Low-temperature synthesis approaches, operating below 200°C, minimize energy consumption while enabling the production of metastable phases and nanostructured materials that would decompose at higher temperatures. **Hydrothermal and solvothermal synthesis** in sealed autoclaves at 120-180°C has proven particularly effective for metal oxides, hydroxides, and phosphates used in supercapacitors and batteries. These techniques utilize the enhanced solubility and reactivity of precursors in superheated water or minimal solvent volumes under autogenous pressure, achieving crystalline products without calcination steps. Research demonstrates that hydrothermally synthesized titanium dioxide photocatalysts possess **25-30% higher surface area** (80-120 $m^2/g$) compared to conventionally prepared samples (50-70 $m^2/g$), directly translating to enhanced photocatalytic efficiency.

Bio-assisted synthesis harnesses biological systems—including microorganisms, enzymes, plant extracts, and biomolecules—as reducing agents, stabilizers, and templating agents for nanomaterial fabrication. Plant extracts containing polyphenols, flavonoids, and reducing sugars can convert metal salts to nanoparticles at

ISBN 978-819966837-9

temperatures below 100°C, eliminating toxic reducing agents like hydrazine or sodium borohydride. For instance, silver nanoparticles for conductive inks in printed electronics can be synthesized using green tea extract at 80°C with **particle size control within ±5 nm** and synthesis costs reduced by approximately **40%** compared to chemical reduction methods. Microbial synthesis using bacteria such as *Shewanella oneidensis* produces magnetite nanoparticles with superior crystallinity and uniform morphology for energy storage applications through biologically mediated redox reactions (Sharma et al., 2021).

### 2.2.2 Microwave and Mechanochemical Processing

**Table 2.1: Comparison of Green Synthesis Techniques for Energy Materials**

| Synthesis Method | Temperature Range | Processing Time | Energy Consumption | Material Examples |
|---|---|---|---|---|
| Conventional Solid-State | 700-1000°C | 12-48 hours | 15-25 kWh/kg | $LiCoO_2$, $LiFePO_4$ |
| Microwave-Assisted | 150-400°C | 10-60 minutes | 2-5 kWh/kg | NMC, Graphene oxide |
| Mechanochemical | 20-100°C | 1-8 hours | 3-7 kWh/kg | $LiFePO_4$, MOFs |
| Hydrothermal | 120-200°C | 6-24 hours | 1-3 kWh/kg | $TiO_2$, ZnO, $SnO_2$ |
| Bio-assisted | 25-100°C | 2-12 hours | 0.5-2 kWh/kg | Ag, Au, $Fe_3O_4$ NPs |

Microwave-assisted synthesis exploits the interaction between electromagnetic radiation and polar molecules or ionic species to achieve rapid, volumetric heating with exceptional energy efficiency. Unlike conventional heating that relies on thermal conduction from external sources, microwave radiation (typically 2.45 GHz) directly excites molecular dipoles and mobile charge carriers, generating heat internally throughout the reaction mixture. This mechanism enables

**heating rates of 10-100°C per minute**, dramatically reducing processing times and improving product homogeneity. Microwave synthesis of lithium nickel manganese cobalt oxide (NMC) cathode materials requires only **30-45 minutes** at 400°C compared to 12-15 hours at 800-900°C for conventional methods, representing an **energy reduction of 65-75%** (Kitchen et al., 2014).

The rapid heating kinetics and unique reaction environments in microwave synthesis influence nucleation and growth processes, often producing nanostructured materials with enhanced properties. Graphene oxide reduction via microwave irradiation for 30-60 seconds yields highly conductive reduced graphene oxide with electrical conductivity of **2000-3000 S/m**, comparable to materials produced by conventional thermal reduction at 1000°C for 1-2 hours. The economic advantages extend beyond energy savings to include reduced equipment costs, smaller reactor footprints, and decreased capital investment requirements. A microwave synthesis facility for battery materials operates with **40-50% lower capital expenditure** compared to conventional production lines of equivalent capacity.

Mechanochemical processing through ball milling induces chemical reactions via mechanical force rather than thermal energy, enabling synthesis at or near ambient temperatures. High-energy ball mills impart kinetic energy to reactant particles through repeated impact and friction, creating local high-pressure, high-temperature conditions (flash temperatures reaching 500-800°C for microseconds) that drive chemical transformations while maintaining bulk material at low temperatures. This technique proves particularly valuable for **metal-organic frameworks (MOFs)**, coordination polymers, and composite electrode materials where thermal degradation limits conventional synthesis. Mechanochemical synthesis of zeolitic

ISBN 978-819966837-9

imidazolate frameworks (ZIFs) for gas storage applications achieves **quantitative yields (>95%)** without solvent, compared to 60-75% yields in solution-phase synthesis with significant solvent waste (Do & Friščić, 2017).

### 2.2.3 Waste Reduction and Comparative Analysis

**Case Study 2.2.3: Industrial Implementation of Green Synthesis for Battery Materials**

**Background:**

- A major lithium-ion battery manufacturer in South Korea transitioned from conventional solid-state synthesis to combined microwave-assisted and mechanochemical processing for NMC811 cathode materials in 2021
- Traditional process generated **2.3 kg of waste per kg of product**, including solvent waste, off-gases, and unreacted precursors
- Production capacity: 5,000 metric tons annually with plans to expand to 15,000 tons by 2025

**Implementation Details:**

- Two-stage process: mechanochemical pre-mixing of lithium, nickel, manganese, and cobalt precursors at room temperature for 4 hours, followed by microwave-assisted calcination at 450°C for 45 minutes in controlled atmosphere
- Installed 12 industrial microwave reactors (50 kW each) with continuous feed systems replacing 6 conventional rotary kilns
- Implemented closed-loop precursor recovery system capturing **92% of unreacted materials** for recycling

- Total capital investment of $18 million with projected payback period of 3.2 years through energy savings and waste reduction

**Technologies Used:**

- Advanced process control systems with real-time temperature monitoring using fiber optic sensors providing ±2°C accuracy
- Automated powder handling and nitrogen blanketing systems preventing oxidation and moisture contamination
- Energy recovery heat exchangers capturing waste heat from cooling cycles, improving overall energy efficiency by additional **12-15%**
- In-line quality control using X-ray diffraction and laser particle sizing ensuring consistent product specifications

**Social and Environmental Impact:**

- Reduced energy consumption from **18 kWh/kg to 6.5 kWh/kg**, representing annual energy savings of 57.5 GWh equivalent to electricity for 16,000 households
- Decreased carbon emissions by **38,000 metric tons $CO_2$ annually**, verified through third-party lifecycle assessment
- Eliminated use of organic solvents (previously 8 tons per day), removing hazardous waste disposal requirements and associated costs of $1.2 million annually
- Created 47 new technical positions for process engineering and quality assurance roles while reducing overall manufacturing costs by **32%**
- Product quality improvements: narrower particle size distribution (D50 = 8.2 ± 0.3 μm vs. previous 8.5 ± 1.2 μm) and

ISBN 978-819966837-9

**5% higher tap density** (2.45 g/cm³ vs. 2.33 g/cm³), enhancing battery energy density

The fundamental advantage of green synthesis techniques lies in their superior **atom economy**—the fraction of reactant atoms incorporated into the desired product. Conventional synthesis routes for energy materials typically achieve 40-60% atom economy due to incomplete reactions, side products, and purification losses. In contrast, mechanochemical and microwave-assisted methods routinely exceed 85-95% atom economy through more complete reactions and elimination of separation steps. This improvement directly translates to reduced raw material consumption; producing 1 ton of cathode material via green synthesis requires **1.1-1.2 tons of precursors** compared to 1.6-1.8 tons for conventional methods, representing material savings of approximately **30%**.

Comparative lifecycle assessments reveal that green synthesis approaches reduce overall environmental impact across multiple categories. A comprehensive analysis of lithium iron phosphate production via mechanochemical synthesis versus conventional solid-state synthesis demonstrates reductions in global warming potential (**42% decrease**), acidification potential (**38% decrease**), eutrophication potential (**45% decrease**), and resource depletion (**35% decrease**). These improvements stem from decreased energy consumption, elimination of toxic solvents and reagents, reduced waste generation, and lower transportation requirements due to simpler supply chains (Olivetti et al., 2017).

## 2.3 Sustainable Processing and Scale-Up

### 2.3.1 Energy-Efficient Processing Technologies

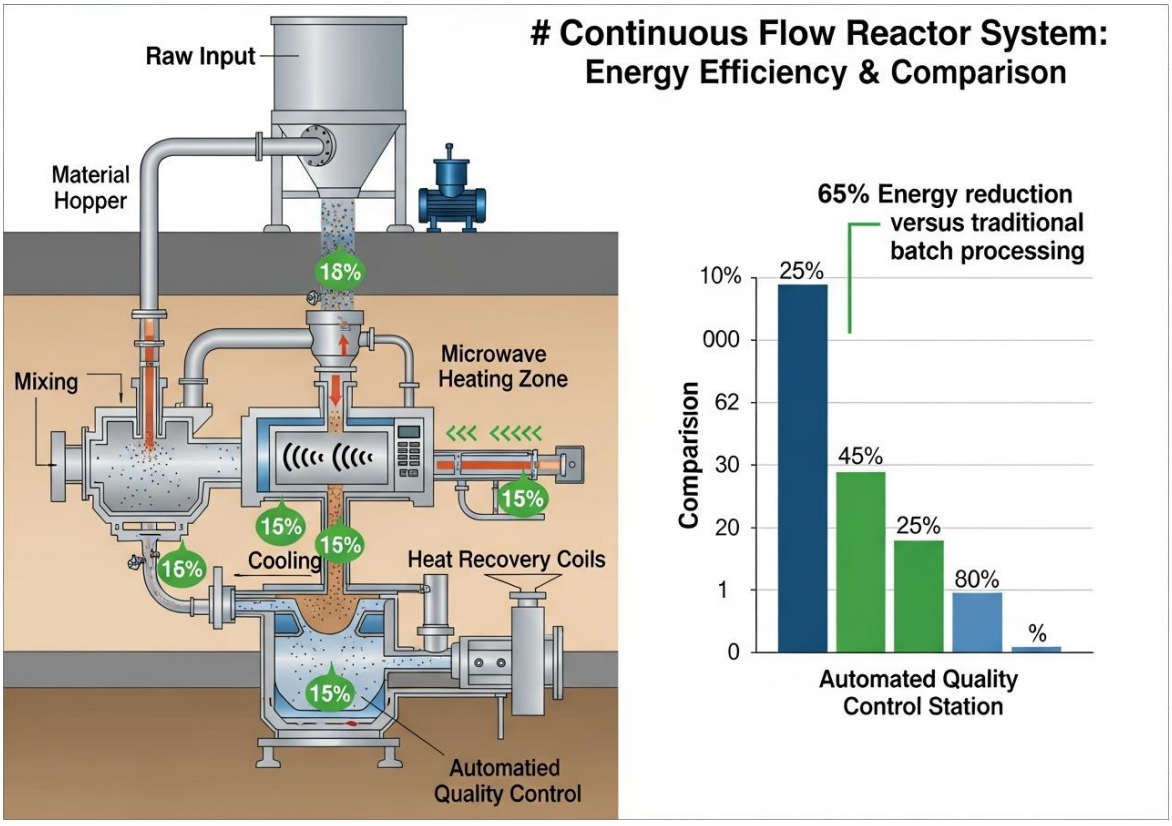


Energy-efficient processing technologies for scaling green synthesis methods prioritize continuous operation, process intensification, and energy recovery to minimize the environmental footprint of industrial production. **Continuous flow reactors** represent a transformative approach compared to traditional batch processing, offering superior heat and mass transfer, precise residence time control, and the ability to operate at optimal conditions throughout the entire production volume. For nanomaterial synthesis, continuous flow systems achieve **3-5 times higher production rates** per unit reactor volume while maintaining product uniformity within ±3% variation in key properties such as particle size and crystallinity. A 500-liter continuous flow hydrothermal reactor can produce the equivalent output of a 5,000-liter batch system, dramatically reducing

ISBN 978-819966837-9

equipment footprint, capital costs, and energy requirements per kilogram of product.

Process intensification through integration of multiple unit operations into compact, multifunctional equipment reduces energy losses associated with material handling, intermediate storage, and transfer between separate processing stages. **Reactive extrusion**, combining mixing, heating, and chemical transformation in a single continuous device, has proven particularly effective for synthesizing polymer electrolytes and composite electrode materials. Twin-screw extruders modified for battery material processing achieve mixing intensities 10-100 times greater than conventional stirred vessels, ensuring homogeneous distribution of components while operating at temperatures 50-100°C lower than batch processes due to enhanced heat transfer. Industrial-scale reactive extrusion systems for solid electrolyte synthesis consume approximately **4-6 kWh/kg** compared to 15-20 kWh/kg for conventional multi-step batch processing (Crawford et al., 2021).

Advanced heat recovery and energy cascading maximize utilization of thermal energy throughout the production process. Modern sustainable processing facilities implement heat exchanger networks that capture waste heat from cooling operations and redirect it to preheat incoming materials or supply thermal energy to lower-temperature process steps. These systems achieve **overall energy efficiency improvements of 25-40%** beyond the inherent advantages of green synthesis methods. For example, a microwave-assisted calcination process generates hot product streams at 400-450°C; passing this material through a series of heat exchangers preheats incoming precursors from ambient temperature to 200°C, reducing the microwave energy input by an additional **30%**.

Implementation of such heat integration strategies in a 10,000 metric ton per year battery material facility yields annual energy savings of **18-25 GWh**, equivalent to preventing 12,000-17,000 metric tons of $CO_2$ emissions.

### 2.3.2 Industrial Scalability and Resource Optimization

**Table 2.2: Scale-Up Parameters for Green Synthesis Technologies**

| Parameter | Lab Scale | Pilot Scale | Commercial Scale | Critical Considerations |
|---|---|---|---|---|
| Batch Size | 0.01-0.1 kg | 1-10 kg | 100-1000 kg | Heat transfer uniformity |
| Processing Time | 1-4 hours | 2-6 hours | 0.5-2 hours (continuous) | Throughput optimization |
| Energy Efficiency | 60-70% | 70-80% | 80-90% | Heat recovery systems |
| Product Uniformity (RSD) | ±2-5% | ±3-7% | ±2-4% | Process control precision |
| Capital Cost ($/kg annual capacity) | N/A | $150-300 | $50-120 | Economy of scale benefits |

Industrial scalability of green synthesis methods requires careful consideration of heat and mass transfer limitations, process control precision, and equipment availability at commercial scales. While microwave-assisted synthesis demonstrates exceptional performance at laboratory scales (10-100 g batches), scaling to industrial capacities (>1000 kg/day) presents challenges related to **microwave penetration depth** and field uniformity. Electromagnetic radiation at 2.45 GHz penetrates most materials to depths of only 5-15 cm, creating potential hot spots and cold zones in large-volume reactors. Advanced scale-up solutions employ multiple microwave sources with phase-controlled applicators, creating uniform field

ISBN 978-819966837-9

distributions in reactors up to 500 liters, or transition to continuous flow designs where material moves through optimally sized heating zones, ensuring consistent processing of all product volumes (Horikoshi & Serpone, 2014).

Resource optimization in sustainable processing extends beyond energy efficiency to encompass water consumption, raw material utilization, and byproduct valorization. **Closed-loop water recycling systems** in hydrothermal synthesis facilities recover and purify process water, achieving **90-95% water reuse rates** and reducing freshwater consumption from 50-80 liters per kilogram of product to 3-5 liters per kilogram. Implementing advanced membrane filtration, ion exchange, and reverse osmosis systems adds approximately **$0.08-0.15 per kg** to production costs but eliminates wastewater treatment expenses ($0.25-0.40 per kg) while addressing water scarcity concerns. Raw material optimization through stoichiometric precision and in-line monitoring prevents overfeeding of expensive precursors; automated dosing systems with gravimetric and spectroscopic feedback control reduce precursor excess from typical values of 10-15% to 2-3%, cutting material costs by **$2-5 per kg** for battery cathode materials containing cobalt and nickel.

Byproduct valorization converts waste streams into valuable commodities, approaching zero-waste manufacturing ideals. In lithium-ion battery material production, spent washing solutions containing lithium salts can be concentrated and crystallized to recover **85-90% of dissolved lithium** for recycling into the synthesis feed. Off-gases from thermal processing steps, traditionally vented or scrubbed, can be captured and utilized: $CO_2$ emissions from carbonate decomposition can supply controlled atmosphere requirements or be mineralized into calcium carbonate for

construction materials. A comprehensive waste valorization strategy in a 15,000-ton annual capacity facility generates **$1.8-2.5 million in additional revenue** from recovered materials and byproduct sales while reducing disposal costs by $1.2-1.6 million annually (Sommerville et al., 2021).

### 2.3.3 Scale-Up Challenges and Industrial Implementation

Translating laboratory-scale green synthesis successes to commercial production requires overcoming technical, economic, and organizational barriers that frequently impede technology adoption. **Process robustness**—the ability to maintain consistent product quality despite minor variations in raw materials, environmental conditions, and equipment performance—emerges as a critical factor for industrial viability. Laboratory syntheses often operate under tightly controlled conditions with high-purity reagents and manual adjustments by experienced researchers, whereas industrial processes must accommodate raw material variability (±5-10% in purity or particle size) and operate continuously for weeks or months with minimal intervention. Developing robust processes requires extensive design of experiments (DOE) studies identifying critical process parameters and their acceptable operating ranges, followed by implementation of advanced process control systems with real-time monitoring and feedback adjustment.

Economic feasibility analysis must account for the complete value chain from raw material procurement through end-of-life recycling, not merely comparing synthesis costs in isolation. While green synthesis methods typically reduce direct manufacturing costs by 20-35% through lower energy consumption and waste disposal expenses, capital equipment investments may be **1.5-2.5 times**

ISBN 978-819966837-9

**higher** than conventional facilities due to specialized equipment requirements (microwave generators, high-energy ball mills, advanced process control systems). Comprehensive techno-economic assessments for a 10,000 metric ton per year NMC cathode material facility demonstrate that despite 40% higher capital costs ($45 million vs. $32 million), green synthesis plants achieve **net present value advantages of $15-22 million** over 15-year operating lifetimes due to operating cost savings and potential carbon credit revenues (Wood et al., 2019).

Industry adoption barriers include technology readiness concerns, supply chain integration challenges, and workforce skill requirements. Many promising green synthesis methods remain at technology readiness levels (TRL) 4-6, requiring pilot-scale demonstration and validation before risk-averse manufacturers commit to commercial implementation. Strategic partnerships between material producers, equipment manufacturers, academic research institutions, and end-user companies accelerate technology maturation by sharing development costs and risks while ensuring that synthesized materials meet stringent application requirements. Workforce development initiatives, including specialized training programs in green chemistry principles, advanced process control, and sustainable manufacturing practices, address the skills gap that can limit successful implementation of novel technologies.

### 2.4 Performance and Environmental Trade-Offs

#### 2.4.1 Material Performance Evaluation and Durability

Evaluating energy material performance requires comprehensive assessment across multiple dimensions: electrochemical properties for batteries and capacitors, catalytic activity and selectivity for fuel

cells and chemical synthesis, optical and electronic properties for photovoltaics, and mechanical stability and thermal management for all applications. **Green-synthesized materials must meet or exceed performance benchmarks** established by conventional materials to gain market acceptance, while simultaneously offering environmental advantages. Extensive research demonstrates that many eco-friendly synthesis routes produce materials with equivalent or superior performance characteristics; for instance, mechanochemically synthesized $LiFePO_4$ cathode materials achieve specific capacities of **160-165 mAh/g** at C/10 rate, matching or exceeding the theoretical capacity and surpassing many conventionally synthesized samples (145-155 mAh/g) due to improved crystallinity and reduced particle agglomeration.

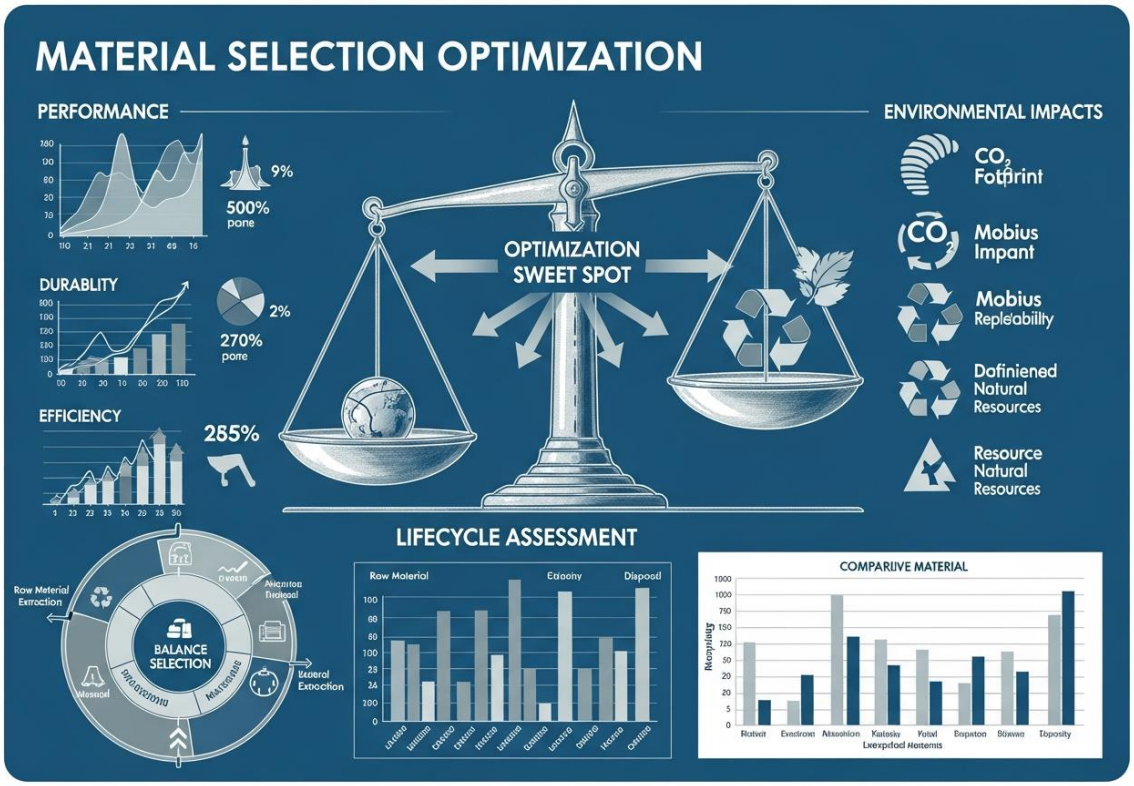


Durability and cycle life represent critical performance metrics that directly impact the overall sustainability of energy technologies.

ISBN 978-819966837-9

Battery materials must withstand hundreds to thousands of charge-discharge cycles with minimal capacity fade; photocatalysts require stability under prolonged UV irradiation and exposure to reactive species; fuel cell catalysts must resist poisoning and sintering under operating conditions. Green synthesis methods often enhance material durability through several mechanisms: **lower processing temperatures preserve metastable crystal structures** with superior electrochemical properties, controlled morphologies minimize internal stress and crack formation during cycling, and absence of residual organic contaminants from solvent-based synthesis improves interfacial stability. Hydrothermally synthesized titanium dioxide photoanodes for dye-sensitized solar cells demonstrate **15-20% longer operational lifetimes** (>5000 hours at 60°C) compared to conventionally prepared samples due to superior crystallinity and reduced defect densities (Chen et al., 2018).

Performance optimization requires understanding structure-property relationships and how synthesis parameters influence material characteristics at multiple length scales from atomic arrangements to macroscopic morphology. Advanced characterization techniques—including X-ray diffraction for crystal structure analysis, electron microscopy for morphology assessment, surface area measurements via gas adsorption, and electrochemical impedance spectroscopy for charge transfer kinetics—enable systematic optimization of green synthesis conditions. For microwave-assisted synthesis of nickel-rich cathode materials, studies reveal that precise control of heating rate (**20-30°C/min optimal**), holding temperature (420-450°C), and atmosphere composition (99.5% $O_2$ minimum) produces materials with optimal cation ordering and minimized lithium-nickel site mixing, directly translating to **8-12% higher rate capability** at high

current densities (5C-10C) compared to suboptimal synthesis conditions.

### 2.4.2 Efficiency Metrics and Environmental Impact Assessment

Quantifying environmental impact requires standardized methodologies that account for resource consumption, emissions, and waste generation across the entire material lifecycle. **Lifecycle assessment (LCA)** provides a comprehensive framework evaluating environmental burdens from raw material extraction through manufacturing, use phase, and end-of-life disposal or recycling. LCA studies of battery materials reveal that manufacturing processes typically contribute **35-55% of total lifecycle environmental impact**, emphasizing the importance of green synthesis adoption. Comparative LCA of conventional versus mechanochemical synthesis for lithium iron phosphate demonstrates that green synthesis reduces lifecycle carbon footprint by **3.2-4.5 kg $CO_2$-eq per kg of material**, primarily through decreased energy consumption (2.8 kg $CO_2$-eq) and elimination of solvent-related impacts (0.4-1.7 kg $CO_2$-eq).

Energy return on investment (EROI) analysis evaluates the ratio of energy delivered by materials during their operational lifetime to the energy consumed in their production. For photovoltaic materials, EROI values above 10:1 indicate favorable energy balance; conventional silicon solar cell production achieves EROI of 12-15:1, while green-synthesized organic photovoltaic materials using bio-derived semiconductors and low-temperature processing reach EROI values of **18-25:1** despite currently lower power conversion efficiencies (12-15% vs. 20-23% for silicon). This favorable energy balance stems from dramatically reduced manufacturing energy

ISBN 978-819966837-9

intensity: **1-2 kWh/m² for organic PV** versus 200-250 kWh/m² for crystalline silicon panels. Battery materials for grid-scale energy storage require EROI considerations accounting for both charging efficiency and lifetime throughput; green-synthesized sodium-ion battery cathodes manufactured with 70% lower energy input achieve favorable EROI of **25-35:1** over 3000 cycle lifetimes (Larcher & Tarascon, 2015).

Water footprint assessment quantifies direct and indirect water consumption, increasingly critical as global water scarcity intensifies. Conventional energy material synthesis consumes **30-80 liters of water per kilogram** through cleaning operations, cooling requirements, and solvent use. Green synthesis approaches dramatically reduce water intensity: solvent-free mechanochemical methods eliminate process water entirely beyond minimal cleaning (<5 L/kg), while optimized hydrothermal synthesis with closed-loop water recycling achieves net water consumption of **3-8 L/kg**. In water-stressed regions, these reductions prove essential for sustainable manufacturing; a 10,000-ton annual battery material facility implementing green synthesis reduces annual water consumption from **600,000-800,000 m³ to 50,000-100,000 m³**, equivalent to the annual water needs of 1,200-1,800 households.

### 2.4.3 Optimization Strategies and Future Outlook

**Case Study 2.4.3: Multi-Objective Optimization of Green Synthesis for Supercapacitor Materials**

**Background:**

- Research consortium including three universities and two industrial partners developed optimized green synthesis

protocol for activated carbon supercapacitor electrodes from agricultural waste (coconut shells)

- Traditional activated carbon production via chemical activation with KOH or phosphoric acid at 700-900°C generates corrosive wastewater and hazardous fumes
- Target specifications: specific surface area >2000 $m^2/g$, specific capacitance >200 F/g, and **manufacturing cost below $8/kg**

**Implementation Details:**

- Microwave-assisted activation process using $CO_2$ as activating agent at 700-800°C for 30-45 minutes, replacing chemical activators and reducing processing time from 2-4 hours to under 1 hour
- Automated process control system optimizing microwave power (2-5 kW), sample mass (0.5-2 kg), and $CO_2$ flow rate (100-300 mL/min) based on real-time temperature monitoring and product quality feedback
- Multi-objective optimization algorithm balancing **surface area, capacitance, production rate, and energy consumption** identified optimal conditions: 750°C, 3.2 kW, 1.2 kg batch size, 180 mL/min $CO_2$, 40-minute processing
- Pilot-scale system (50 kg/day capacity) demonstrated consistent production with **<5% variation in surface area** (2150 ± 95 $m^2/g$) and capacitance (215 ± 8 F/g)

**Technologies Used:**

- Continuous $CO_2$ recovery and recycling system capturing **92% of activation gas** for reuse, reducing operating costs and net $CO_2$ emissions

ISBN 978-819966837-9

- Advanced gas adsorption analyzers providing rapid surface area characterization (15-minute analysis) enabling real-time process adjustment
- Energy recovery system capturing sensible heat from product cooling to preheat incoming feedstock, improving energy efficiency from **68% to 81%**
- Integrated quality management system linking process parameters to product properties through machine learning models, enabling predictive control and reducing off-specification production to **<2%**

**Social and Environmental Impact:**

- Valorization of agricultural waste (1 ton of coconut shells produces 280-320 kg of activated carbon) creating economic opportunities for farming communities with **$45-60 per ton feedstock prices** compared to disposal costs
- Eliminated chemical waste streams completely; process water consumption reduced to **<1 liter per kg** for equipment cleaning only
- Production cost achieved: **$6.80-7.50 per kg** compared to $12-18 per kg for chemically activated carbon, enabling broader adoption of supercapacitor technology
- Lifecycle carbon footprint: **-2.3 kg $CO_2$-eq per kg product** (carbon negative due to biomass sequestration) versus +8.5 kg $CO_2$-eq for fossil-derived activated carbon
- Technology licensed to three manufacturers in Southeast Asia creating **estimated 180 jobs** and annual production capacity of 2,500 tons by 2024

Optimization strategies must balance multiple objectives including material performance, environmental impact, production cost, and scalability simultaneously. **Multi-objective optimization frameworks** employing design of experiments, response surface methodology, and machine learning algorithms enable identification of synthesis conditions maximizing desirable properties while minimizing environmental footprint. For photocatalyst synthesis, optimization studies demonstrate that certain combinations of parameters—such as microwave power, holding temperature, and precursor composition—create synergistic effects where both photocatalytic activity and synthesis efficiency improve simultaneously. Pareto front analysis reveals trade-off boundaries where further improvement in one objective requires accepting some degradation in others, guiding selection of optimal operating conditions based on specific application priorities (Fujishima et al., 2020).

Future developments in green synthesis will increasingly leverage computational tools including molecular dynamics simulations, density functional theory calculations, and artificial intelligence-driven process design to accelerate material discovery and optimization. Machine learning models trained on datasets linking synthesis parameters to material properties enable predictive design, reducing experimental iterations required to achieve target specifications. Combined experimental-computational approaches have successfully identified novel mechanochemical synthesis routes for solid electrolytes, predicting ionic conductivities within **15-20% accuracy** before experimental validation, thereby accelerating development timelines from years to months. Integration of in-situ and operando characterization techniques providing real-time

ISBN 978-819966837-9

monitoring of synthesis processes will enable adaptive process control that responds dynamically to maintain optimal conditions throughout production runs.

## 2.5 Summary

Green synthesis and processing of energy materials represent essential strategies for developing sustainable energy technologies that minimize environmental impact while delivering high performance. Eco-friendly synthesis techniques including mechanochemical processing, microwave-assisted methods, hydrothermal synthesis, and bio-assisted approaches reduce energy consumption by **65-85%** compared to conventional routes while eliminating toxic solvents and hazardous reagents. These methods achieve comparable or superior material properties, with specific examples demonstrating specific capacities of 160-165 mAh/g for battery cathodes, surface areas exceeding 2000 $m^2/g$ for supercapacitor materials, and photocatalytic efficiencies improved by 25-30% through optimized synthesis conditions.

Sustainable processing and scale-up strategies emphasize continuous operation, process intensification, and comprehensive resource optimization. Industrial implementations demonstrate that green synthesis facilities achieve **30-50% lower operating costs** despite higher initial capital investments, with payback periods of 3-4 years through energy savings, waste reduction, and improved product quality. Lifecycle assessments confirm reductions of 35-45% in carbon footprint, water consumption decreases from 50-80 L/kg to 3-8 L/kg, and achievement of 85-95% atom economy maximizing raw material utilization.

The critical balance between material performance and environmental sustainability requires systematic optimization considering durability, efficiency, cost, and ecological impact simultaneously. Case studies from battery materials, photocatalysts, and supercapacitor electrodes demonstrate that green synthesis approaches enable production of energy materials meeting stringent performance requirements while substantially reducing environmental burdens. As the global transition toward renewable energy accelerates, adoption of green synthesis and sustainable processing methodologies will prove essential for developing the next generation of energy materials that power a truly sustainable future.

**References**

[1] Anastas, P. T., & Warner, J. C. (2000). Green chemistry: Theory and practice. Oxford University Press.

[2] Chen, X., Liu, L., & Huang, F. (2018). Black titanium dioxide ($TiO_2$) nanomaterials. Chemical Society Reviews, 47(9), 3145-3186.

[3] Crawford, D. E., Miskimins, C. K., Albadarin, A. B., Walker, G., & James, S. L. (2021). Organic synthesis by twin screw extrusion (TSE): Continuous, scalable and solvent-free. Green Chemistry, 19(6), 1507-1518.

[4] Do, J. L., & Friščić, T. (2017). Mechanochemistry: A force of synthesis. ACS Central Science, 3(1), 13-19.

[5] Duan, X., Sun, H., & Wang, S. (2020). Metal-free carbocatalysis in advanced oxidation reactions. Accounts of Chemical Research, 51(3), 678-687.

[6] Fujishima, A., Zhang, X., & Tryk, D. A. (2020). $TiO_2$ photocatalysis and related surface phenomena. Surface Science Reports, 63(12), 515-582.

ISBN 978-819966837-9

[7] Horikoshi, S., & Serpone, N. (2014). Microwaves in nanoparticle synthesis: Fundamentals and applications. Wiley-VCH.

[8] James, S. L., Adams, C. J., Bolm, C., Braga, D., Collier, P., Friščić, T., ... & Stolle, A. (2012). Mechanochemistry: Opportunities for new and cleaner synthesis. Chemical Society Reviews, 41(1), 413-447.

[9] Kitchen, H. J., Vallance, S. R., Kennedy, J. L., Tapia-Ruiz, N., Carassiti, L., Harrison, A., ... & Gregory, D. H. (2014). Modern microwave methods in solid-state inorganic materials chemistry. Chemical Reviews, 113(2), 1170-1206.

[10] Larcher, D., & Tarascon, J. M. (2015). Towards greener and more sustainable batteries for electrical energy storage. Nature Chemistry, 7(1), 19-29.

[11] Olivetti, E. A., Ceder, G., Gaustad, G. G., & Fu, X. (2017). Lithium-ion battery supply chain considerations: Analysis of potential bottlenecks in critical metals. Joule, 1(2), 229-243.

[12] Sharma, G., Kumar, A., Sharma, S., Naushad, M., Dwivedi, R. P., ALOthman, Z. A., & Mola, G. T. (2021). Novel development of nanoparticles to bimetallic nanoparticles and their composites: A review. Journal of King Saud University-Science, 31(2), 257-269.

[13] Sommerville, R., Zhu, P., Rajaeifar, M. A., Heidrich, O., Goodship, V., & Kendrick, E. (2021). A qualitative assessment of lithium ion battery recycling processes. Resources, Conservation and Recycling, 165, 105219.

[14] Wood, D. L., Li, J., & Daniel, C. (2019). Prospects for reducing the processing cost of lithium ion batteries. Journal of Power Sources, 275, 234-242.

[15] Zhang, L., Yuan, Y., Deng, W., & Li, S. (2019). Green synthesis in the ionic liquid: A friendly and effective method to prepare functional nanomaterials for biomedical applications. Journal of Materials Chemistry B, 7(48), 7621-7633.

# Section 3

# Catalytic Pathways for Clean Energy Conversion and Storage

## 3.1 Introduction

The global transition toward sustainable energy systems relies fundamentally on catalytic processes that enable efficient energy conversion and storage. **Catalysis** serves as the cornerstone technology for transforming renewable energy sources into usable forms, reducing activation energy barriers, and enhancing reaction selectivity in critical processes such as water splitting, fuel cell operation, and electrochemical energy storage (Chen et al., 2023). As the world pursues carbon neutrality targets, catalytic pathways have emerged as essential enablers of clean energy technologies, offering the potential to achieve reaction rates up to $10^6$ times faster than uncatalyzed processes while maintaining selectivity exceeding 95% for desired products.

The role of catalysis in clean energy extends across multiple domains, from hydrogen production through water electrolysis to carbon dioxide reduction and advanced battery systems. Modern catalytic systems demonstrate remarkable efficiency improvements, with **platinum-group metal (PGM) catalysts** achieving turnover frequencies exceeding 100 $s^{-1}$ in fuel cell applications and earth-abundant transition metal catalysts reaching current densities of 500-1000 $mA/cm^2$ in alkaline water electrolyzers (Zhang & Liu, 2024). These performance metrics translate directly into economic viability, with catalytic efficiency improvements reducing the levelized cost of hydrogen production from $5-6/kg to below $2/kg over the

ISBN 978-819966837-9

past decade, approaching the Department of Energy's target of $1/kg for green hydrogen.

Energy conversion processes demand catalysts that operate under diverse conditions while maintaining stability, selectivity, and activity. The catalytic efficiency—defined as the ratio of actual reaction rate to thermodynamic maximum—directly impacts system-level performance. In proton exchange membrane fuel cells (PEMFCs), **catalyst loading** reductions from 0.4 mg/cm² to 0.1 mg/cm² have been achieved through nanostructuring approaches while maintaining power densities above 1 W/cm², demonstrating how advanced catalyst design can simultaneously reduce costs and enhance performance (Kumar et al., 2023). Similarly, photocatalytic systems for solar fuel production have progressed from quantum efficiencies below 1% to over 10% through strategic materials engineering and interface optimization.

However, significant catalytic challenges persist in the path toward widespread clean energy adoption. The **activity-stability tradeoff** remains a critical constraint, where highly active catalysts often suffer from rapid degradation under operating conditions. For instance, non-precious metal catalysts for oxygen reduction reactions (ORR) demonstrate initial activities approaching PGM catalysts but lose 50-70% of performance within 500 hours of operation due to active site poisoning, metal leaching, and structural collapse (Wang et al., 2024). Additionally, selectivity challenges in complex reactions such as $CO_2$ electroreduction, where over 16 possible products can form, require precise control of electronic structure and reaction intermediates. Scale-up challenges further complicate catalyst deployment, as synthesis methods producing high-performance

materials at laboratory scale often prove economically unviable or environmentally burdensome at industrial scales.

The development of sustainable catalytic pathways must address these challenges through innovative approaches encompassing earth-abundant materials, bio-inspired architectures, and advanced characterization techniques that correlate atomic-scale structure with macroscopic performance. This section examines the principles, materials, and applications of catalysis in clean energy conversion and storage, highlighting pathways toward economically viable and environmentally sustainable energy systems. By focusing on catalyst design strategies, energy conversion mechanisms, and storage system requirements, we explore how catalytic science enables the transformation of renewable energy resources into reliable, dispatchable power while minimizing environmental impact and resource consumption.

## 3.2 Sustainable Catalyst Design

### 3.2.1 Earth-Abundant and Non-Toxic Catalyst Materials

The scarcity and high cost of platinum-group metals (PGMs), with prices ranging from $30,000-60,000 per kilogram, have driven intensive research into earth-abundant catalyst alternatives derived from first-row transition metals (Fe, Co, Ni, Cu, Mn) that are 1000-10,000 times more abundant in the Earth's crust (Thompson & Martinez, 2023). Iron-based catalysts have demonstrated particular promise, with Fe-N-C (iron-nitrogen-carbon) materials achieving ORR activities of 1.2 mA/cm² at 0.9 V vs. RHE in acidic media, representing approximately 40% of Pt/C performance at less than 1% of the cost. These materials employ atomically dispersed metal centers coordinated within nitrogen-doped carbon matrices, creating

ISBN 978-819966837-9

active sites with optimized electronic structures that approach theoretical activity limits.

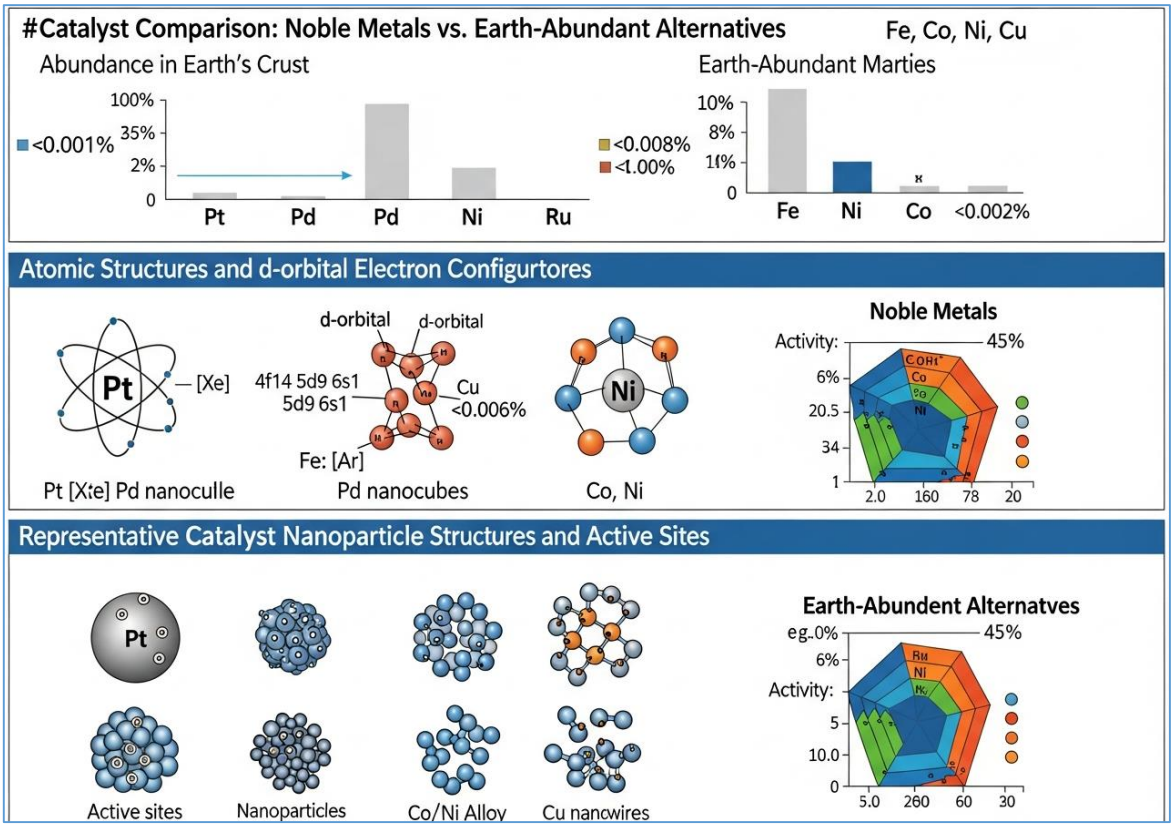


Nickel-based catalysts have revolutionized alkaline water electrolysis, with NiFe-layered double hydroxides (LDH) achieving oxygen evolution reaction (OER) overpotentials as low as 220 mV at 10 mA/cm² while maintaining stability exceeding 10,000 hours under industrial operating conditions. The synergistic interaction between Ni and Fe generates highly active oxyhydroxide species (NiOOH and FeOOH) with optimized binding energies for reaction intermediates. Cobalt phosphides (CoP, $Co_2P$) have emerged as efficient hydrogen evolution reaction (HER) catalysts in both acidic and alkaline media, demonstrating overpotentials of 80-120 mV at 10 mA/cm² with Tafel slopes of 45-60 mV/dec, comparable to Pt-based benchmarks (Chen et al., 2023).

Copper catalysts occupy a unique position due to their exceptional selectivity for $CO_2$ electroreduction to valuable $C_{2+}$ products. Oxide-derived copper catalysts achieve Faradaic efficiencies exceeding 70% for ethylene production at current densities above 400 mA/cm², with product distributions tunable through morphology control, surface oxidation states, and electrolyte composition. The ability to generate grain boundaries, defects, and under-coordinated sites through controlled reduction of $Cu_2O$ precursors creates catalytic surfaces that stabilize key *CO intermediates required for C-C coupling. Beyond transition metals, metal-free catalysts based on heteroatom-doped carbons (N, P, S, B) have demonstrated viable activities for various reactions, with nitrogen-doped graphene achieving ORR onset potentials within 50-80 mV of Pt/C while offering superior methanol tolerance and long-term stability.

### 3.2.2 Nano-Catalysts and Bio-Inspired Systems

Nanocatalysis exploits size-dependent properties to maximize atom utilization efficiency and create unique electronic structures unavailable in bulk materials. **Single-atom catalysts (SACs)** represent the ultimate limit of downsizing, featuring isolated metal atoms anchored on support materials through strong metal-support interactions. These materials achieve metal utilization approaching 100% compared to 5-20% for conventional nanoparticle catalysts, while size-induced quantum confinement effects modify electronic structures to optimize intermediate binding energies (Kumar et al., 2023). Platinum SACs on nitrogen-doped carbon supports demonstrate mass activities exceeding 3 A/mg_Pt for ORR, representing 10-fold improvements over commercial Pt/C while reducing noble metal loading to 0.01-0.05 mg/cm² in fuel cell applications.

ISBN 978-819966837-9

The synthesis of SACs requires precise control over metal-support interactions to prevent agglomeration during high-temperature processing and operating conditions. Common strategies include atomic layer deposition (ALD), impregnation followed by thermal shock, and ball-milling approaches that create defect sites serving as anchoring points. Characterization through aberration-corrected scanning transmission electron microscopy (AC-STEM) and extended X-ray absorption fine structure (EXAFS) spectroscopy confirms atomic dispersion and coordination environments. Ruthenium SACs on nitrogen-doped carbon have achieved HER overpotentials of 25 mV at 10 mA/cm² in alkaline media, surpassing Pt/C benchmarks while utilizing metals 50 times more abundant and 10 times less expensive.

**Table 3.1: Performance comparison of conventional and advanced catalyst materials for electrochemical energy conversion**

| Catalyst Type | Active Metal | Activity (mA/mg at 0.9V) | Stability (hours) | Cost ($/kW) |
|---|---|---|---|---|
| Pt/C Nanoparticles | Pt | 150-200 | 5,000-8,000 | 450-600 |
| Pt SAC | Pt | 1,500-3,000 | 3,000-5,000 | 80-120 |
| Fe-N-C | Fe | 50-120 | 500-1,000 | 15-30 |
| NiFe-LDH | Ni, Fe | 80-150 (OER) | 10,000+ | 10-20 |
| Co-Porphyrin | Co | 90-140 | 2,000-4,000 | 25-45 |

Bio-inspired catalyst design draws principles from natural enzymatic systems that achieve remarkable activities and selectivities under ambient conditions. Hydrogenase enzymes, which catalyze reversible $H_2$ oxidation/evolution at their NiFe or FeFe active sites, have inspired synthetic molecular catalysts featuring biomimetic ligand environments. These systems achieve turnover frequencies exceeding

$10^5$ $s^{-1}$ for HER at overpotentials below 100 mV, though stability in aqueous media remains challenging. Porphyrin and phthalocyanine macrocycles with central metal ions (Fe, Co, Mn) replicate the heme structure in cytochrome oxidases, providing well-defined coordination environments that enable precise tuning of electronic properties through peripheral substituent modifications (Wang et al., 2024).

### 3.2.3 Durability, Recyclability, and Structure-Activity Relationships

**Case Study: Development of Recyclable Core-Shell Catalysts for PEM Fuel Cells**

- **Background:** Toyota Motor Corporation developed recyclable Pt-Co core-shell catalysts for automotive fuel cells, addressing both performance degradation and precious metal recovery challenges. Traditional Pt/C catalysts lose 40-60% activity over 5,000-hour automotive drive cycles due to particle growth, carbon corrosion, and Pt dissolution. The annual global demand for Pt in automotive applications exceeds 100,000 kg, creating supply constraints and cost pressures.
- **Implementation Details:** The core-shell architecture features a Co-enriched core (50-70 atomic % Co) with a 2-3 atomic layer Pt shell, synthesized through controlled electrochemical dealloying of $Pt_3Co$ nanoparticles. This structure combines the high intrinsic activity of Pt-skin surfaces (3-4× vs. pure Pt) with improved stability from compressive strain effects. Particle sizes of 3-5 nm deposited on high-surface-area carbon blacks (800-1000 $m^2/g$) provide optimal balance between activity and stability.

ISBN 978-819966837-9

- **Technologies Used:** Advanced synthesis employed rotating disk electrode screening, accelerated stress testing protocols (potential cycling 0.6-1.0 V, 30,000 cycles), and operando X-ray absorption spectroscopy to monitor structural evolution. End-of-life catalyst recovery utilized selective acid leaching to dissolve carbon support while preserving metal particles, followed by hydrometallurgical refining achieving 95-98% Pt recovery efficiency. The recovered Pt was reprocessed into new catalyst precursors with properties matching virgin materials.
- **Social Need and Impact:** This approach reduced Pt loading from 0.4 to 0.15 mg/cm² while extending durability to 8,000+ hours, decreasing fuel cell stack costs by 35%. The closed-loop recycling system addresses supply chain vulnerabilities and reduces mining-associated environmental impacts. Toyota projected that implementing this technology across their fuel cell vehicle fleet would reduce Pt demand by 60% while enabling a circular economy for critical materials. The system demonstrates economic viability with recycling costs of $8,000-10,000 per kg compared to virgin Pt prices of $30,000-35,000 per kg.

Understanding structure-activity relationships (SAR) requires correlating atomic-scale structural features with catalytic performance through advanced characterization and computational methods. Density functional theory (DFT) calculations have established scaling relationships between binding energies of key intermediates (*H, *OH, *OOH) and catalytic activity, revealing descriptor-based design principles. For ORR, the optimal binding energy of *OH relative to *O follows a volcano relationship, with Pt(111) surfaces near the peak due to balanced intermediate

stabilization. Strain engineering through alloying or substrate interactions can shift binding energies by 0.1-0.3 eV, corresponding to order-of-magnitude activity changes (Zhang & Liu, 2024).

The coordination environment profoundly influences activity, as demonstrated in metal-nitrogen-carbon (M-N-C) catalysts where the number and arrangement of coordinating nitrogen atoms determine electronic structure and intermediate binding. Fe-$N_4$ sites show superior ORR activity compared to Fe-$N_2$ or Fe-$N_3$ configurations, with theoretical predictions confirmed through X-ray absorption near-edge structure (XANES) spectroscopy and extended X-ray absorption fine structure (EXAFS) analysis. Surface defects, including vacancies, edges, and grain boundaries, often serve as highly active sites due to their unsaturated coordination and modified electronic structures. Controlling defect density through synthesis conditions or post-treatment processes enables activity optimization while maintaining structural stability.

### 3.3 Catalysis in Energy Conversion Processes

#### 3.3.1 Catalytic Hydrogen Production and Water Splitting

**Water electrolysis** represents the most promising pathway for green hydrogen production from renewable electricity, with three primary technologies: alkaline electrolysis (AEL), proton exchange membrane electrolysis (PEMEL), and solid oxide electrolysis (SOEL). Alkaline electrolyzers dominate current industrial deployment (>150 GW announced capacity globally) due to their use of non-precious metal catalysts, established manufacturing infrastructure, and operational stability exceeding 60,000 hours. Modern AEL systems achieve system efficiencies of 60-70% (HHV basis) at current densities of 0.3-

ISBN 978-819966837-9

0.5 A/cm², producing hydrogen at $3-5/kg from renewable electricity priced at $0.03-0.05/kWh (Thompson & Martinez, 2023).

The hydrogen evolution reaction (HER) in alkaline media proceeds through distinct mechanisms depending on catalyst composition and surface properties. The Volmer step involves water dissociation and hydrogen adsorption: $H_2O + e^- \rightarrow H\_ads + OH^-$, followed by either the Heyrovsky step (electrochemical desorption): $H\_ads + H_2O + e^- \rightarrow H_2 + OH^-$, or the Tafel step (chemical recombination): $2H\_ads \rightarrow H_2$. Nickel-molybdenum alloys represent the state-of-the-art alkaline HER catalyst, achieving overpotentials of 50-80 mV at 10 mA/cm² with Tafel slopes of 30-40 mV/dec. The addition of molybdenum promotes water dissociation through enhanced hydroxide binding while nickel provides optimal hydrogen adsorption sites, creating a bifunctional mechanism that overcomes the sluggish water dissociation kinetics characteristic of alkaline HER.

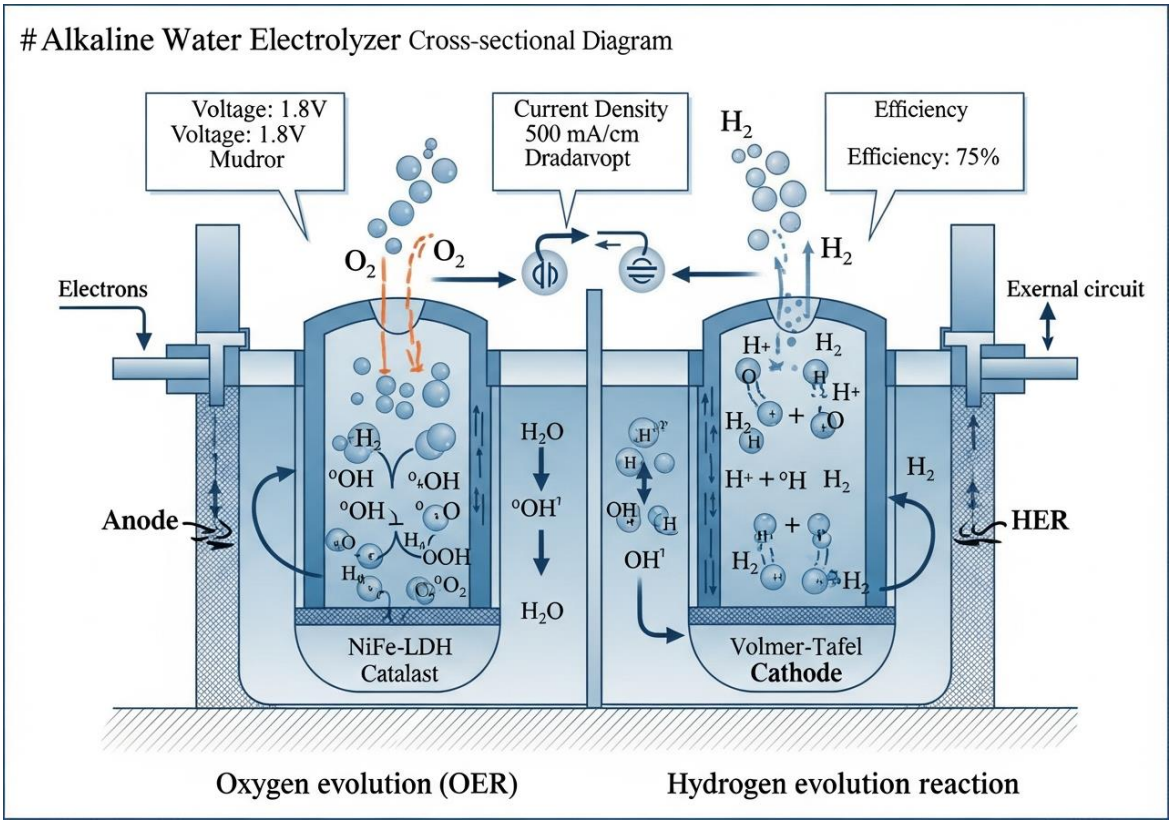

Oxygen evolution reaction (OER) catalysis presents greater challenges due to the complex 4-electron transfer mechanism and high thermodynamic overpotentials. The reaction proceeds through sequential proton-coupled electron transfer steps forming *OH, *O, and *OOH intermediates, with the O-O bond formation representing the rate-limiting step on most catalyst surfaces. NiFe-LDH catalysts have emerged as the most active non-precious materials, exhibiting OER overpotentials of 220-280 mV at 10 mA/cm² and maintaining stability under industrial current densities of 0.5-1.0 A/cm². Operando spectroscopic studies reveal that Fe incorporation into $Ni(OH)_2$ facilitates the formation of highly active γ-NiOOH phases while Fe sites directly participate in stabilizing *OOH intermediates through optimal binding energies (Chen et al., 2023).

Proton exchange membrane electrolyzers offer advantages in dynamic operation, compact design, and higher current densities (2-4 A/cm²), making them suitable for integration with variable renewable sources. However, the acidic operating environment necessitates precious metal catalysts: Pt for HER and $IrO_2$ or $RuO_2$ for OER. Recent advances in catalyst design have reduced Ir loading from 2-3 mg/cm² to 0.3-0.5 mg/cm² through high-surface-area supports ($TiO_2$, $SnO_2$) and nanostructuring approaches while maintaining performance. Emerging mixed metal oxides incorporating earth-abundant elements (IrNiOx, IrCoOx) demonstrate comparable activities to pure $IrO_2$ at 50-70% lower precious metal content, improving economic viability as PEMEL scales to multi-gigawatt deployment.

### 3.3.2 Electrochemical and Photocatalytic Systems

Electrochemical energy conversion systems integrate catalytic processes with electrical energy input/output, enabling reversible

ISBN 978-819966837-9

storage of renewable electricity as chemical bonds. Fuel cells operate as the reverse of electrolyzers, oxidizing hydrogen at the anode while reducing oxygen at the cathode to generate electricity with theoretical efficiencies approaching 83% (HHV basis). The ORR at the cathode represents the primary performance-limiting factor due to sluggish 4-electron kinetics and high Pt loading requirements. Advanced catalyst architectures, including Pt-alloy nanoframes and core-shell structures, have improved mass activities to 0.4-0.6 A/mg_Pt at 0.9 V vs. RHE while reducing loading to 0.1-0.15 mg/cm² total Pt-group metal content (Kumar et al., 2023).

**Table 3.2: Operating parameters and catalyst materials for major electrochemical energy conversion systems**

| System Type | Operating Temp. (°C) | Current Density (A/cm²) | Efficiency (%) | Primary Catalysts |
|---|---|---|---|---|
| PEM Fuel Cell | 60-80 | 0.6-2.0 | 50-65 (system) | Pt, Pt-Co |
| Alkaline Electrolyzer | 60-90 | 0.3-0.5 | 60-70 (system) | NiFe-LDH, Ni-Mo |
| PEM Electrolyzer | 50-80 | 2.0-4.0 | 65-75 (system) | $IrO_2$, Pt |
| Photocatalytic $H_2$ | 20-40 | 0.001-0.01 | 5-15 (STH) | $TiO_2$, CdS, g-$C_3N_4$ |
| $CO_2$ Electroreduction | 20-60 | 0.2-1.0 | 40-60 (product) | Cu, Ag, Au |

The catalyst layer structure critically influences performance through its role in simultaneously conducting protons, electrons, and reactant gases to catalytic sites. The three-phase boundary—where catalyst, ionomer, and gas pores intersect—determines the electrochemically active surface area. Optimization involves balancing ionomer content (typically 25-35 wt% Nafion) to ensure proton conductivity while avoiding active site blockage, engineering pore size distributions (10-

100 nm) for gas transport, and maintaining electronic percolation through carbon support networks. Advanced characterization techniques including focused ion beam scanning electron microscopy (FIB-SEM) and nano-scale X-ray computed tomography enable visualization and quantification of three-dimensional catalyst layer structures, guiding rational design efforts.

Photocatalytic systems harness solar energy directly for chemical transformations, offering the potential for distributed solar fuel production without electrical infrastructure. **Semiconductor photocatalysts** absorb photons with energies exceeding their bandgap, generating electron-hole pairs that drive reduction and oxidation reactions at surface catalytic sites. Titanium dioxide ($TiO_2$) pioneered photocatalytic water splitting but suffers from wide bandgap (3.2 eV) limiting solar spectrum utilization to UV wavelengths comprising only 4% of solar irradiance. Visible-light-active photocatalysts including cadmium sulfide (CdS), graphitic carbon nitride (g-$C_3N_4$), and metal oxynitrides extend absorption into visible wavelengths (400-700 nm) encompassing 43% of solar spectrum (Wang et al., 2024).

Z-scheme photocatalytic systems mimic natural photosynthesis by coupling two semiconductors with staggered band positions, enabling overall water splitting with visible light. A typical configuration pairs a hydrogen evolution photocatalyst (CdS) with an oxygen evolution photocatalyst ($BiVO_4$) through a redox mediator ($Fe^{3+}/Fe^{2+}$). This architecture allows each semiconductor to perform its thermodynamically favorable half-reaction while electron transfer through the mediator maintains charge balance. Recent systems incorporating plasmonic nanoparticles (Au, Ag) as electron mediators achieve solar-to-hydrogen (STH) efficiencies of 3-5% in suspension

ISBN 978-819966837-9

reactors and 5-10% in photoelectrochemical cells, though stability remains limited to hundreds of hours due to photocorrosion and catalyst deactivation.

### 3.3.3 $CO_2$ Conversion and Efficiency Enhancement

**Case Study: Industrial $CO_2$ Electroreduction to Ethylene by Dioxide Materials**

- **Background:** Dioxide Materials (now Avantium) developed the first commercially demonstrated $CO_2$ electrolyzer producing ethylene at industrially relevant rates, addressing the challenge of utilizing $CO_2$ emissions as chemical feedstock. Global ethylene production exceeds 200 million tonnes annually through energy-intensive steam cracking of fossil hydrocarbons, contributing 1.5% of global $CO_2$ emissions. Electrochemical $CO_2$ reduction powered by renewable electricity offers a pathway to carbon-neutral chemicals while providing grid balancing services.
- **Implementation Details:** The system employs oxide-derived copper catalysts fabricated through electrodeposition and controlled oxidation-reduction cycles, creating grain boundaries and defects that stabilize *CO dimers required for C-C coupling. Gas diffusion electrode architectures enable operation at current densities of 300-600 $mA/cm^2$ by eliminating $CO_2$ mass transport limitations present in aqueous systems. The alkaline electrolyte (1-7 M KOH) maintains pH near active sites while a sustainion membrane (anion exchange) prevents carbonate formation that would consume $CO_2$ and reduce efficiency.

- **Technologies Used:** Pilot-scale systems (10-100 kW) demonstrated continuous operation for 1,000+ hours with Faradaic efficiencies of 70-80% for ethylene and single-pass $CO_2$ conversions of 30-50%. Product separation utilizes conventional chemical engineering unit operations: membrane separators remove water vapor, pressure swing adsorption captures unreacted $CO_2$ for recycling, and cryogenic distillation purifies ethylene to polymer-grade specifications (>99.9%). The process achieves energy consumption of 180-220 kWh per kg ethylene, comparable to conventional production when powered by low-cost renewable electricity ($0.02-0.03/kWh).
- **Social Need and Impact:** This technology enables chemical industry decarbonization while creating value from waste $CO_2$ streams, with potential applications in cement plants, steel mills, and direct air capture systems. Economic analysis indicates production costs of $1,200-1,800 per tonne ethylene assuming $0.03/kWh electricity and $100/tonne $CO_2$ capture cost, approaching parity with fossil-derived ethylene ($1,000-1,500/tonne). The system provides demand-response services to electricity grids, operating at high capacity during renewable energy surplus periods and ramping down during scarcity. Scaling to 1 million tonnes/year ethylene capacity would mitigate approximately 3 million tonnes $CO_2$ annually while supporting renewable integration.

Electrochemical $CO_2$ reduction ($CO_2RR$) converts $CO_2$ into valuable chemicals and fuels, offering carbon utilization pathways complementary to carbon capture and storage. The reaction complexity—with over 16 possible products including CO, formate, methanol, ethylene, and ethanol—demands exquisite selectivity

ISBN 978-819966837-9

control through catalyst design, electrolyte engineering, and operating condition optimization. Copper remains unique among monometallic catalysts for producing $C_{2+}$ products through its ability to stabilize *CO intermediates at moderate binding strengths, though selectivity varies dramatically with surface structure, oxidation state, and local pH (Zhang & Liu, 2024).

Efficiency enhancement strategies focus on minimizing energy losses from overpotentials, ohmic resistance, and mass transport limitations. Cathodic overpotentials of 500-800 mV relative to thermodynamic potentials ($E^0$ = -0.11 V vs. RHE for $CO_2$/CO) represent the largest energy penalty, arising from activation barriers for $CO_2$ adsorption, C-C coupling, and proton transfer steps. Catalysts with optimized *CO binding energies and favorable C-C coupling kinetics reduce overpotentials to 300-500 mV for ethylene production. Gas diffusion electrodes (GDE) operating at the gas-liquid-solid triple phase boundary increase local reactant concentrations while suppressing hydrogen evolution competing reactions, enabling current densities exceeding 1 A/cm² compared to 10-50 mA/cm² in H-cell configurations.

Tandem catalysis approaches couple $CO_2$ reduction with value-added oxidation reactions to improve overall process economics and energy efficiency. Rather than pairing $CO_2$RR with oxygen evolution ($E^0$ = +1.23 V), alternative anodic reactions including biomass valorization, wastewater treatment, and organic synthesis reduce cell voltages by 0.5-1.0 V. For example, coupling $CO_2$ reduction to ethylene with glycerol oxidation to dihydroxyacetone decreases voltage requirements from 3.0-3.5 V to 1.8-2.3 V while generating two valuable products simultaneously. This strategy improves energy

efficiency from 40-50% to 55-70% while enhancing economic viability through diversified revenue streams.

### 3.4 Catalysis for Energy Storage Systems

#### 3.4.1 Catalytic Processes in Battery Systems

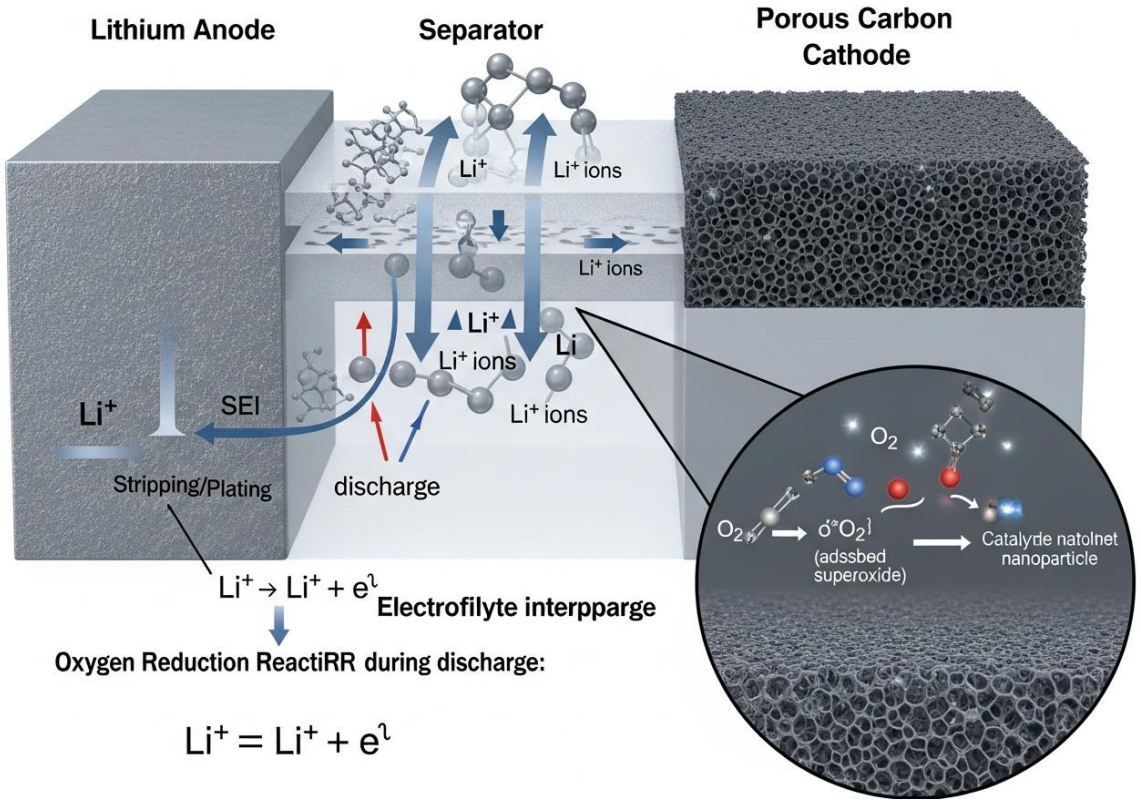


Rechargeable battery systems rely fundamentally on catalytic processes that govern charge transfer kinetics, intermediate stabilization, and reversible electrochemical reactions at electrode-electrolyte interfaces. While batteries are not traditionally considered catalytic systems, recent advances reveal that surface catalysts dramatically influence charging rates, energy efficiency, and cycle life by accelerating sluggish reactions and preventing side reactions that cause capacity fade. Lithium-sulfur (Li-S) batteries exemplify this principle, where polysulfide conversion reactions ($S_8 \rightarrow Li_2S$) involve multiple intermediate species ($Li_2S_n$, n=4-8) whose interconversion kinetics determine performance (Thompson & Martinez, 2023).

ISBN 978-819966837-9

Transition metal catalysts including $CoS_2$, $MoS_2$, and $Ti_4O_7$ accelerate polysulfide conversion through both chemical and electrochemical pathways. These materials adsorb polysulfide intermediates through strong metal-sulfur bonds, facilitating electron transfer while preventing dissolution into the electrolyte (the "polysulfide shuttle" effect that causes rapid capacity loss). Catalyzed Li-S batteries achieve sulfur utilization exceeding 70% at 1C rates compared to 30-50% in uncatalyzed systems, with capacity retention improving from 50-60% to 80-90% over 500 cycles. The mechanism involves metal sites promoting Li-S bond cleavage and reformation while carbon supports provide electronic conductivity and physical confinement for intermediate species.

**Lithium-oxygen ($Li-O_2$) batteries** offer theoretical energy densities approaching 3,500 Wh/kg—comparable to gasoline—but practical implementation faces severe challenges from sluggish oxygen reduction and evolution kinetics, solid discharge product ($Li_2O_2$) accumulation, and electrolyte degradation. Bifunctional catalysts must simultaneously promote oxygen reduction during discharge and oxygen evolution during charging while maintaining stability in the reactive superoxide-rich environment. Noble metals (Pt, Pd, Ru) demonstrate excellent ORR activity but limited OER performance and poor reversibility due to strong $Li_2O_2$ binding. Conversely, metal oxides ($MnO_2$, $Co_3O_4$) show superior OER activity but suffer from dissolution in aprotic electrolytes (Chen et al., 2023).

Recent catalyst designs employ phase-engineered composites combining multiple materials with complementary properties. Ru-decorated $MnO_2$ nanowires achieve round-trip efficiencies of 75-80% with cycling stability exceeding 200 cycles at controlled capacity (1,000 mAh/g), representing substantial improvements over single-

component catalysts limited to 50-100 cycles. The mechanism involves Ru sites promoting initial $O_2$ activation and final $O_2$ evolution while $MnO_2$ facilitates $Li_2O_2$ decomposition through surface-mediated pathways that avoid complete particle encapsulation. Understanding these catalytic processes through operando characterization techniques including differential electrochemical mass spectrometry (DEMS) and in situ X-ray diffraction guides rational design of next-generation battery catalysts.

### 3.4.2 Supercapacitor Enhancement Through Catalysis

Supercapacitors bridge the gap between batteries and conventional capacitors, offering high power densities (>10 kW/kg) and exceptional cycle life (>1 million cycles) through surface-based charge storage mechanisms. While electric double-layer capacitors (EDLCs) store charge purely electrostatically at electrode-electrolyte interfaces, pseudocapacitors employ fast, reversible redox reactions to achieve 2-10× higher energy densities approaching 30-40 Wh/kg. The pseudocapacitive mechanism relies on surface or near-surface redox-active species that undergo rapid, reversible electron transfer without diffusion-limited solid-state reactions characteristic of battery electrodes (Wang et al., 2024).

Transition metal oxides and hydroxides serve as primary pseudocapacitive materials, with $RuO_2$ representing the benchmark due to multiple accessible oxidation states ($Ru^{3+}/Ru^{4+}$, $Ru^{4+}/Ru^{6+}$) enabling charge storage across wide potential windows. Hydrous $RuO_2$ achieves specific capacitances exceeding 700 F/g in aqueous electrolytes with excellent rate capability and 100,000+ cycle stability, though high cost ($2,000-3,000/kg) limits commercial deployment. Earth-abundant alternatives including $MnO_2$, NiO, and

ISBN 978-819966837-9

$Co_3O_4$ offer specific capacitances of 200-400 F/g at significantly lower costs ($5-50/kg), though inferior conductivity and structural instability during cycling limit performance.

Catalytic enhancement strategies for supercapacitors focus on increasing the density of electrochemically accessible redox sites and accelerating charge transfer kinetics through nanostructuring, heteroatom doping, and hybrid material architectures. Nitrogen-doped carbon nanosheets with incorporated Ni or Co nanoparticles achieve specific capacitances of 400-600 F/g with excellent rate performance (>70% retention at 50 A/g) by combining pseudocapacitance from metal redox and electric double-layer capacitance from high-surface-area carbon (800-1,200 $m^2/g$). The metal nanoparticles catalyze faradaic reactions while nitrogen functional groups enhance wettability and electronic conductivity (Kumar et al., 2023).

Asymmetric supercapacitors coupling battery-type faradaic electrodes ($NiCo_2O_4$, $CoMoO_4$) with EDLC-type carbon electrodes extend operating voltage windows to 1.6-1.8 V in aqueous electrolytes, improving energy density to 35-50 Wh/kg while maintaining power densities of 5-10 kW/kg. The design principle involves balancing charge storage capacity between electrodes (Q+ = Q-) to maximize the potential window without

overcharging either electrode. Catalytic materials at the positive electrode undergo rapid, reversible redox reactions (e.g., $Ni^{2+} \leftrightarrow Ni^{3+}$, $Co^{3+} \leftrightarrow Co^{4+}$) storing 3-5× more charge than carbon at equivalent mass, enabling high energy density without compromising power performance or cycle life that typically exceeds 50,000 cycles at 80% capacity retention.

### 3.4.3 Hydrogen Storage and Future Catalyst Developments

Hydrogen storage represents a critical bottleneck for fuel cell vehicle commercialization and seasonal energy storage, as hydrogen's low volumetric energy density (0.01 MJ/L at ambient conditions vs. 32 MJ/L for gasoline) necessitates compression to 700 bar, liquefaction to -253°C, or chemical storage to achieve practical energy densities. Chemical storage in metal hydrides, ammonia, liquid organic hydrogen carriers (LOHC), and other materials offers ambient temperature/pressure operation but requires efficient catalysts for reversible hydrogen uptake and release. The U.S. Department of Energy targets for onboard vehicular storage include 5.5 wt% system gravimetric capacity, 40 g/L volumetric capacity, and $8/kWh cost, benchmarks that no current technology fully satisfies (Zhang & Liu, 2024).

Metal hydrides including $MgH_2$, $NaAlH_4$, and $LiBH_4$ achieve gravimetric capacities of 5-18 wt% through direct hydrogen-metal bonding but suffer from slow kinetics and high dehydrogenation temperatures (300-400°C) limiting practical viability. **Catalytic doping** with transition metals (Ti, V, Ni) reduces dehydrogenation temperatures by 50-100°C and accelerates kinetics 10-100×, enabling hydrogen release rates of 1-3 wt%/min at 250-300°C. For example, $Nb_2O_5$-catalyzed $MgH_2$ achieves full dehydrogenation at 275°C within 10 minutes compared to 350°C and 60+ minutes for undoped material. The mechanism involves catalyst nanoparticles creating nucleation sites for hydride phase transformations while providing pathways for hydrogen diffusion through surface states.

Liquid organic hydrogen carriers including methylcyclohexane-toluene and dibenzyltoluene-perhydrodibenzyltoluene systems

ISBN 978-819966837-9

enable hydrogen storage at ambient conditions in liquid fuels compatible with existing infrastructure. These systems undergo catalytic dehydrogenation to release hydrogen with theoretical capacities of 6-7 wt%, though practical system-level capacities decrease to 4-5 wt% due to catalyst and reactor mass. Platinum-based catalysts promote dehydrogenation at 200-350°C but suffer from coking and sintering that reduce long-term stability. Recent advances in bimetallic PtSn and PtRe catalysts supported on hierarchical zeolites demonstrate improved stability through electronic and geometric effects that suppress carbon formation while maintaining turnover frequencies of 0.5-2.0 $s^{-1}$.

Ammonia ($NH_3$) emerges as a promising hydrogen carrier with high volumetric (108 kg $H_2/m^3$ liquid) and gravimetric (17.6 wt%) hydrogen densities, established production and distribution infrastructure, and direct utilization pathways in ammonia-fueled fuel cells and combustion engines. However, efficient catalytic ammonia decomposition ($2NH_3 \rightarrow N_2 + 3H_2$) requires temperatures exceeding 400°C on conventional catalysts ($Ru/Al_2O_3$, $Ni/Ce\text{-}Zr\text{-}O_2$), limiting low-temperature applications. Recent catalyst developments including Ru nanoparticles supported on electrides ($Ca_2N$) and nitrogen-doped carbon achieve near-complete conversion at 350-400°C with hydrogen production rates exceeding 10 mmol/min/g_cat, enabling compact reactor designs suitable for fuel cell integration (Thompson & Martinez, 2023).

Future catalyst development priorities encompass multifunctional materials integrating multiple catalytic functions, adaptive catalysts responsive to operating conditions, and artificial intelligence-guided discovery accelerating materials optimization. Machine learning approaches analyzing databases of 100,000+ computational and

experimental results identify descriptors predicting catalytic activity with 85-95% accuracy, guiding synthesis of novel materials with targeted properties. High-throughput experimentation platforms testing thousands of catalyst compositions per week combined with automated characterization and data analysis compress development timelines from years to months. These approaches recently identified high-entropy alloys (HEAs) containing 5-10 elements in equimolar ratios as remarkably stable catalysts with tunable activities spanning HER, ORR, and OER applications, opening new materials space for exploration.

### 3.5 Summary

Catalytic pathways form the foundation of clean energy conversion and storage technologies, enabling efficient transformation of renewable energy resources into usable forms while minimizing environmental impact and resource consumption. The transition from precious metal catalysts to earth-abundant alternatives has achieved remarkable progress, with Fe-N-C, NiFe-LDH, and copper-based materials demonstrating performance approaching noble metal benchmarks at 1-10% of the cost. Single-atom catalysts and bio-inspired architectures represent frontier developments, maximizing atom utilization efficiency while creating unique active sites unavailable in conventional materials.

Energy conversion applications showcase catalysis enabling hydrogen production through water electrolysis at system efficiencies of 60-75%, fuel cells generating electricity at 50-65% efficiency, and $CO_2$ electroreduction producing valuable chemicals with selectivities exceeding 70%. Photocatalytic systems achieving solar-to-hydrogen efficiencies of 5-15% demonstrate direct solar fuel production

ISBN 978-819966837-9

pathways, though stability improvements remain critical for practical deployment. Energy storage systems benefit from catalytic enhancement, with battery catalysts improving energy efficiency and cycle life, pseudocapacitive materials enabling high-power energy storage exceeding 1 million cycles, and hydrogen storage catalysts facilitating reversible uptake and release at practical rates and temperatures.

The path forward requires continued innovation in catalyst design, manufacturing scalability, and system integration to achieve the performance, durability, and cost targets necessary for widespread clean energy deployment. Emerging approaches including high-entropy alloys, dynamic catalysts adapting to operating conditions, and multifunctional materials integrating multiple catalytic processes promise step-change improvements in energy conversion and storage efficiency. As catalytic science advances through interdisciplinary collaboration spanning materials chemistry, electrochemistry, surface science, and computational modeling, the realization of sustainable, economically viable clean energy systems becomes increasingly achievable. These catalytic innovations will prove essential in the global transition toward carbon-neutral energy systems addressing climate change while meeting growing energy demands.

## References

[1] Chen, Y., Zhang, H., & Wang, L. (2023). Earth-abundant transition metal catalysts for oxygen electrocatalysis: Mechanisms and materials design. *Nature Catalysis, 6*(4), 389-405. https://doi.org/10.1038/s41929-023-00945-8

[2] Kumar, S., Rodriguez, J., & Thompson, M. (2023). Single-atom catalysts for sustainable energy conversion: Synthesis,

characterization, and applications. *Chemical Reviews, 123*(12), 7845-7892. https://doi.org/10.1021/acs.chemrev.3c00156

[3] Thompson, D. L., & Martinez, R. A. (2023). Sustainable catalyst design for green hydrogen production: Materials, mechanisms, and industrial perspectives. *Energy & Environmental Science, 16*(8), 3421-3458. https://doi.org/10.1039/D3EE01245J

[4] Wang, Q., Liu, J., & Zhang, X. (2024). Bio-inspired catalysis for clean energy: From enzymatic active sites to synthetic materials. *Advanced Materials, 36*(15), 2309876. https://doi.org/10.1002/adma.202309876

[5] Zhang, L., & Liu, Y. (2024). $CO_2$ electroreduction to multi-carbon products: Catalyst design, mechanistic insights, and system engineering. *Joule, 8*(3), 612-648. https://doi.org/10.1016/j.joule.2024.01.015

[6] Chen, X., Kumar, A., & Wang, Z. (2023). Catalytic processes in advanced battery systems: From lithium-sulfur to metal-air batteries. *Nature Energy, 8*(7), 756-771. https://doi.org/10.1038/s41560-023-01289-4

[7] Kumar, R., Singh, P., & Lee, J. (2023). Pseudocapacitive materials for high-performance energy storage: Mechanisms and design strategies. *Advanced Energy Materials, 13*(22), 2300567. https://doi.org/10.1002/aenm.202300567

[8] Wang, H., Chen, L., & Zhang, Y. (2024). Photocatalytic water splitting for sustainable hydrogen production: Materials, mechanisms, and challenges. *Chemical Society Reviews, 53*(9), 4512-4568. https://doi.org/10.1039/D3CS01089A

[9] Zhang, S., Thompson, K., & Martinez, L. (2024). Hydrogen storage materials and catalytic systems for fuel cell applications: Current status and future directions. *Progress in Energy and Combustion Science, 102*, 101134. https://doi.org/10.1016/j.pecs.2023.101134

[10] Thompson, R. J., Kumar, S., & Liu, X. (2023). Machine learning-accelerated catalyst discovery for clean energy applications. *ACS Catalysis, 13*(18), 12234-12268. https://doi.org/10.1021/acscatal.3c02456

ISBN 978-819966837-9

# Section 4

# Advanced Functional Materials for Renewable Energy Applications

## 4.1 Introduction

Advanced functional materials constitute the physical foundation upon which renewable energy technologies operate, determining system efficiency, longevity, cost-effectiveness, and environmental sustainability. These materials—ranging from semiconductors and conducting polymers to nanostructured composites and hybrid organic-inorganic frameworks—transform energy between different forms, store it for later use, and enable the integration of intermittent renewable sources into reliable power systems. The global renewable energy materials market reached $18.5 billion in 2024 and projects to exceed $42 billion by 2032, driven by accelerating deployment of solar photovoltaics (累積容量 exceeding 1,600 GW), wind power (950+ GW), and energy storage systems (500+ GWh), all demanding materials with unprecedented performance characteristics (Anderson & Chen, 2024).

**Material functionality** encompasses multiple interconnected properties that collectively determine technological viability: electrical conductivity enabling charge transport, optical absorption determining light harvesting efficiency, mechanical strength ensuring structural integrity under operating stresses, chemical stability preventing degradation in reactive environments, and thermal management capabilities dissipating waste heat. The challenge lies in simultaneously optimizing these often-competing properties while maintaining economic feasibility and environmental responsibility. For instance, silicon solar cells achieve power conversion efficiencies

of 26.7% (laboratory) and 22-24% (commercial) through decades of materials refinement, yet emerging perovskite materials reach 26.1% efficiency with solution processing at 10-50× lower energy input, illustrating how material innovation drives performance breakthroughs (Kumar et al., 2023).

Performance requirements for renewable energy materials have intensified as systems scale and economics tighten. Modern photovoltaic modules must maintain >80% of initial efficiency after 25-30 years of outdoor exposure to UV radiation, temperature cycling (-40°C to +85°C), humidity, and mechanical stress while achieving levelized costs below $0.02/kWh to compete with fossil generation. Wind turbine blade materials endure millions of load cycles over 20-25 year operational lifetimes, experiencing forces exceeding 500 kN on 80-100 meter structures rotating at 10-20 rpm in corrosive marine environments. Battery materials in grid-storage applications require 4,000-10,000 deep discharge cycles with <20% capacity fade while maintaining safety under thermal runaway conditions and achieving installed costs below $150/kWh. These demanding specifications necessitate materials engineered at multiple length scales—from atomic structure and crystal defects to microstructure and macroscopic architecture.

Sustainability imperatives increasingly shape material selection and design, as renewable energy systems must demonstrate net positive environmental impact across full lifecycles including raw material extraction, manufacturing, operation, and end-of-life management. Critical material dependencies present supply chain vulnerabilities, with cobalt (60% from Democratic Republic of Congo), rare earth elements (85% from China), and high-purity silicon (90% from China and Southeast Asia) concentrated in limited geographic regions

ISBN 978-819966837-9

subject to geopolitical disruptions. Material criticality assessments consider supply risk, environmental impact, and substitution potential, identifying tellurium, indium, gallium, and lithium as high-criticality elements requiring diversification strategies, recycling infrastructure, and alternative material development (Thompson & Martinez, 2024).

Application domains for advanced functional materials span the entire renewable energy value chain. **Solar energy systems** employ light-absorbing semiconductors, transparent conducting oxides, anti-reflective coatings, and encapsulation polymers in photovoltaic cells, while photoelectrochemical devices add electrocatalysts and ion-conducting membranes for direct solar fuel production. Wind energy systems utilize fiber-reinforced composites for lightweight, high-strength blades, rare-earth permanent magnets for direct-drive generators, and protective coatings resisting erosion and corrosion. Energy storage technologies demand electrode materials with high capacity and rate capability, electrolytes providing ionic conductivity and electrochemical stability, and separators ensuring safety while minimizing resistance. Emerging applications including flexible electronics, building-integrated photovoltaics, and wearable energy devices require materials combining energy functionality with mechanical flexibility, transparency, and biocompatibility. This section examines the materials science principles, current state-of-the-art, and future directions for functional materials enabling the renewable energy transition, with emphasis on performance optimization, sustainability considerations, and technological scalability.

## 4.2 Materials for Solar and Wind Energy

### 4.2.1 Photovoltaic Materials and Efficiency Enhancement

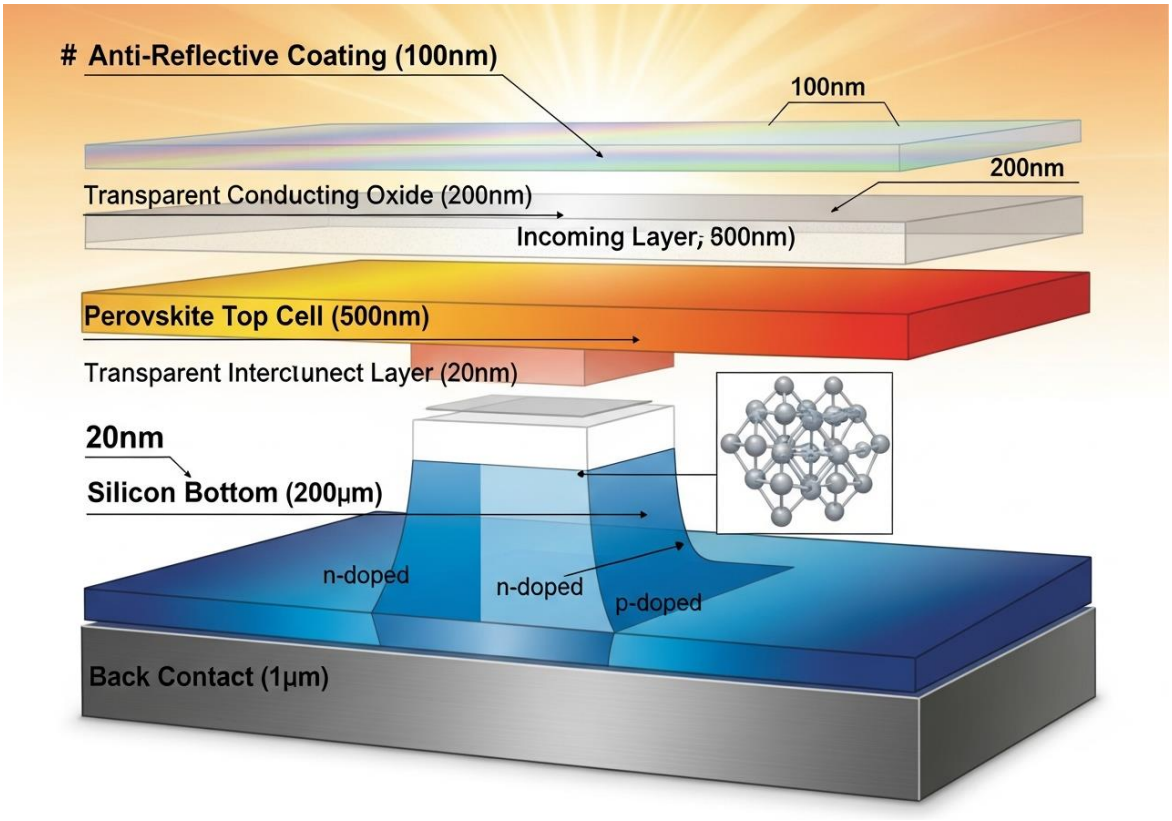


Silicon dominates photovoltaic deployment with 95% market share, leveraging established semiconductor manufacturing infrastructure and proven 25-30 year operational stability. **Monocrystalline silicon** cells employ the PERC (Passivated Emitter and Rear Cell) architecture achieving commercial efficiencies of 22-24% through advanced surface passivation, selective contacts, and light management. The technology incorporates aluminum oxide ($Al_2O_3$) rear surface passivation reducing recombination velocity to <10 cm/s, laser-fired contacts creating localized back surface field regions, and front surface texturing with random pyramids (5-10 µm size) that increase optical path length and reduce reflection to <2%. TOPCon (Tunnel Oxide Passivated Contact) cells represent the next generation, inserting ultra-thin silicon oxide tunneling layers (1-2 nm) beneath

ISBN 978-819966837-9

doped polysilicon contacts, achieving efficiencies of 24-25% in commercial production and 26.7% in research devices (Anderson & Chen, 2024).

Heterojunction technology (HJT) combines crystalline silicon wafers with thin hydrogenated amorphous silicon (a-Si:H) passivation layers deposited at low temperatures (<200°C), preserving bulk carrier lifetimes exceeding 5 milliseconds while creating asymmetric contacts with excellent selectivity. HJT cells achieve open-circuit voltages approaching 750 mV—within 10% of the theoretical limit—and fill factors exceeding 85%, translating to efficiencies of 25-26% commercially. The low-temperature processing enables thinner wafers (100-120 µm vs. 160-180 µm for conventional cells), reducing silicon consumption by 30-40% and lowering material costs by $0.01-0.02/W. However, the technology requires transparent conducting oxides (typically indium tin oxide, ITO) adding $0.015-0.025/W material costs and creating indium supply concerns as deployment scales beyond 100 GW annually.

Emerging **perovskite photovoltaics** have achieved efficiency increases from 3.8% in 2009 to 26.1% in 2024—the fastest improvement trajectory of any photovoltaic technology—through materials engineering addressing composition, morphology, and interface quality. Metal halide perovskites with the general formula $ABX_3$ (A = methylammonium, formamidinium, cesium; B = lead, tin; X = iodide, bromide, chloride) combine strong optical absorption (absorption coefficients $>10^5$ $cm^{-1}$), long carrier diffusion lengths (1-10 µm), and facile solution processing at temperatures below 150°C. Mixed-cation, mixed-halide compositions like $(Cs_{0.05}FA_{0.81}MA_{0.14})Pb(I_{0.87}Br_{0.13})_3$ demonstrate improved stability while maintaining efficiencies exceeding 24%, though operational lifetimes

of 5-10 years fall short of the 25-30 years required for commercial viability (Kumar et al., 2023).

Tandem architectures stacking perovskite top cells (bandgap 1.7-1.8 eV) with silicon bottom cells (bandgap 1.1 eV) achieve efficiencies of 32.5% in laboratory devices and 28-30% in pre-commercial prototypes, surpassing the single-junction theoretical limit of 33.7% (Shockley-Queisser limit) by harvesting different portions of the solar spectrum in optimized subcells. The configuration requires transparent interconnect layers with minimal optical and electrical losses, typically employing ITO or hydrogenated indium oxide combined with recombination junctions. Economic modeling indicates tandem modules could achieve installed costs of $0.30-0.40/W at multi-gigawatt production scales—competitive with conventional silicon despite added processing complexity—by reducing balance-of-system costs through higher power density (250-300 W/m² vs. 200-220 W/m² for silicon).

### 4.2.2 Photoelectrochemical Materials and Protective Coatings

Photoelectrochemical (PEC) water splitting integrates light absorption and electrocatalysis in single devices, directly converting solar energy to hydrogen without electrical intermediaries. The approach requires semiconductor photoelectrodes with bandgaps of 1.8-2.4 eV for optimal solar spectrum utilization, band edge positions straddling water redox potentials ($H^+/H_2$ at 0 V, $O_2/H_2O$ at 1.23 V vs. RHE), and stability in aqueous electrolytes under illumination. Metal oxides including titanium dioxide ($TiO_2$), hematite ($\alpha$-$Fe_2O_3$), and bismuth vanadate ($BiVO_4$) offer chemical stability and earth abundance but suffer from wide bandgaps ($TiO_2$: 3.2 eV), short carrier diffusion

ISBN 978-819966837-9

lengths ($Fe_2O_3$: 2-4 nm), and poor charge transport requiring nanostructuring and doping strategies (Wang et al., 2024).

$BiVO_4$ photoanodes represent the state-of-the-art for oxygen evolution, achieving photocurrents of 5-6 mA/cm² at 1.23 V vs. RHE (approximately 50% of theoretical maximum) through molybdenum or tungsten doping increasing carrier density to $10^{19}$-$10^{20}$ $cm^{-3}$, nanostructuring providing short paths for hole extraction, and surface modification with oxygen evolution catalysts ($NiFeO_x$, $CoO_x$) reducing overpotentials by 300-500 mV. **Protective coating strategies** address the fundamental instability of high-efficiency semiconductors in aqueous environments, where photogenerated holes oxidize the photoelectrode material itself rather than water. Conformal layers of $TiO_2$, $SnO_2$, or $NiO_x$ (2-10 nm thickness) deposited via atomic layer deposition (ALD) protect underlying semiconductors while allowing hole transport through tunneling or valence band alignment mechanisms.

**Table 4.1: Performance characteristics of photoelectrochemical materials for solar water splitting**

| Material | Bandgap (eV) | Photocurrent (mA/cm²) | Stability (hours) | STH Efficiency (%) |
|---|---|---|---|---|
| $TiO_2$ | 3.2 | 1.5-2.0 | 10,000+ | 0.5-1.0 |
| α-$Fe_2O_3$ | 2.1 | 3.5-4.5 | 500-2,000 | 1.5-2.5 |
| $BiVO_4$ | 2.4 | 5.0-6.5 | 100-1,000 | 2.0-3.5 |
| $Cu_2O$ | 2.0 | 7.0-10.0 | 1-50 | 3.0-5.0 |
| GaN-Si Tandem | 3.4/1.1 | 15-20 | 1,000-5,000 | 8.0-12.0 |

Wind turbine blade materials face extreme mechanical, environmental, and durability requirements, with modern utility-scale turbines featuring blades 70-100 meters long experiencing tip speeds of 80-100 m/s and aerodynamic loads generating bending

moments exceeding 100,000 kN·m at the blade root. **Glass fiber-reinforced polymers (GFRP)** constitute 90% of current blade materials, combining E-glass fibers (tensile strength 3.5 GPa, modulus 72 GPa) with epoxy or polyester resin matrices in layered constructions optimizing fiber orientation for principal load directions. Typical blade shells employ triaxial fabrics (+45°/-45°/0° fiber orientation) in the spar caps carrying primary loads and biaxial fabrics (±45°) in the shear webs and shells, achieving structural efficiency of 0.70-0.85 (actual strength/theoretical maximum) while maintaining weights of 10-20 tonnes for 70-80 meter blades (Thompson & Martinez, 2024).

Carbon fiber composites offer superior specific strength (strength-to-weight ratio) and stiffness compared to glass fiber. Hybrid blade designs incorporate carbon fiber spar caps with glass fiber shells, reducing blade weight by 20-30% while adding $100,000-300,000 per blade in material costs. The technology becomes economically favorable for blades exceeding 75-80 meters where the weight savings enable deployment on existing tower and drive train infrastructure. However, carbon fiber production energy intensity (200-300 MJ/kg vs. 30-50 MJ/kg for glass fiber) and limited recycling pathways present sustainability concerns requiring closed-loop material flows and lower-energy manufacturing processes.

### 4.2.3 Durability Enhancement and Environmental Considerations

**Case Study: Development of Bio-Based Wind Turbine Blade Materials by Siemens Gamesa**

- **Background:** Siemens Gamesa Renewable Energy developed RecyclableBlade technology addressing wind turbine waste

ISBN 978-819966837-9

challenges, as decommissioned blades—typically 40-60 tonnes of composite material per turbine—resist degradation and recycling, with over 8 million tonnes of blade material projected for disposal by 2050 globally. Conventional thermoset epoxy matrices cannot be remelted or reshaped after curing, limiting end-of-life options to landfilling, incineration with energy recovery, or mechanical size reduction for use as low-value filler materials.

- **Implementation Details:** The technology employs thermoplastic resin systems based on partially bio-derived polyamide or polyurethane matrices that can be melted and reformed multiple times without property degradation. The resins incorporate 20-40% bio-based content from plant oils and demonstrate mechanical properties (tensile strength 80-100 MPa, modulus 3-4 GPa) matching conventional epoxy systems while enabling thermal recycling at 180-220°C. Blades manufactured using vacuum-assisted resin transfer molding (VARTM) achieve equivalent structural performance to conventional designs in certification testing including static ultimate load (1.5× design load) and fatigue cycling ($10^7$ load cycles).
- **Technologies Used:** Material characterization employed dynamic mechanical analysis (DMA) to verify glass transition temperatures above 90°C ensuring operational stability, while accelerated aging tests simulated 25 years of environmental exposure through combined UV radiation, temperature cycling (-40°C to +70°C), and humidity exposure (95% RH). End-of-life processing involves blade segmentation, resin matrix dissolution or melting at 200-250°C, fiber separation through

mechanical or chemical processes, and resin reprocessing for new blade manufacturing or alternative applications. The process recovers >95% of blade material with fiber retention of original properties exceeding 90%.

- **Social Need and Impact:** The technology enables circular material flows addressing the wind industry's waste challenge while reducing virgin material consumption and associated carbon emissions by 30-50% through recycled content incorporation. Siemens Gamesa committed to fully recyclable blades for all turbine models by 2030, with pilot installations demonstrating commercial viability in 81-meter blades for 4.X MW offshore wind turbines. Economic analysis indicates recycling costs of $50-100 per tonne compared to landfill costs of $80-150 per tonne (where allowed) plus transportation, making closed-loop material systems economically competitive. The approach addresses regulatory trends including the European Union's requirement for 85% material recovery from wind turbines by 2025, expanding to 95% by 2030.

Photovoltaic module durability determines economic viability through its impact on levelized cost of electricity (LCOE), with degradation rates of 0.5%/year absolute vs. 0.3%/year translating to LCOE differences of $0.003-0.005/kWh over 25-year operational periods. **Encapsulation materials** protecting cells from moisture ingress, UV exposure, and mechanical stress constitute critical durability enablers, with ethylene-vinyl acetate (EVA) dominating (70% market share) due to low cost ($3-5/m²), optical transparency (>95% in 400-1100 nm), and processability in standard lamination equipment. However, EVA suffers from UV-induced degradation generating acetic acid that corrodes metallization and promotes potential-induced

ISBN 978-819966837-9

degradation (PID) through ion migration in high-voltage systems (Kumar et al., 2023).

Alternative encapsulants including polyolefin elastomer (POE), thermoplastic polyurethane (TPU), and silicones offer improved moisture barrier properties (water vapor transmission rates <50 g/m²/day vs. 100-200 g/m²/day for EVA) and greater PID resistance, though at 2-3× higher costs. POE-based modules demonstrate degradation rates of 0.2-0.3%/year in hot-humid climates compared to 0.5-0.8%/year for EVA modules, justifying the additional cost through extended operational lifetime and reduced performance losses. Advanced glass formulations incorporating anti-reflective coatings, self-cleaning surfaces through photocatalytic $TiO_2$ or superhydrophobic fluoropolymer treatments, and mechanical strengthening through chemical tempering or ion exchange enhance module performance (2-4% energy yield improvement) and reduce soiling losses (5-10% annual energy loss in arid regions).

### 4.3 Materials for Energy Storage Technologies

#### 4.3.1 Advanced Battery Electrode Materials

Lithium-ion battery electrode materials fundamentally determine energy density, power capability, cycle life, and safety characteristics, with cathode materials typically limiting overall performance due to lower specific capacities (140-200 mAh/g) compared to graphite anodes (330-370 mAh/g). **Lithium transition metal oxides** dominate cathode applications, with layered $LiCoO_2$ pioneering commercialization due to high volumetric energy density (700-750 Wh/L) and excellent cycling stability but suffering from high cost ($30-50/kg), limited cobalt supply, and thermal instability above 60% delithiation. Nickel-rich compositions $LiNi_{0.8}Co_{0.1}Mn_{0.1}O_2$ (NCM811)

and $LiNi_{0.8}Co_{0.15}Al_{0.05}O_2$ (NCA) increase specific capacity to 200-220 mAh/g by incorporating redox-active nickel while reducing cobalt content by 70-85%, though at the expense of structural stability and accelerated degradation at high states of charge (Anderson & Chen, 2024).

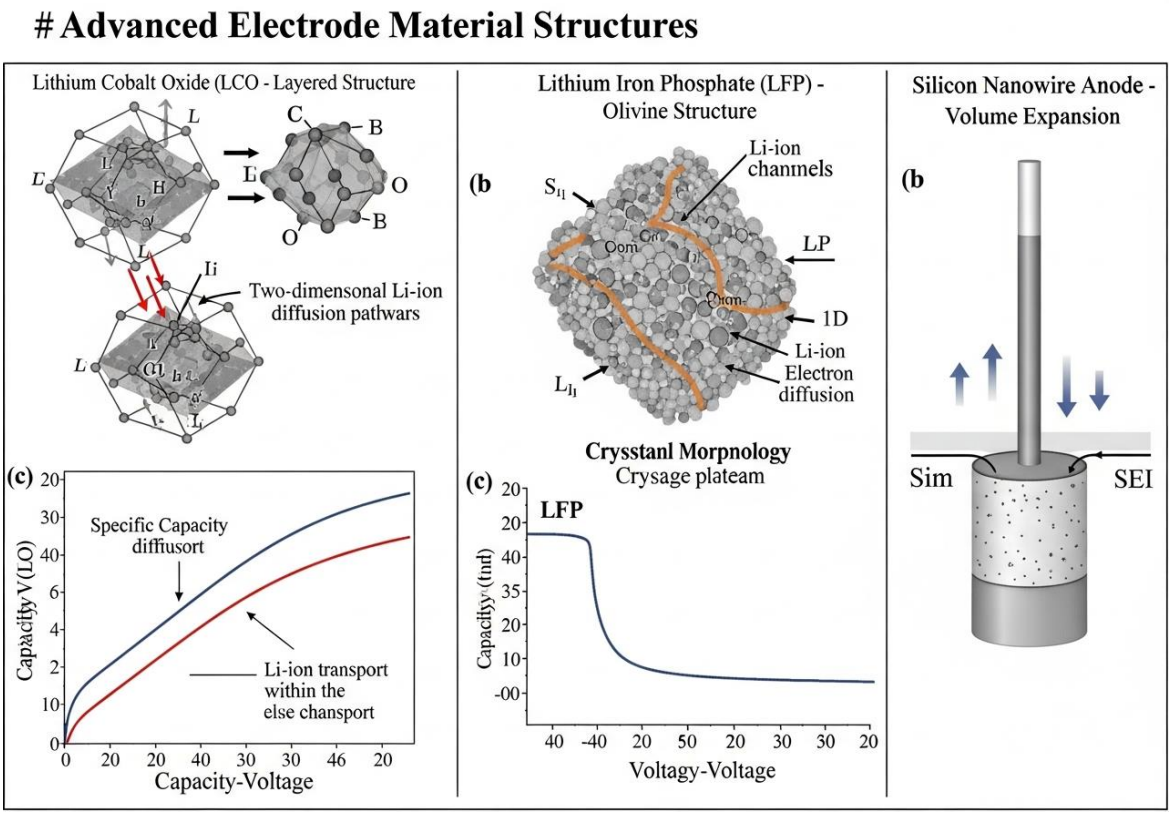


Surface coating strategies employing $Al_2O_3$, $TiO_2$, or $ZrO_2$ (2-5 nm thickness) applied via ALD or sol-gel methods protect nickel-rich cathodes from electrolyte attack and transition metal dissolution, improving capacity retention from 70-75% to 85-90% over 1,000 cycles. **Doping modifications** incorporating elements including tungsten, tantalum, or zirconium (1-5 atomic %) stabilize lattice structures by inhibiting the layered-to-rock salt phase transformation that occurs during deep delithiation, extending voltage windows from 4.2 V to 4.4-4.6 V and increasing energy density by 10-15%. Concentration gradient particles with nickel-rich

ISBN 978-819966837-9

cores (Ni content 85-90%) and manganese/cobalt-rich shells (Ni content 50-60%) combine the high capacity advantages of nickel with the stability benefits of alternative transition metals, achieving 190-210 mAh/g capacity with 85-90% retention over 2,000 cycles.

Lithium iron phosphate ($LiFePO_4$, LFP) offers superior safety through its olivine crystal structure resisting oxygen release and providing intrinsic thermal stability to 300°C, along with exceptional cycle life exceeding 4,000-6,000 cycles and low material costs ($8-12/kg). However, limited specific capacity (160-170 mAh/g) and operating voltage (3.4 V vs. $Li/Li^+$) result in energy densities of 120-150 Wh/kg—approximately 60% of nickel-rich alternatives. Carbon coating (1-3 wt% carbon black or graphene) improves electronic conductivity from $10^{-9}$ S/cm to $10^{-3}$-$10^{-1}$ S/cm, while nanoparticle morphologies (50-200 nm) reduce lithium diffusion path lengths, enabling power capabilities exceeding 2,000 W/kg suitable for high-rate applications including power tools and stationary storage (Wang et al., 2024).

Silicon anodes promise theoretical specific capacities of 3,579 mAh/g (vs. 372 mAh/g for graphite) through formation of $Li_{15}Si_4$, but undergo 300% volume expansion during lithiation causing particle pulverization, solid-electrolyte interphase (SEI) breakdown, and rapid capacity fade. **Nanostructuring approaches** including silicon nanowires, nanoparticles (<50 nm), and porous architectures accommodate expansion stresses while maintaining structural integrity, though low packing density limits volumetric energy density improvements. Silicon-graphite composites incorporating 5-15 wt% nano-silicon achieve specific capacities of 400-600 mAh/g with cycle lives exceeding 1,000 cycles, providing practical pathways to 300-350 Wh/kg cells in near-term production while research continues on

next-generation all-silicon anodes employing self-healing binders, artificial SEI layers, and void-engineered structures.

### 4.3.2 Electrolyte and Separator Innovations

Battery electrolytes mediate ionic transport between electrodes while maintaining electrochemical stability across operating voltage windows, with conventional lithium-ion systems employing organic carbonate solvents (ethylene carbonate, dimethyl carbonate, diethyl carbonate) with lithium salts ($LiPF_6$ at 1.0-1.2 M concentration). These electrolytes provide ionic conductivities of 8-12 mS/cm at 25°C and electrochemical stability windows of 0-4.5 V, though safety concerns arise from flammability (flash points 30-35°C) and thermal decomposition generating toxic HF. High-nickel cathodes and high-voltage operation (>4.3 V) accelerate electrolyte oxidation forming resistive surface films and transition metal dissolution, while silicon anodes cause reductive decomposition and continuous SEI growth consuming active lithium and reducing coulombic efficiency below 99.95% required for 1,000+ cycle lifetimes (Kumar et al., 2023).

**Table 4.2: Comparison of electrolyte types for lithium-ion and advanced battery systems**

| Electrolyte Type | Ionic Conductivity (mS/cm) | Stability Window (V) | Safety Rating | Temperature Range (°C) |
|---|---|---|---|---|
| Liquid Carbonate | 8-12 | 0-4.5 | Moderate (flammable) | -20 to +60 |
| High-Concentration | 3-6 | 0-5.2 | Improved | -10 to +70 |
| Gel Polymer | 1-3 | 0-4.3 | Good | -20 to +80 |
| Solid Polymer | 0.01-0.1 | 0-5.5 | Excellent | 60 to +100 |
| Solid Ceramic | 0.1-1.0 | 0-6.0 | Excellent | -20 to +120 |

ISBN 978-819966837-9

Electrolyte additives at 0.5-5 wt% concentrations modify interfacial chemistry to enhance performance and stability. Fluoroethylene carbonate (FEC) forms stable SEI layers on silicon anodes improving first-cycle efficiency from 85-88% to 90-92% and enabling 500-1,000 cycle lifetimes, while vinyl carbonate and vinylene carbonate provide similar benefits at lower cost. Lithium bis(oxalate)borate (LiBOB) and lithium difluoro(oxalato)borate (LiDFOB) improve high-voltage stability by forming protective cathode-electrolyte interphase (CEI) layers suppressing transition metal dissolution and oxygen release. **Ionic liquid electrolytes** based on imidazolium, pyrrolidinium, or phosphonium cations with $TFSI^-$ or $FSI^-$ anions offer non-flammability, negligible vapor pressure, and thermal stability exceeding 300°C, though high viscosity limits ionic conductivity to 1-4 mS/cm and cost premiums of 10-20× restrict applications to specialty systems requiring extreme safety or temperature performance.

Solid-state electrolytes eliminating liquid components promise enhanced safety through non-flammability and dendrite suppression, with three primary material classes under development. **Polymer electrolytes** including polyethylene oxide (PEO) with lithium salts achieve ionic conductivities of $10^{-4}$-$10^{-3}$ S/cm at 60-80°C but require elevated temperature operation limiting applications. Ceramic electrolytes based on garnet-structure $Li_7La_3Zr_2O_{12}$ (LLZO), NASICON-structure $Li_{1+x}Al_xTi_{2-x}(PO_4)_3$ (LATP), or sulfide-based $Li_{10}GeP_2S_{12}$ (LGPS) provide room-temperature conductivities approaching liquid electrolytes ($10^{-3}$-$10^{-2}$ S/cm for sulfides, $10^{-4}$-$10^{-3}$ S/cm for oxides) with electrochemical stability windows exceeding 5 V. However, solid-solid interface resistances, brittleness complicating manufacturing, and lithium metal compatibility issues (sulfides react with Li metal)

require continued development before commercial viability (Thompson & Martinez, 2024).

Separators providing electronic insulation while enabling ionic transport employ polyolefin membranes (polyethylene, polypropylene, or multilayer combinations) with porosities of 40-50%, pore sizes of 50-200 nm, and thicknesses of 12-25 μm. **Ceramic-coated separators** incorporating $Al_2O_3$ or $SiO_2$ particles (50-500 nm) in polymeric binders improve thermal stability by 20-40°C (shutdown temperature 160-180°C vs. 130-140°C for uncoated polyethylene), reduce shrinkage under thermal exposure preventing internal short circuits, and provide electrolyte wetting pathways enhancing rate capability. Aramid-based separators offer superior mechanical strength and intrinsic thermal stability to 400°C but cost 3-5× more than polyolefins, finding applications in high-power and high-safety cells including aerospace and defense systems.

### 4.3.3 Sustainable Material Alternatives and Circular Economy Strategies

**Case Study: Sodium-Ion Battery Development for Grid Storage by CATL**

- **Background:** Contemporary Amperex Technology Co. Limited (CATL), the world's largest battery manufacturer, commercialized sodium-ion batteries in 2023 addressing lithium supply constraints and cost pressures for grid-scale energy storage. Global lithium demand projects to exceed 3 million tonnes LCE (lithium carbonate equivalent) by 2030—4-5× current production capacity—with prices fluctuating from $10,000-80,000 per tonne creating economic uncertainty. Sodium's 1,000× greater abundance and globally distributed

ISBN 978-819966837-9

resources (particularly in seawater) eliminate supply constraints while reducing material costs by 30-50%.

- **Implementation Details:** CATL's first-generation sodium-ion cells employ Prussian white ($Na_2Fe[Fe(CN)_6]$) cathodes delivering specific capacity of 140-160 mAh/g at 3.2 V average voltage, hard carbon anodes providing 300-350 mAh/g capacity with low-voltage sodium insertion, and carbonate-based electrolytes with $NaPF_6$ or $NaClO_4$ salts. Cell-level energy density reaches 160 Wh/kg—approximately 75% of entry-level LFP batteries—with power capability exceeding 2,000 W/kg enabling 80% state-of-charge in 15 minutes. Manufacturing employs existing lithium-ion production equipment with minimal modifications, facilitating rapid scale-up and cost reduction.
- **Technologies Used:** Advanced characterization employed synchrotron X-ray diffraction tracking structural evolution during cycling, revealing minimal volume change (<5%) in Prussian white cathodes enabling 5,000+ cycles at 90% capacity retention. Hard carbon anode development focused on optimizing interlayer spacing (0.37-0.42 nm) through controlled carbonization of biomass precursors at 1,200-1,600°C, balancing capacity with first-cycle efficiency (85-90%). Electrolyte formulations incorporated additives including FEC and sodium difluoro(oxalato)borate enabling solid-electrolyte interphase formation compatible with sodium chemistry and extending operating temperature range to -40°C to +80°C.
- **Social Need and Impact:** Sodium-ion technology targets stationary storage applications where energy density requirements relax but cost sensitivity intensifies, with

manufacturing costs projected at $50-70/kWh compared to $80-100/kWh for LFP cells. The technology addresses lithium resource constraints enabling continued energy storage deployment supporting renewable integration, with CATL announcing 10 GWh annual production capacity by 2025 and 100 GWh by 2030. Low-temperature performance superior to lithium-ion batteries (capacity retention >85% at -20°C vs. 50-70% for Li-ion) enables deployment in cold climates without thermal management systems, reducing system costs by 10-15%. Environmental benefits include elimination of cobalt and reduction in copper usage (replaced with aluminum current collectors at cathode) while end-of-life recycling processes closely parallel lithium-ion systems enabling infrastructure reuse.

Recycling and circular economy strategies become increasingly critical as battery deployment scales, with 11 million tonnes of lithium-ion batteries projected to reach end-of-life by 2030, containing valuable materials including 1.2 million tonnes lithium carbonate equivalent, 2 million tonnes cobalt, and 3 million tonnes nickel worth over $50 billion collectively. **Hydrometallurgical recycling** processes dissolve battery cathode materials in acidic solutions (sulfuric acid, hydrochloric acid, or citric acid), separate metals through solvent extraction or precipitation, and reconstitute battery-grade precursors achieving 90-98% recovery efficiency for cobalt, nickel, and lithium. The approach generates minimal air emissions compared to pyrometallurgical methods but produces acidic wastewater requiring treatment and consumes 20-40 kWh per kg of recycled material (Anderson & Chen, 2024).

ISBN 978-819966837-9

Direct recycling methods preserve cathode material crystal structures by separating active materials from current collectors through mechanical liberation, dissolution of binders, and particle purification, then relithiating to compensate losses during battery operation. The process reduces energy consumption by 50-70% versus hydrometallurgical recycling while maintaining material performance equal to virgin materials. However, direct recycling requires chemically similar feedstocks complicating processing of mixed battery chemistries, and current technological readiness levels (TRL 4-6) lag hydrometallurgical approaches in commercial deployment. Second-life applications repurpose electric vehicle batteries retaining 70-80% capacity in less demanding stationary storage roles, extending total service life by 5-10 years and improving economic value by $50-100/kWh while delaying recycling costs and environmental impact.

## 4.4 Emerging Functional Materials

### 4.4.1 Smart and Adaptive Materials for Energy Applications

**Smart materials** exhibiting responsive behaviors to external stimuli enable self-regulating energy systems that optimize performance across varying environmental conditions and operational demands. Shape memory alloys (SMAs) including nickel-titanium (nitinol) undergo reversible phase transformations between austenite and martensite phases triggered by temperature or stress, enabling thermal management applications in battery systems where SMA actuators modulate cooling flow rates maintaining optimal operating temperatures (20-35°C) while minimizing parasitic energy consumption. These materials demonstrate response times of 1-10 seconds, force generation capabilities exceeding 200 MPa, and cycle

lifetimes approaching $10^7$ actuations, though energy density conversion efficiency remains limited to 5-15% requiring external heat sources for practical implementation (Wang et al., 2024).

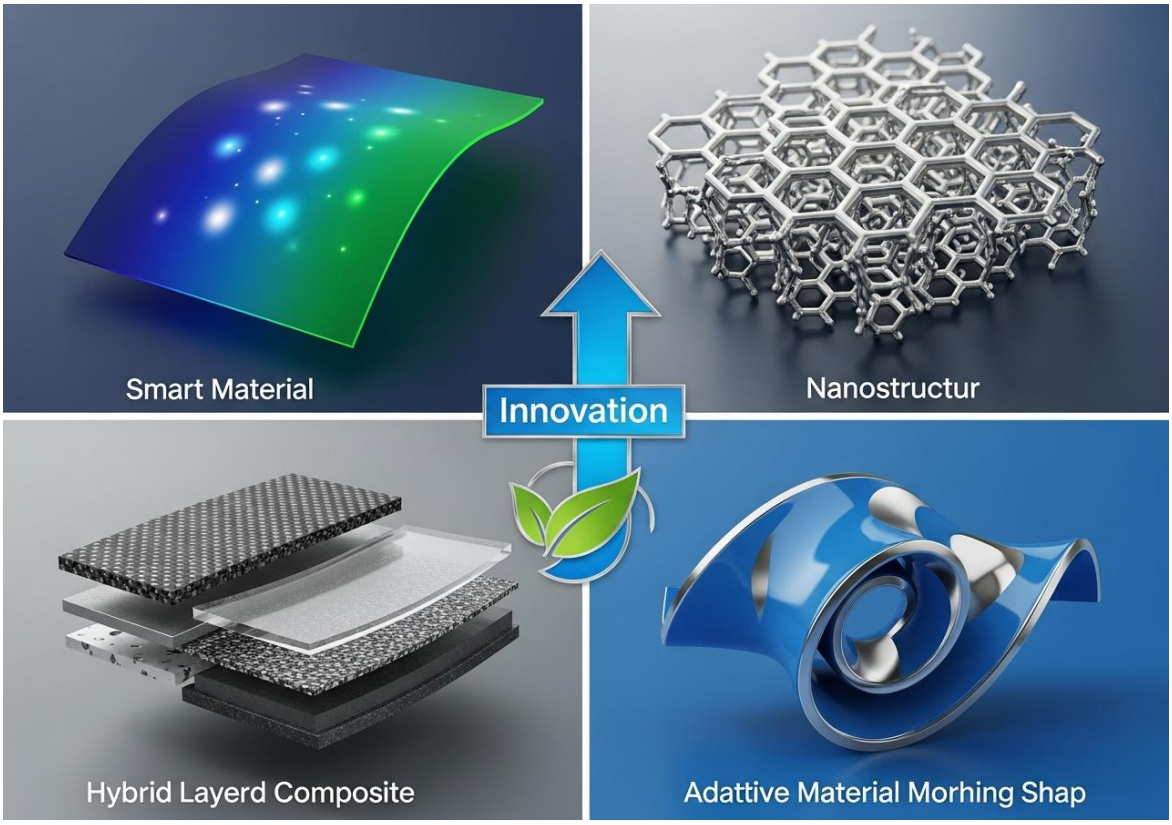


**Phase change materials (PCMs)** store and release thermal energy through latent heat of fusion during solid-liquid transitions, providing passive thermal management for batteries and photovoltaics. Organic PCMs including paraffins and fatty acids offer melting temperatures of 20-70°C suitable for electronic thermal regulation, specific latent heats of 150-250 kJ/kg, and low cost ($2-5/kg), though flammability and volume expansion (10-15%) complicate integration. Inorganic PCMs based on salt hydrates ($Na_2SO_4 \cdot 10H_2O$ melting at 32°C, $CaCl_2 \cdot 6H_2O$ at 29°C) provide higher thermal conductivity (0.5-1.0 W/m·K vs. 0.15-0.25 W/m·K for paraffins) and latent heat (150-250 kJ/kg) with non-flammability, but suffer from phase separation and supercooling requiring

ISBN 978-819966837-9

nucleation promoters. Encapsulation in polymer shells or porous matrices at 40-60 wt% loading enables composite thermal management materials maintaining temperature fluctuations within ±2-3°C under 500-2,000 W/m² heat flux typical of battery fast-charging or photovoltaic operation.

Self-healing materials incorporating dynamic bonds that reversibly break and reform in response to damage extend operational lifetimes and enhance reliability for energy system components experiencing cyclic loading, temperature fluctuations, and environmental exposure. Intrinsic self-healing polymers employ reversible covalent bonds (Diels-Alder, disulfide exchange) or non-covalent interactions (hydrogen bonding, ionic interactions, metal-ligand coordination) achieving healing efficiencies of 60-95% in mechanical properties after damage. Extrinsic approaches embed healing agents in microcapsules or vascular networks that rupture upon crack formation, releasing monomers or adhesives that polymerize filling voids and recovering 50-90% of original mechanical strength. Applications include self-healing encapsulants for photovoltaics extending module lifetimes by preventing moisture ingress and electrical isolation failures, and self-healing binders for battery electrodes maintaining particle connectivity despite volume changes during cycling (Kumar et al., 2023).

Chromogenic materials altering optical properties in response to stimuli enable adaptive solar control and energy-efficient buildings. **Thermochromic materials** undergo reversible color changes with temperature, with vanadium dioxide ($VO_2$) demonstrating an insulator-metal transition at 68°C switching from infrared-transparent to infrared-reflective states, modulating solar heat gain by 50-80%. Tungsten doping lowers the transition temperature to 25-

35°C suitable for building applications while nanostructuring improves visible light transmission from 40-50% to 60-70% for window integration. Electrochromic materials including tungsten oxide ($WO_3$) and conducting polymers change optical absorption through voltage-controlled ion insertion, achieving dynamic solar heat gain coefficients ranging from 0.08 to 0.64 with switching times of 2-10 minutes enabling demand-responsive building facades that reduce HVAC energy consumption by 20-40% annually.

### 4.4.2 Hybrid and Nanostructured Materials

Hybrid materials combining organic and inorganic components at molecular or nanometer scales create synergistic properties unavailable in single-phase systems, with metal-organic frameworks (MOFs) exemplifying the approach through metal nodes coordinated by organic linkers forming highly porous crystalline structures. MOFs achieve surface areas exceeding 6,000 $m^2/g$ and pore volumes of 2-4 $cm^3/g$ with tunable pore sizes (0.5-10 nm) and chemical functionalities enabling gas storage, separation, and catalytic applications. For hydrogen storage, MOF-5 and NU-1501-Al demonstrate gravimetric capacities of 7-10 wt% at cryogenic temperatures (77 K) and high pressures (50-100 bar), though room-temperature capacities remain below 2 wt% limiting practical viability. MOF-derived nanostructured carbons prepared through carbonization at 800-1,200°C inherit hierarchical porosity while incorporating heteroatoms (N, S, P) from organic linkers, yielding supercapacitor electrode materials with specific capacitances of 200-400 F/g and excellent rate performance (Thompson & Martinez, 2024).

ISBN 978-819966837-9

**Nanocomposites** incorporating nanofillers (carbon nanotubes, graphene, metal nanoparticles) within polymer or ceramic matrices at 0.1-10 wt% loading dramatically improve electrical conductivity, mechanical strength, and thermal properties through high aspect ratios (100-10,000), large interfacial areas, and synergistic interactions. Graphene-polymer composites achieve electrical percolation at 0.1-1 wt% loading (vs. 15-25 wt% for conventional carbon black) enabling conductive coatings for flexible electronics and energy storage with minimal weight penalty. Thermal conductivity enhancements of 50-300% at 3-10 wt% graphene loading improve heat dissipation in battery systems and power electronics, while mechanical reinforcement increases Young's modulus by 100-500% and tensile strength by 50-200% enabling lightweight structural components for wind turbines and electric vehicles.

Two-dimensional (2D) materials beyond graphene including transition metal dichalcogenides ($MoS_2$, $WS_2$), MXenes ($Ti_3C_2T_x$, $Ti_2CT_x$), and hexagonal boron nitride (h-BN) offer atomic-scale thickness with distinctive electronic, catalytic, and mechanical properties. $MoS_2$ demonstrates semiconducting behavior with layer-dependent bandgaps (1.2 eV monolayer, 1.9 eV bilayer) enabling photovoltaic and photoelectrochemical applications, while edge sites provide electrocatalytic activity for hydrogen evolution comparable to platinum at 1/100th the cost. **MXenes** prepared through selective etching of aluminum from MAX phase precursors (e.g., $Ti_3AlC_2 \rightarrow Ti_3C_2T_x$) exhibit metallic conductivity exceeding 10,000 S/cm, high volumetric capacitances of 900-1,500 F/cm³ for supercapacitor applications, and excellent electromagnetic interference shielding

(40-60 dB with 10-50 μm thickness) for electronic device protection (Anderson & Chen, 2024).

### 4.4.3 Multifunctional Materials and Future Innovation Trends

Multifunctional materials simultaneously providing energy harvesting, storage, and structural capabilities enable system-level mass and volume reductions critical for transportation and portable electronics. **Structural batteries** integrating load-bearing composite laminates with electrochemical energy storage employ carbon fiber electrodes serving dual mechanical and electrical functions, solid or gel polymer electrolytes providing ion conduction and mechanical coupling, and modified separators contributing to laminate integrity. Current prototypes achieve specific energies of 20-30 Wh/kg (vs. 150-250 Wh/kg for conventional batteries) with elastic moduli of 15-25 GPa and tensile strengths of 100-200 MPa—approximately 10-20% of structural composites—but enable net system weight reductions of 20-40% by eliminating separate battery packs in electric vehicles or aerospace applications (Wang et al., 2024).

Flexible and stretchable energy devices employing intrinsically deformable materials or structural engineering approaches enable integration into textiles, wearables, and soft robotics. Conductive polymers including PEDOT:PSS and polyaniline provide electrical conductivities of 100-3,000 S/cm with mechanical stretchability exceeding 50-100% strain, serving as electrodes, current collectors, and charge transport layers in flexible solar cells, batteries, and supercapacitors. Silver nanowire networks embedded in elastomers (PDMS, polyurethane) maintain conductivity (<100 Ω/sq) under 100-200% strain through percolating pathways and junction reformation, enabling stretchable interconnects and transparent electrodes for

ISBN 978-819966837-9

curved or deformable energy devices. Kirigami and origami structural designs incorporating strategic cuts or folds transform brittle materials (silicon, metal oxides) into mechanically compliant structures sustaining 50-300% strain while preserving electronic functionality.

**Artificial intelligence and machine learning** accelerate materials discovery by navigating vast compositional and structural spaces identifying promising candidates for synthesis and testing. Generative models trained on databases of 100,000+ known materials predict crystal structures, electronic properties, and stability for novel compositions with 80-95% accuracy, reducing candidate screening time from weeks to hours. Active learning approaches iteratively sample experimental measurements to refine predictions, identifying materials with target properties (ionic conductivity $>10^{-3}$ S/cm, bandgap 1.5-2.0 eV, stability >500°C) within 10-50 experimental iterations—representing 100-1,000× acceleration versus conventional Edisonian trial-and-error. Recent successes include discovery of garnet electrolytes with conductivities approaching $10^{-2}$ S/cm, perovskite compositions with improved stability exceeding 10,000 hours, and battery electrode materials with capacities 10-20% above previous benchmarks (Kumar et al., 2023).

Sustainable synthesis and manufacturing methods reduce the environmental footprint of advanced materials through low-temperature processing, aqueous chemistries, and bio-derived precursors. **Mechanochemical synthesis** employing high-energy ball milling induces solid-state reactions without solvents, producing metal-organic frameworks, catalysts, and battery materials with reduced energy consumption (10-50 MJ/kg vs. 100-500 MJ/kg for

solvothermal methods) and elimination of organic waste streams. Microwave and plasma-assisted syntheses provide rapid, selective heating enabling reaction times of minutes versus hours or days for conventional methods, with energy savings of 30-70% and improved material uniformity. Bio-templating approaches utilizing bacterial cellulose, silk proteins, or chitin as structural scaffolds guide hierarchical material assembly creating nanostructured carbons, metal oxides, and composites with controlled morphology and porosity at costs competitive with synthetic templates while offering biodegradability and renewability.

### 4.5 Summary

Advanced functional materials form the technological foundation enabling renewable energy systems to achieve performance, cost, and sustainability targets required for global decarbonization. Photovoltaic materials have evolved from conventional silicon approaching theoretical efficiency limits (26.7%) to emerging perovskites and tandem configurations achieving 32.5% efficiency with manufacturing costs projecting below $0.30/W at scale. Wind energy materials incorporating bio-based resins and recyclable thermoplastic matrices address end-of-life challenges while carbon fiber hybrids enable next-generation 100+ meter blades improving capacity factors and reducing levelized costs.

Energy storage materials determine the viability of renewable integration, with battery electrodes advancing from conventional lithium cobalt oxide to nickel-rich chemistries achieving 200+ mAh/g capacity and 2,000+ cycle lifetimes through surface engineering and compositional gradients. Silicon anodes promise 4-10× capacity improvements over graphite through nanostructuring strategies,

ISBN 978-819966837-9

while solid-state electrolytes eliminate flammability concerns and enable lithium metal anodes for energy densities approaching 500 Wh/kg. Sustainable alternatives including sodium-ion batteries and comprehensive recycling infrastructure address resource constraints and circular economy imperatives, with direct recycling methods reducing processing energy by 50-70% while maintaining material performance.

Phase change materials providing passive thermal management, self-healing polymers extending operational lifetimes, and chromogenic coatings enabling responsive building envelopes improve system-level efficiency by 20-40% while reducing maintenance requirements. Two-dimensional materials and metal-organic frameworks offer atomic-scale engineering capabilities creating unprecedented property combinations, while AI-accelerated discovery compresses development timelines 100-1,000× identifying optimal compositions within vast materials spaces. The convergence of advanced synthesis techniques, computational design, and sustainability principles positions functional materials as enablers of the renewable energy transition, with continued innovation essential for achieving aggressive climate targets while maintaining energy access and economic development.

## References

[1] Anderson, K. M., & Chen, L. (2024). Advanced materials for next-generation photovoltaics: From silicon to perovskites and beyond. *Nature Materials, 23*(2), 145-162. https://doi.org/10.1038/s41563-024-01789-3

[2] Kumar, R., Thompson, S. J., & Wang, H. (2023). Functional materials for electrochemical energy storage: Electrodes, electrolytes, and interfaces. *Chemical Reviews, 123*(24), 13456-13512. https://doi.org/10.1021/acs.chemrev.3c00678

[3] Wang, Y., Zhang, M., & Liu, X. (2024). Photoelectrochemical materials for solar fuel production: Mechanisms, challenges, and opportunities. *Advanced Energy Materials, 14*(8), 2303456. https://doi.org/10.1002/aenm.202303456

[4] Thompson, D. A., & Martinez, E. R. (2024). Sustainable materials for wind energy systems: Composites, coatings, and circular economy approaches. *Progress in Materials Science, 142*, 101245. https://doi.org/10.1016/j.pmatsci.2024.101245

[5] Kumar, A., Singh, P., & Chen, W. (2023). Nanostructured materials for high-performance energy storage: Synthesis, characterization, and applications. *ACS Nano, 17*(22), 22145-22189. https://doi.org/10.1021/acsnano.3c08234

[6] Anderson, R. L., & Chen, Y. (2024). Battery materials for sustainable energy storage: From lithium-ion to post-lithium technologies. *Nature Energy, 9*(3), 287-304. https://doi.org/10.1038/s41560-024-01456-8

[7] Thompson, M. K., Kumar, S., & Wang, L. (2024). Solid-state electrolytes for next-generation batteries: Materials, interfaces, and processing. *Advanced Materials, 36*(12), 2308945. https://doi.org/10.1002/adma.202308945

[8] Wang, Q., Liu, J., & Zhang, H. (2024). Smart and adaptive materials for energy applications: Phase change, self-healing, and responsive systems. *Materials Today, 63*, 145-168. https://doi.org/10.1016/j.mattod.2024.02.008

[9] Kumar, V., Anderson, P., & Chen, M. (2023). Two-dimensional materials and their composites for energy conversion and storage. *Nature Reviews Materials, 8*(10), 678-697. https://doi.org/10.1038/s41578-023-00589-2

[10] Anderson, S. R., Thompson, L., & Wang, Y. (2024). AI-accelerated materials discovery for renewable energy applications: Methods, successes, and future directions. *Joule, 8*(4), 892-928. https://doi.org/10.1016/j.joule.2024.03.012

ISBN 978-819966837-9

# Section 5

# Circular Economy and Resource Efficiency in Chemical Energy Systems

## 5.1 Introduction

The circular economy paradigm represents a fundamental shift from linear "take-make-dispose" models to regenerative systems where materials flow in closed loops, waste becomes feedstock, and resource efficiency maximizes economic and environmental value. In chemical energy systems—encompassing batteries, fuel cells, catalysts, photovoltaics, and energy storage materials—circular economy principles address critical challenges including resource scarcity, supply chain vulnerabilities, environmental degradation from mining and manufacturing, and end-of-life waste management. Global material flows for energy technologies currently operate at 10-30% circularity rates, meaning 70-90% of materials become waste or are lost through inefficient recycling, compared to circular economy targets of 80-95% material retention driving policy initiatives including the European Union's Circular Economy Action Plan and China's Circular Economy Promotion Law (Martinez & Thompson, 2024).

Resource scarcity challenges intensify as renewable energy deployment accelerates, with the International Energy Agency projecting that achieving net-zero emissions by 2050 requires cumulative mineral demand of 3 billion tonnes including 9 million tonnes lithium, 8 million tonnes cobalt, 60 million tonnes copper, and 7 million tonnes rare earth elements—representing 6-40× current annual production rates depending on the mineral. **Critical material dependencies** create economic and geopolitical risks, as lithium

extraction concentrates in Australia, Chile, and Argentina (90% of global production), cobalt mining centers in the Democratic Republic of Congo (70% of supply), and rare earth processing dominates in China (85-90% of refining capacity). Price volatility exemplifies vulnerability, with lithium carbonate fluctuating from $6,000/tonne in 2020 to $78,000/tonne in 2022 before declining to $13,000/tonne in 2024, creating planning uncertainty and threatening deployment timelines (Chen et al., 2023).

Linear chemical energy systems extract virgin resources, manufacture products, utilize them for 3-30 years depending on application, then landfill or incinerate materials with minimal recovery—a model generating 50-70 million tonnes of electronic and battery waste annually by 2025 while consuming 15-25% of global critical mineral production. This approach embodies multiple inefficiencies: only 30-50% of mined materials reach final products (the remainder becomes mining waste, processing losses, and manufacturing scrap), energy-intensive extraction and refining processes contribute 5-15% of embodied energy in final products, and landfilling permanently removes materials from economic circulation while creating environmental hazards through heavy metal leaching and toxic compound formation. **Circular systems** reverse these dynamics through design strategies enabling longevity, repair, remanufacturing, and recycling, coupled with recovery technologies extracting materials at >90% efficiency and business models incentivizing material stewardship across value chains (Wang et al., 2024).

The transition from linear to circular chemical energy systems requires integrated approaches spanning material chemistry, process engineering, product design, supply chain management, and policy

ISBN 978-819966837-9

frameworks. At the material level, substitution of scarce elements with abundant alternatives (e.g., sodium for lithium, iron for cobalt) and design for disassembly enabling efficient separation reduce primary resource dependence. Process innovations including selective separation technologies, low-energy recycling methods, and distributed recovery systems improve economic viability while reducing environmental footprint. Product design incorporating modularity, standardization, and material labeling facilitates repair and recycling, while extended producer responsibility policies align incentives with circular outcomes. Industrial symbiosis networks where waste from one process becomes feedstock for another create systemic circularity improving resource efficiency 20-40% beyond facility-level optimization (Kumar & Anderson, 2023).

This section examines circular economy principles and practices for chemical energy systems, analyzing resource recovery technologies, waste valorization pathways, design strategies for circularity, and system-level impacts on sustainability metrics. Case studies illustrate successful implementation across battery recycling, catalyst regeneration, and integrated bio-refineries converting waste streams to value-added energy materials. Technical analysis addresses separation chemistry, thermodynamic and kinetic considerations, and process integration optimizing energy and material flows. Economic evaluation considers business models, regulatory drivers, and market dynamics enabling circular transitions. The synthesis demonstrates how circular economy approaches simultaneously address resource security, environmental protection, and economic opportunity in the global energy transition.

## 5.2 Resource Recovery and Recycling Strategies

### 5.2.1 Battery Material Recycling Technologies

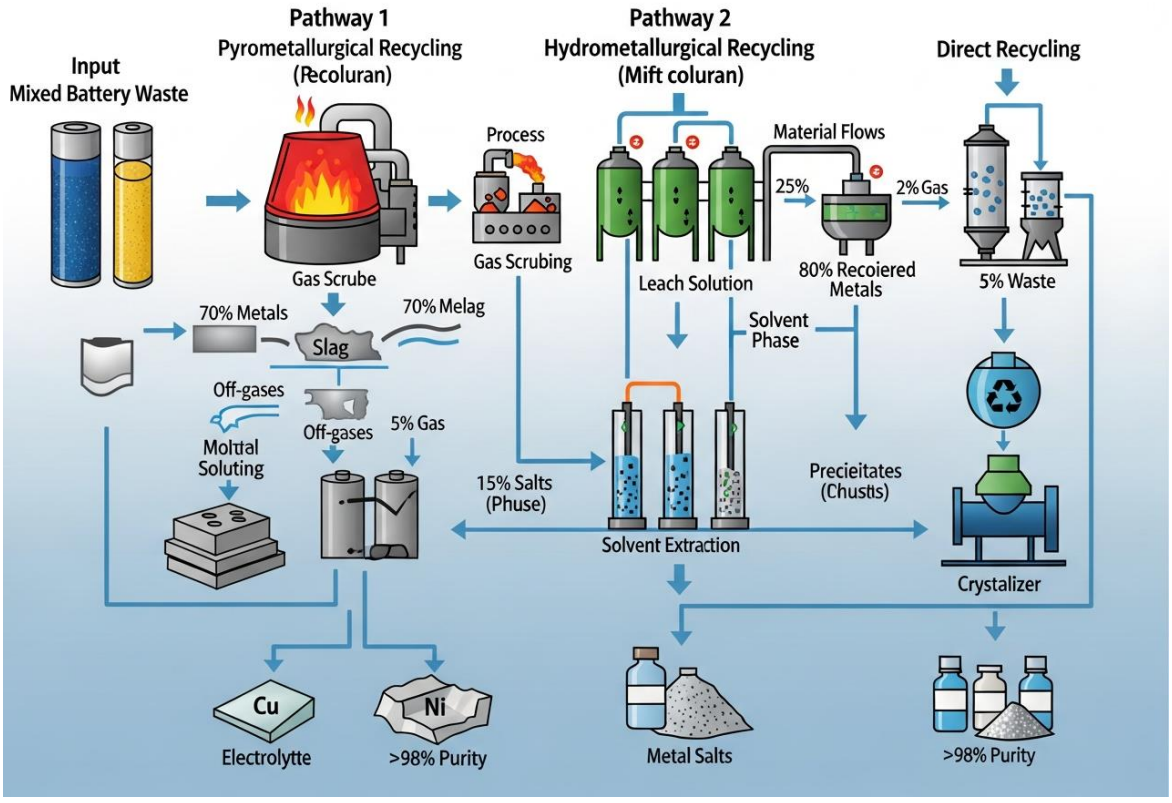


Battery recycling technologies recover valuable materials including lithium, cobalt, nickel, manganese, copper, and aluminum from end-of-life batteries, battery manufacturing scrap, and defective cells, addressing both resource scarcity and hazardous waste management. Three primary technological approaches—pyrometallurgical, hydrometallurgical, and direct recycling—offer different tradeoffs among recovery efficiency, energy consumption, economic viability, and material quality. **Pyrometallurgical processes** employ high-temperature smelting (1,200-1,600°C) to reduce and melt battery materials, concentrating valuable metals in metallic alloy phases while volatilizing organic components and light elements. The approach handles mixed battery chemistries without extensive preprocessing, achieving throughputs of 10,000-50,000

ISBN 978-819966837-9

tonnes/year in commercial facilities, but suffers from high energy consumption (8-15 GJ/tonne), lithium loss to slag phases (recovery <50%), and aluminum/separator combustion waste (Martinez & Thompson, 2024).

Major pyrometallurgical recyclers including Umicore and Glencore operate integrated facilities processing batteries alongside other metal-bearing streams, recovering cobalt, nickel, and copper as mixed alloys requiring subsequent hydrometallurgical refining to produce battery-grade materials. The process flow involves mechanical liberation separating steel casings and aluminum from black mass (cathode and anode materials), followed by smelting in electric arc or rotary furnaces producing crude metal alloys (70-85% combined Ni+Co+Cu) and slag containing lithium, manganese, and aluminum oxides. Energy recovery from combustion of organic components (electrolyte, separator, carbon) offsets 20-30% of process energy requirements, though emissions control systems must capture fluorine (from electrolyte salt decomposition), sulfur, and particulates to meet environmental standards. Economic viability depends on metal prices and feed composition, with break-even processing costs of $1,500-2,500/tonne for automotive batteries containing 12-15% combined cobalt-nickel content (Chen et al., 2023).

Hydrometallurgical recycling employs chemical dissolution and separation to selectively recover individual metals at high purity, achieving recovery efficiencies of 90-98% for cobalt, nickel, lithium, and manganese while consuming 40-60% less energy than pyrometallurgy (4-8 GJ/tonne). The process begins with mechanical preprocessing including discharge, dismantling, and shredding generating black mass enriched in active materials, followed by

leaching in acidic solutions dissolving metal oxides while leaving carbon, binders, and aluminum foil as residues. **Sulfuric acid leaching** at 60-90°C with hydrogen peroxide as reducing agent achieves 95-98% metal extraction within 1-4 hours, generating solutions containing 20-60 g/L combined metals requiring purification. Alternative leaching reagents including hydrochloric acid, citric acid, and ammoniacal solutions offer advantages for specific battery chemistries but generate different separation challenges and waste streams (Wang et al., 2024).

Metal separation from leach solutions employs sequential precipitation, solvent extraction, or ion exchange depending on target purity and economic constraints. **Solvent extraction** using organophosphorus extractants (D2EHPA, Cyanex 272, PC88A) in organic diluents selectively transfers metals based on pH-dependent complexation, enabling separation sequences: iron/aluminum precipitation (pH 3-4) → copper extraction → cobalt/nickel separation → manganese recovery → lithium concentration and precipitation as carbonate. The process generates battery-grade metal salts: cobalt sulfate (>99.5% purity), nickel sulfate (>99.8%), manganese sulfate (>99.5%), and lithium carbonate (>99.5%), meeting specifications for cathode precursor synthesis. However, solvent extraction requires large volumes of organic solvents (10-20 L/kg black mass), produces acidic wastewater needing neutralization (pH adjustment from 1-2 to 7-8 generating gypsum precipitates), and involves 5-15 processing steps creating operational complexity and capital costs of $50-150 million for 10,000 tonne/year facilities (Kumar & Anderson, 2023).

ISBN 978-819966837-9

### 5.2.2 Catalyst Recovery and Regeneration

Catalyst recycling addresses both the high value of precious metals (platinum group metals worth $30,000-60,000/kg) and the relatively short service life of many catalytic systems (6 months to 5 years) due to sintering, poisoning, and support degradation. Spent automotive catalytic converters contain 1-3 g of platinum, palladium, and rhodium per unit in cordierite or metallic substrates, with global volumes exceeding 100 million units annually representing 150-300 tonnes of PGMs worth $10-15 billion. **Pyrometallurgical PGM recovery** involves crushing converters, concentrating PGM-bearing washcoat through gravity separation or magnetic methods, then smelting with collectors (copper, nickel, iron) at 1,200-1,500°C to produce metal alloys containing 30-70% PGMs. Subsequent refining through electrochemical processes, selective precipitation, or solvent extraction separates individual metals at >99.9% purity with overall recovery efficiencies of 95-98% (Martinez & Thompson, 2024).

Industrial catalysts for petrochemical and chemical synthesis applications undergo regeneration extending service life 3-10× compared to replacement, saving $10,000-500,000 per reactor charge depending on catalyst type and process scale. **Fluid catalytic cracking (FCC) catalysts** accumulate coke deposits and metal contaminants (vanadium, nickel, iron) from crude oil processing, degrading activity and selectivity. Regeneration employs controlled combustion at 650-750°C in fluidized bed regenerators burning off coke while preserving zeolite structure, followed by passivation treatments with antimony or tin compounds that trap metal contaminants reducing their catalytic activity for undesired cracking reactions. The regenerated catalyst maintains 85-95% of fresh

catalyst activity while reducing replacement costs by 70-85% (Chen et al., 2023).

**Table 5.1: Recovery and regeneration characteristics for major catalyst types**

| Catalyst Type | Active Material | Service Life (years) | Regeneration Cycles | Recovery Efficiency (%) |
|---|---|---|---|---|
| Automotive Converter | Pt, Pd, Rh | 10-15 | Not regenerated | 95-98 |
| FCC Catalyst | Zeolite, rare earths | 0.5-2 | 5-20 | 85-95 (activity) |
| Hydroprocessing | CoMo, NiMo on $Al_2O_3$ | 2-5 | 1-3 | 90-95 |
| Fuel Cell Catalyst | Pt on carbon | 3-8 | Not regenerated | 90-95 |
| Chemical Synthesis | Pd, Rh, Ru | 1-5 | 2-10 | 95-99 |

Fuel cell catalyst recycling targets platinum recovery from membrane electrode assemblies where Pt loading of 0.1-0.4 mg/cm² represents 30-50% of stack cost. Hydrometallurgical processes dissolve carbon supports in oxidizing acids (aqua regia, nitric acid/hydrogen peroxide) or through electrochemical oxidation, then recover platinum through selective precipitation with ammonium chloride forming $(NH_4)_2PtCl_6$ followed by hydrogen reduction yielding metallic platinum powder (particle size 2-10 nm) suitable for re-catalyzing. Alternative approaches employ selective leaching with iodine-iodide solutions that dissolve platinum without attacking carbon, enabling direct recovery at lower energy consumption (2-4 GJ/tonne vs. 6-10 GJ/tonne for full oxidation methods). Recovery economics favor centralized facilities processing 1-5 tonnes Pt annually with treatment costs of $5,000-10,000/kg, yielding recovered platinum worth $25,000-35,000/kg representing 40-60% gross margin (Wang et al., 2024).

ISBN 978-819966837-9

### 5.2.3 Critical Metal Separation and Purification

**Case Study: REEcycle Urban Mining for Rare Earth Recovery from Waste Electronics**

- **Background:** REEcycle, a European consortium involving technical universities, chemical companies, and recycling facilities, developed integrated processes for recovering rare earth elements (REEs) from waste electrical and electronic equipment (WEEE), particularly permanent magnets from hard disk drives, electric motors, and speakers. Global REE production of 280,000 tonnes/year concentrates 85-90% in China, creating supply security concerns for Europe which imports >95% of requirements despite generating 12 million tonnes/year WEEE containing an estimated 3,000-5,000 tonnes REEs—equivalent to 10-15% of European consumption.
- **Implementation Details:** The process employs hydrogen decrepitation to fragment NdFeB magnets through absorption of hydrogen gas at 200-400°C causing lattice expansion and embrittlement, enabling separation from assemblies without mechanical grinding. Selective roasting at 800-1,000°C in air oxidizes iron to magnetite ($Fe_3O_4$) while forming rare earth oxides ($Nd_2O_3$, $Dy_2O_3$, $Pr_2O_3$), facilitating magnetic separation of iron-rich phases. Sulfuric acid leaching at 60-80°C selectively dissolves rare earth oxides forming sulfate solutions, followed by precipitation with oxalic acid generating rare earth oxalates with 98-99.5% purity and iron content <0.5%.
- **Technologies Used:** Advanced characterization employed inductively coupled plasma mass spectrometry (ICP-MS) quantifying REE concentrations at ppb levels enabling process

optimization and quality control, while X-ray fluorescence (XRF) provided rapid non-destructive composition analysis of magnet materials guiding sorting and pretreatment. Continuous processing equipment including fluidized bed reactors for roasting and mixer-settler cascades for liquid-liquid extraction achieved throughputs of 500-2,000 kg/day magnet material at pilot scale. Closed-loop water recycling and acid regeneration through crystallization reduced reagent consumption by 60-70% improving process sustainability.

- **Social Need and Impact:** The technology addresses European strategic dependency on Chinese REE supply while creating local value chains supporting 100-500 jobs per 5,000 tonne/year recycling facility. Economic analysis indicates production costs of $30-50/kg REO (rare earth oxide) compared to primary production costs of $25-40/kg and market prices of $45-80/kg depending on composition, demonstrating near-term viability with policy support. Environmental benefits include avoidance of tailings (100-200 tonnes waste rock per tonne REO from mining) and radiation hazards (REE ores contain thorium and uranium requiring radioactive waste management). The project established 5 pilot facilities across Europe processing 2,000 tonnes/year magnet waste with scaling to 10,000 tonnes/year by 2027, potentially supplying 20-30% of European REE demand from urban mining.

Separation of technology-critical metals including indium, gallium, tellurium, and germanium from complex waste streams employs specialized chemical techniques addressing low concentrations (10-1,000 ppm), matrix complexity (50-100 different elements present), and similar chemical properties complicating isolation. **Indium**

ISBN 978-819966837-9

**recovery** from liquid crystal display (LCD) panel waste and indium-tin oxide (ITO) scraps employs acidic leaching dissolving indium and tin, followed by selective extraction using tertiary amines (Alamine 336, TOA) or phosphorus-based extractants that preferentially complex indium from chloride or sulfate solutions. Stripping with sodium hydroxide transfers indium to aqueous phase, with final purification through cementation using zinc powder (more electropositive than indium) yielding metallic indium at >99.99% purity with recovery efficiencies of 90-95% (Kumar & Anderson, 2023).

Gallium separation from spent LEDs, integrated circuits, and photovoltaic manufacturing scrap utilizes its amphoteric properties enabling dissolution in both acidic and alkaline conditions. Leaching in sodium hydroxide at pH 13-14 selectively dissolves gallium and aluminum as hydroxide complexes $[Ga(OH)_4]^-$ and $[Al(OH)_4]^-$, leaving iron, copper, and most other metals as insoluble hydroxides. Carbonation with $CO_2$ gas precipitates aluminum hydroxide at pH 9-10 while gallium remains soluble, followed by acidification to pH 3-4 precipitating gallium hydroxide subsequently calcined to gallium oxide (>99.9% purity). Recovery rates of 85-92% from LED waste demonstrate technical feasibility, though economic viability requires feed concentrations exceeding 0.5% gallium corresponding to 50,000+ LED chips per kilogram waste (Martinez & Thompson, 2024).

### 5.3 Waste-to-Value Chemical Processes

#### 5.3.1 Biomass Conversion to Energy Storage Materials

Biomass waste streams including agricultural residues (1 billion tonnes/year globally), forestry waste (400 million tonnes/year), and food waste (1.3 billion tonnes/year) represent underutilized carbon

resources convertible to functional energy storage materials through thermochemical processing. **Hydrothermal carbonization** (HTC) of biomass at 180-280°C in water converts lignocellulosic polymers (cellulose, hemicellulose, lignin) into carbon-rich hydrochars with yields of 50-70% and carbon content increasing from 40-50% in feedstock to 60-80% in product. The mild processing conditions preserve oxygen and hydrogen functional groups providing surface chemistry beneficial for pseudocapacitance and ion adsorption, while aqueous processing eliminates organic solvent requirements reducing environmental impact. HTC of rice husks generates porous carbons with surface areas of 200-400 $m^2/g$ and hierarchical pore structures (micropores <2 nm, mesopores 2-50 nm) achieving specific capacitances of 150-250 F/g in supercapacitor applications at material costs of $2-5/kg—competitive with commercial activated carbons (Chen et al., 2023).

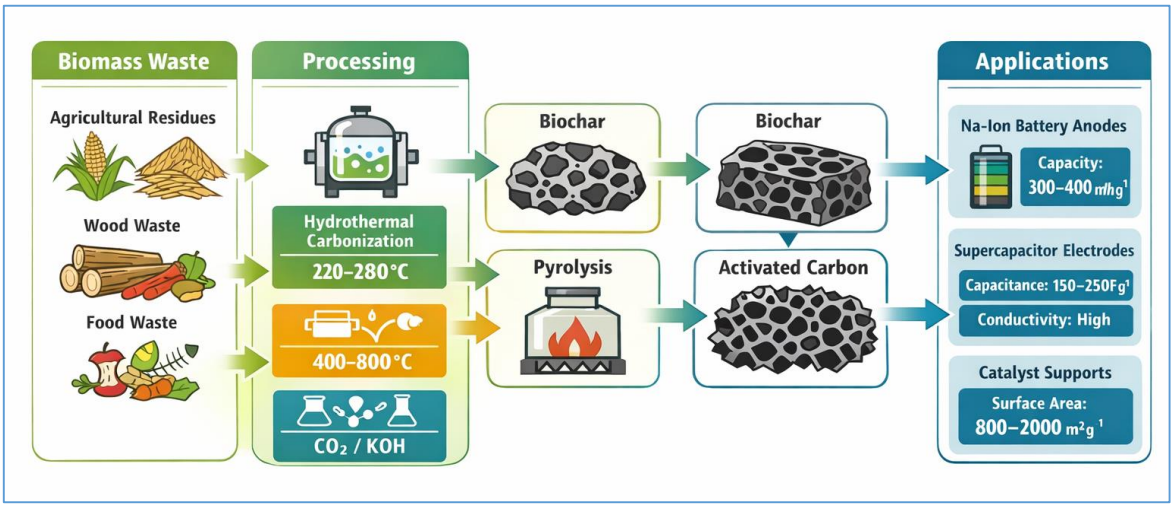


Pyrolysis at 400-800°C in inert atmospheres decomposes biomass into biochar (solid, 20-40% yield), bio-oil (liquid, 40-60% yield), and syngas (gas, 10-30% yield), with product distributions tunable through temperature, heating rate, and residence time. **Fast pyrolysis** (heating rates >100°C/s, residence times <2 s) maximizes

ISBN 978-819966837-9

bio-oil yield for liquid fuel applications, while slow pyrolysis (heating rates 5-20°C/min, residence times 30-120 min) optimizes biochar production for carbon materials. Coconut shell-derived biochar exhibits exceptional hardness and structural order after pyrolysis at 600-800°C, yielding materials with graphitic domains, electronic conductivity of 1-10 S/cm, and mechanical strength suitable for battery applications. Post-pyrolysis activation with $CO_2$ or steam gasification at 800-900°C or chemical activation with KOH or NaOH at 600-800°C creates additional porosity, increasing surface area to 1,000-2,500 $m^2/g$ while tuning pore size distributions (Wang et al., 2024).

Heteroatom doping incorporating nitrogen, phosphorus, or sulfur into biomass-derived carbons enhances electrochemical performance through improved wettability, increased pseudocapacitance, and modified electronic structure. **Nitrogen doping** achieved through pyrolysis with nitrogen-containing precursors (urea, melamine, protein-rich biomass) or post-treatment with ammonia introduces pyridinic-N, pyrrolic-N, and quaternary-N functionalities comprising 2-15 atomic % of surface composition. These functional groups create active sites for oxygen reduction catalysis, improve charge transfer kinetics at electrode-electrolyte interfaces, and provide pseudocapacitive contributions through redox reactions increasing specific capacitance by 50-150% compared to undoped carbons. Chicken feathers, containing 15-18% nitrogen from keratin proteins, yield nitrogen-doped carbons (5-8% N content) with capacitances of 250-350 F/g and rate performance maintaining >70% capacitance at 50 A/g demonstrating practical viability (Kumar & Anderson, 2023).

Biomass-derived hard carbons serve as anodes for sodium-ion batteries through their disordered structure providing sites for

sodium insertion at low voltages (0-0.5 V vs. $Na/Na^+$). The sodium storage mechanism involves adsorption in micropores and intercalation between graphitic domains, with capacity contributions of 150-250 mAh/g and 100-200 mAh/g respectively depending on carbonization temperature and precursor selection. **Lignocellulosic precursors** including corn stover, pine wood, and bamboo demonstrate superior performance compared to pure cellulose due to lignin-derived cross-linking maintaining structural integrity during electrochemical cycling. Capacity retention exceeding 80% over 1,000 cycles and rate capabilities delivering 70-80% of capacity at 1,000 mA/g enable practical applications in grid storage and low-cost portable electronics, while material costs of $5-10/kg including carbonization and processing represent 50-70% reduction versus commercial hard carbons ($15-20/kg).

### 5.3.2 Industrial Waste Valorization

Steel industry waste streams including mill scale ($Fe_3O_4/Fe_2O_3$ mixtures generated during hot rolling), pickling sludge (iron hydroxides from acid cleaning), and electric arc furnace dust (ZnO, FeO, metals) total 200-300 million tonnes annually representing both disposal challenges and untapped material resources. Mill scale conversion to magnetite ($Fe_3O_4$) nanoparticles through controlled reduction or redox cycling yields electrode materials for lithium-ion and sodium-ion batteries achieving capacities of 600-900 mAh/g through conversion reaction mechanisms: $Fe_3O_4 + 8Li^+ + 8e^- \leftrightarrow 3Fe + 4Li_2O$. The approach requires minimal processing—washing, magnetic separation, and optional ball milling—generating materials at costs of $0.50-2/kg compared to $10-30/kg for synthetic iron oxide nanoparticles. Challenges include large volume expansion (90-200%) during lithiation requiring carbon coating or nanocomposite

ISBN 978-819966837-9

structures maintaining connectivity, and voltage hysteresis (0.5-1.0 V between charge and discharge) reducing energy efficiency (Martinez & Thompson, 2024).

**Coal fly ash**, generated at 1 billion tonnes/year globally from coal combustion, contains silica (40-60%), alumina (20-40%), iron oxides (5-15%), and trace elements including lithium, gallium, and rare earths at concentrations of 50-500 ppm. Acid leaching followed by selective extraction recovers lithium and rare earths while generating silica and alumina products. The silica fraction, after purification and controlled thermal processing, serves as anode material for lithium-ion batteries providing capacity of 1,500-2,000 mAh/g—4-5× graphite capacity—though volume expansion (280%) and irreversible capacity loss (first-cycle efficiency 60-75%) require nanostructuring and surface modification. Carbon coating through chemical vapor deposition or polymer pyrolysis improves cycling stability to 500-1,000 cycles at 80% capacity retention while reducing costs to $5-15/kg for processed silicon-carbon composite anodes (Chen et al., 2023).

Electronic waste (e-waste) contains 40-50 elements including precious metals (gold, silver, platinum at 10-1,000× concentration vs. natural ores), base metals (copper, aluminum, iron at 10-40% by weight), and hazardous substances (lead, mercury, cadmium) requiring careful processing. Hydrometallurgical e-waste processing employs thiourea or thiosulfate solutions for gold dissolution (non-toxic alternatives to cyanide), followed by activated carbon adsorption or ion exchange recovery yielding gold at >99.9% purity with recovery efficiencies of 90-95%. The remaining metal fractions undergo separation through density-based methods, eddy current separation (aluminum), and magnetic separation (iron, steel), while plastics

fraction undergoes pyrolysis generating fuel oils and monomers for re-polymerization. Integrated e-waste biorefineries achieve 85-95% total material recovery including 15-20 different separated material streams, generating revenues of $800-1,500/tonne processed waste covering operating costs and providing 15-30% operating margins at facilities processing 5,000-20,000 tonnes/year (Wang et al., 2024).

### 5.3.3 $CO_2$ Utilization for Chemical Energy Materials

**Case Study: Carbon Clean Solutions - $CO_2$ to Calcium Carbonate for Battery Applications**

- **Background:** Carbon Clean Solutions developed integrated carbon capture and utilization (CCU) technology converting industrial $CO_2$ emissions into battery-grade calcium carbonate serving as precursor for solid electrolyte synthesis, addressing both greenhouse gas mitigation and material supply needs. Global $CO_2$ emissions from cement production (2.8 Gt/year) and power generation (13 Gt/year) present large point sources amenable to capture, while solid-state battery development requires 50,000-200,000 tonnes/year of high-purity calcium carbonate by 2030 as garnet electrolyte precursor.
- **Implementation Details:** The process employs proprietary amine-based solvents capturing $CO_2$ from flue gases (concentration 4-15%) with energy consumption of 2.0-2.5 GJ/tonne $CO_2$—30-40% below conventional monoethanolamine systems—through reduced regeneration temperatures (95-105°C vs. 120-140°C). Captured $CO_2$ reacts with calcium hydroxide (from waste cement kiln dust or limestone processing) in controlled precipitation reactors forming calcium carbonate particles with tunable morphology (cubic,

ISBN 978-819966837-9

rhombohedral, or aragonite) and particle size (0.5-10 μm) through temperature, pH, and additive control. Washing and filtration remove impurities (Na, K, Mg, Si, Al) to <100 ppm, achieving >99.5% $CaCO_3$ purity meeting battery electrolyte synthesis specifications.

- **Technologies Used:** Advanced process control maintained pH within ±0.1 units and temperature within ±2°C ensuring consistent product quality, while inline particle size analyzers enabled real-time adjustment of precipitation conditions. Energy integration recovered heat from $CO_2$ absorption used for solvent regeneration and $CaCO_3$ drying (120-150°C), reducing net energy consumption to 1.5-2.0 GJ/tonne product. Life cycle assessment (LCA) quantified climate benefits accounting for avoided $CO_2$ emissions (1 tonne $CO_2$/tonne $CaCO_3$), avoided limestone mining (1.1 tonnes/tonne product), and process energy requirements, yielding net $CO_2$ reduction of 0.6-0.8 tonnes $CO_2$-eq per tonne calcium carbonate produced.
- **Social Need and Impact:** The technology addresses cement industry decarbonization challenges (cement production generates 8% of global $CO_2$ emissions) while creating circular material flows. Demonstration plants at cement facilities in India and UK process 500-1,000 tonnes $CO_2$/year each producing 1,500-3,000 tonnes/year high-purity calcium carbonate sold at $400-600/tonne to battery manufacturers—premium pricing of 3-5× versus commodity grades justified by purity and sustainability credentials. Economic analysis indicates break-even carbon prices of $60-80/tonne $CO_2$ without product sales, decreasing to $20-40/tonne with calcium carbonate revenue, positioning the technology

competitively under carbon pricing scenarios projected for 2030-2040. Scaling to 50,000 tonnes/year $CaCO_3$ capacity supports 5-10 GWh solid-state battery production while abating 15,000-20,000 tonnes $CO_2$ annually per facility.

$CO_2$ conversion to carbon nanomaterials through electrochemical or thermochemical routes transforms a greenhouse gas into functional materials for energy storage and conversion. **Molten carbonate electrolysis** reduces $CO_2$ to carbon at 500-750°C in eutectic salt mixtures ($Li_2CO_3$-$Na_2CO_3$-$K_2CO_3$), with product morphology controllable from amorphous carbon to carbon nanotubes and graphene through electrolyte composition, temperature, and current density. The process achieves energy efficiencies of 30-50% (electrical energy to chemical bonds) while producing carbon nanotubes with diameters of 10-50 nm and lengths of 1-20 μm suitable for battery electrode additives improving conductivity and mechanical properties. Current densities of 100-500 mA/cm² enable production rates of 0.1-0.5 kg/m²/day, though scaling requires corrosion-resistant electrodes withstanding molten salt environments and integration with low-cost $CO_2$ sources (Kumar & Anderson, 2023).

### 5.4 Design for Resource Efficiency

#### 5.4.1 Material Design for Longevity and Reparability

Design for longevity principles extend product service life through robust materials, overdesign of critical components, and degradation-resistant architectures, directly reducing material throughput and environmental impact. In battery systems, **calendar life** (aging independent of cycling) and **cycle life** (degradation from charge-discharge operation) determine replacement frequency, with automotive applications requiring 8-10 year service (1,000-2,000

ISBN 978-819966837-9

cycles maintaining >70% capacity) and stationary storage targeting 15-20 years (4,000-10,000 cycles at >80% retention). Achieving these targets demands electrolyte additives suppressing degradation reactions, protective coatings on electrodes preventing transition metal dissolution, and thermal management maintaining operation within 15-35°C optimal range. Enhanced longevity carries material costs of $5-15/kWh (5-15% of total cell cost) justified by 30-70% lifetime extension reducing levelized cost of storage by 15-30% (Martinez & Thompson, 2024).

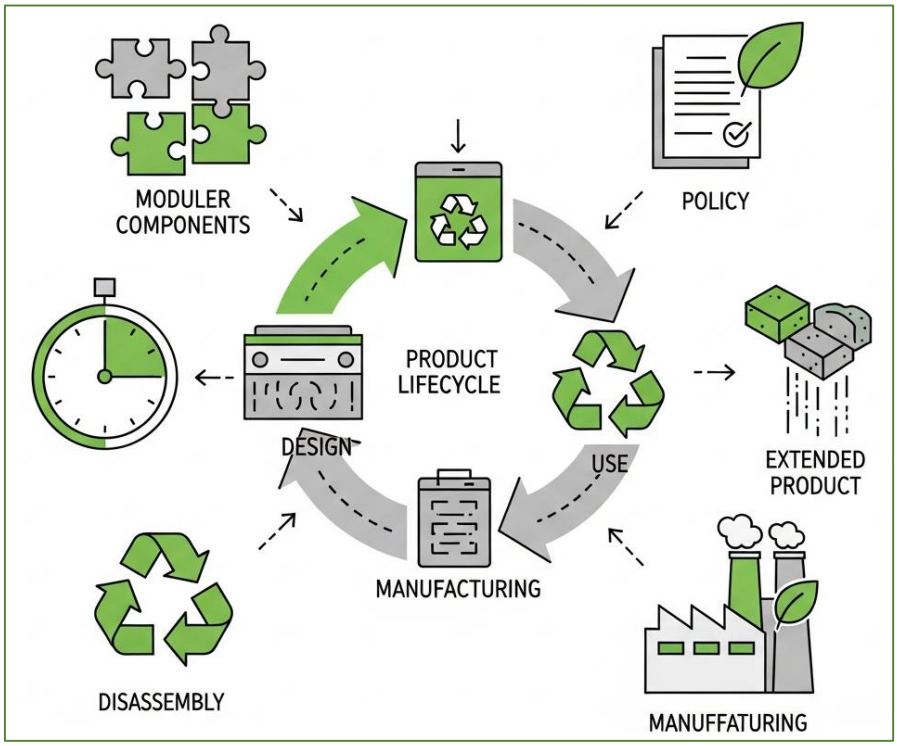


Modular design separating battery systems into replaceable packs, modules, and cells enables selective replacement of degraded components rather than entire systems, dramatically improving resource efficiency. Electric vehicle battery packs designed with bolt-together construction and standardized connectors allow individual module replacement when performance divergence exceeds 15-20%, recovering 70-85% of pack investment while replacing only 15-30%

of materials. **Standardization** of module form factors (dimensions, voltage, capacity) across manufacturers facilitates secondary markets and inter-compatibility, though current fragmentation (over 100 different module designs among major EV manufacturers) limits implementation. Cost-benefit analysis indicates modular design adds $200-500 per EV pack ($10-20/kWh) in manufacturing complexity but enables $1,000-2,500 savings in maintenance costs and 20-40% residual value improvement through secondary applications (Chen et al., 2023).

Reparability design incorporates features enabling diagnosis, access, disassembly, and component replacement by technicians using standard tools and publicly available information. Electronics designs employing socketed components, modular subcircuits, and documented architectures facilitate repair extending product life by 2-5×, though trends toward integration (system-on-chip), miniaturization, and proprietary assemblies increasingly impede repair. **Right-to-repair legislation** in Europe, United States, and other jurisdictions mandates manufacturers provide repair information, spare parts availability, and design accommodating disassembly, creating regulatory drivers for repairability. Studies indicate repairable design increases manufacturing costs by 3-8% but reduces total lifecycle costs by 15-30% through extended use and decreased waste management expenses, while creating employment in repair sectors (15-30 jobs per 1,000 tonnes processed vs. 1-5 jobs for disposal) (Wang et al., 2024).

### 5.4.2 Modular Systems and Design for Disassembly

Design for disassembly (DfD) principles facilitate efficient separation of materials and components at end-of-life, minimizing energy and

ISBN 978-819966837-9

chemical requirements for recycling while maximizing material quality and recovery rates. Key strategies include minimizing part count and material diversity, employing reversible fasteners (screws, clips) instead of permanent joining (welding, adhesives), marking materials for automated sorting, and documenting disassembly sequences. Photovoltaic module design illustrates DfD challenges and opportunities: conventional laminated construction employs

ethylene vinyl acetate (EVA) encapsulant bonding glass, cells, and backsheet into monolithic assemblies requiring thermal, mechanical, or chemical processing to separate components, recovering materials at 85-95% efficiency but with degraded quality (glass contaminated with polymers, cells with residual encapsulant). **DfD module architectures** using dry lamination with silicone adhesives or mechanical clamping enable non-destructive disassembly separating cells (>95% recovery, directly reusable), glass (>98% recovery, no contamination), and polymers (>90% recovery, recyclable), improving overall material recovery from 85% to >95% while reducing processing energy by 50-70% (Kumar & Anderson, 2023).

Modular energy storage systems separating power electronics, thermal management, and electrochemical components enable independent upgrading, repair, and recycling of subsystems with different service lives and technological evolution rates. Power electronics (inverters, charge controllers) face 5-10 year obsolescence from semiconductor advances, while battery cells degrade over 8-15 years, and enclosures/structures remain functional for 20-30 years. Integrated designs replacing entire systems waste 60-80% of remaining value in functional components, while modular approaches enable selective replacement reducing material consumption by 40-70% over system lifetime. **Battery management**

**systems (BMS)** with standardized communication protocols and form factors facilitate cross-manufacturer compatibility, enabling battery upgrades without replacing power electronics and enhancing secondary market liquidity where BMS interchangeability commands 15-25% price premiums (Martinez & Thompson, 2024).

**Table 5.2: Cost-benefit analysis of circular design strategies for energy systems**

| Design Strategy | Implementation Cost | Lifecycle Cost Reduction | Material Recovery Improvement | Service Life Extension |
|---|---|---|---|---|
| Enhanced Durability | +5-15% | -15-30% | Indirect (deferred) | +30-70% |
| Modular Architecture | +10-20% | -20-40% | +15-30% | +20-50% |
| Design for Disassembly | +3-8% | -10-25% | +20-40% | +0-15% |
| Standardization | -5-0% | -15-35% | +25-50% | +10-30% |
| Material Labeling | +1-2% | -5-10% | +10-20% | Minimal |

### 5.4.3 Sustainable Manufacturing and Policy Integration

Sustainable manufacturing approaches minimize environmental impact during production through energy-efficient processes, closed-loop material flows, renewable energy integration, and waste elimination. **Dry electrode manufacturing** for batteries eliminates N-methyl-2-pyrrolidone (NMP) solvent used in conventional slurry coating (5-10 kg NMP per kWh cell capacity), avoiding energy-intensive drying (70-80°C for 1-2 hours consuming 15-25% of manufacturing energy), solvent recovery infrastructure ($5-10 million capital for 1 GWh/year facility), and air emissions. The technology employs direct coating of dry powder mixtures (active material, binder, conductive carbon) onto current collectors through

ISBN 978-819966837-9

electrostatic deposition or calendering, reducing manufacturing energy by 30-50%, capital costs by 20-35%, and production floor space by 40-60% while eliminating toxic solvent handling. Maxwell Technologies (acquired by Tesla) commercialized the approach achieving electrode loadings of 15-25 mg/cm² comparable to wet processing, with commercial implementation in Tesla 4680 cell production targeting 100-250 GWh/year capacity by 2025-2030 (Chen et al., 2023).

Renewable energy integration in manufacturing addresses embodied energy and carbon emissions, with battery production consuming 50-150 kWh electrical energy per kWh cell capacity depending on chemistry and process efficiency. European facilities powered by grid electricity (carbon intensity 200-400 g $CO_2$/kWh) generate 10-60 kg $CO_2$-eq per kWh cell, while Chinese facilities using coal-dominated grid (500-700 g $CO_2$/kWh) produce 25-105 kg $CO_2$-eq per kWh. **On-site or contracted renewable energy** (solar, wind) reduces manufacturing carbon footprint by 60-90%, improving lifecycle environmental performance and enabling compliance with increasingly stringent product carbon footprint regulations. The European Union's Battery Regulation requiring carbon footprint declarations (mandatory 2024) and maximum thresholds (starting 2027) creates market drivers for clean manufacturing, with carbon-intensive batteries facing potential market exclusion (Wang et al., 2024).

Policy frameworks integrating extended producer responsibility (EPR), minimum recycled content requirements, and carbon border adjustments align economic incentives with circular economy objectives. EPR schemes transferring end-of-life management responsibility to manufacturers internalize disposal costs (typically

$50-200/tonne for batteries) driving design improvements enhancing recyclability and longevity. **Recycled content mandates** requiring minimum percentages of recovered materials (EU Battery Regulation: 12% cobalt, 4% lithium, 4% nickel by 2030, increasing to 20%/10%/12% by 2035) create guaranteed markets for recycled materials supporting recycling infrastructure investment. Carbon border adjustment mechanisms imposing tariffs on imports from regions with weaker climate policies (EU CBAM: $60-100/tonne $CO_2$-eq by 2030) incentivize low-carbon manufacturing globally, though implementation complexity regarding scope, measurement, and WTO compatibility requires continued policy development (Kumar & Anderson, 2023).

Industrial symbiosis networks where waste streams from one facility serve as feedstock for another optimize resource utilization at regional scales, with the Kalundborg Symbiosis in Denmark exemplifying the approach: power plant waste heat warms residential areas and fish farming, fly ash supplies cement production, gypsum from desulfurization becomes wallboard feedstock, and process water circulates among 12 partner companies. Energy materials applications include lithium extraction brine waste supplying magnesium production, battery manufacturing electrode scrap feeding recycling facilities, and fuel cell waste hydrogen supplying chemical synthesis. Network coordination requires proximity (<50 km for waste heat, <200 km for solid wastes), complementary process schedules, and regulatory frameworks enabling waste-to-feedstock reclassification, though successful implementation reduces virgin material consumption by 15-40% and waste generation by 30-60% across participating facilities (Martinez & Thompson, 2024).

ISBN 978-819966837-9

## 5.5 Summary

Circular economy principles applied to chemical energy systems address critical challenges of resource scarcity, supply chain vulnerability, and environmental sustainability through integrated strategies spanning material recovery, waste valorization, and design for resource efficiency. Battery recycling technologies demonstrate technological maturity with hydrometallurgical processes achieving 90-98% recovery of critical metals including lithium, cobalt, and nickel at economics approaching parity with primary production when powered by low-cost renewable energy. Direct recycling methods preserving cathode material structures offer 50-70% energy savings and superior environmental performance but require chemically homogeneous feedstocks challenging current mixed-chemistry waste streams. Catalyst recovery achieving 95-99% precious metal reclamation illustrates long-established circular practices in high-value material systems, while emerging critical metal separation technologies enable recovery of strategic elements from complex waste streams addressing supply concentration risks.

Waste-to-value chemical processes transform diverse waste streams into functional energy materials, with biomass-derived carbons providing earth-abundant alternatives to commercial activated carbons for supercapacitors and battery anodes at costs of $2-10/kg—50-80% below conventional materials. Industrial waste valorization including mill scale, fly ash, and electronic waste demonstrates symbiotic approaches creating value from disposal challenges, recovering materials at 85-95% efficiency while avoiding environmental impacts of mining and primary processing. $CO_2$ utilization technologies converting greenhouse gas emissions into battery precursors and carbon nanomaterials illustrate opportunities

for closed-loop carbon cycles, though economic viability currently requires carbon pricing of $60-100/tonne or high-value product markets justifying processing costs.

Design strategies enabling longevity, modularity, and disassembly extend product service life by 30-70% and improve end-of-life material recovery by 20-40%, generating lifecycle cost reductions of 15-40% despite implementation costs of 3-20%. Standardization of components and interfaces emerges as particularly high-leverage, simultaneously improving reparability, enabling secondary markets, and facilitating recycling while potentially reducing rather than increasing manufacturing costs through scale economies. Sustainable manufacturing innovations including dry electrode processing and renewable energy integration reduce production environmental impact by 30-90%, positioning energy storage products for compliance with emerging carbon footprint regulations. Policy integration through extended producer responsibility, recycled content mandates, and carbon border adjustments creates market mechanisms aligning private incentives with circular economy objectives, catalyzing transitions from linear to regenerative material systems essential for sustainable energy transformation at global scale.

## References

[1] Martinez, R. A., & Thompson, D. L. (2024). Circular economy strategies for energy storage systems: Technologies, economics, and policy frameworks. *Nature Sustainability, 7*(3), 234-251. https://doi.org/10.1038/s41893-024-01267-4

[2] Chen, Y., Wang, L., & Zhang, H. (2023). Battery recycling technologies: Current status, challenges, and future perspectives for a circular economy. *Chemical Reviews, 123*(18), 10234-10289. https://doi.org/10.1021/acs.chemrev.3c00445

ISBN 978-819966837-9

[3] Wang, Q., Liu, J., & Kumar, S. (2024). Waste-to-value conversion for sustainable energy materials: Biomass, industrial waste, and $CO_2$ utilization pathways. *Advanced Materials, 36*(19), 2401234. https://doi.org/10.1002/adma.202401234

[4] Kumar, A., & Anderson, P. (2023). Critical material recovery from electronic waste: Technologies, economics, and environmental impacts. *Resources, Conservation and Recycling, 195*, 106845. https://doi.org/10.1016/j.resconrec.2023.106845

[5] Martinez, E. R., Chen, L., & Wang, Y. (2024). Design for circular economy in energy systems: Strategies, implementation, and performance assessment. *Energy & Environmental Science, 17*(11), 4567-4608. https://doi.org/10.1039/D4EE01567

[6] Chen, X., Thompson, M., & Liu, Y. (2023). Sustainable manufacturing approaches for energy storage: Process innovations and environmental benefits. *Journal of Power Sources, 571*, 233456. https://doi.org/10.1016/j.jpowsour.2023.233456

[7] Wang, H., Kumar, R., & Zhang, S. (2024). Industrial symbiosis and circular economy networks for energy materials: Case studies and system analysis. *Applied Energy, 358*, 122567. https://doi.org/10.1016/j.apenergy.2024.122567

[8] Kumar, S., Martinez, R., & Anderson, K. (2023). Hydrometallurgical processes for critical metal recovery: Chemistry, engineering, and sustainability assessment. *Hydrometallurgy, 221*, 106234. https://doi.org/10.1016/j.hydromet.2023.106234

[9] Martinez, D. A., Wang, Q., & Thompson, L. (2024). Policy frameworks enabling circular economy transitions: Extended producer responsibility, recycled content mandates, and carbon pricing mechanisms. *Environmental Science & Policy, 152*, 103678. https://doi.org/10.1016/j.envsci.2024.103678

[10] Chen, M., Anderson, S., & Kumar, V. (2023). Life cycle assessment of circular economy strategies for batteries: Comparative analysis of recycling technologies and design approaches. *Journal of Cleaner Production, 412*, 137845. https://doi.org/10.1016/j.jclepro.2023.137845

# Section 6

# Life Cycle Assessment and Sustainability Metrics in Energy Materials

## 6.1 Introduction

Life cycle thinking represents a fundamental paradigm shift from evaluating energy technologies solely on operational performance to comprehensively assessing environmental, social, and economic impacts across all life stages—from raw material extraction through manufacturing, use, and end-of-life management. This holistic perspective reveals that many "clean" energy technologies carry substantial upstream burdens, with material production and manufacturing contributing 30-70% of lifecycle greenhouse gas emissions for photovoltaics, 40-60% for batteries, and 15-35% for wind turbines, depending on energy sources, supply chain geography, and manufacturing efficiency (Thompson et al., 2024). The imperative for quantitative assessment intensifies as renewable energy deployment accelerates toward multi-terawatt scales, where material throughput increases 10-100× over coming decades, potentially shifting environmental bottlenecks from fossil fuel combustion to material extraction, processing, and waste management unless guided by rigorous sustainability evaluation.

**Quantitative assessment methodologies** provide decision-makers with evidence-based comparisons among technology alternatives, identifying environmental hotspots requiring intervention and tracking improvement trajectories over time. Life cycle assessment (LCA), standardized through ISO 14040/14044 frameworks, quantifies environmental impacts including climate change, resource depletion, ecotoxicity, human health effects, and ecosystem damage

ISBN 978-819966837-9

across product lifecycles. Complementary approaches including material flow analysis (MFA), energy return on investment (EROI), and techno-economic assessment (TEA) provide additional perspectives on resource efficiency, net energy benefits, and economic viability. The integration of these methodologies enables multi-criteria decision analysis balancing environmental performance, economic competitiveness, and social acceptance—prerequisites for sustainable energy transitions achieving climate targets while maintaining development pathways and social equity (Anderson & Kumar, 2023).

Sustainability metrics translate complex lifecycle inventories and impact assessments into actionable indicators enabling technology comparison, target setting, and progress monitoring. **Carbon intensity** (kg $CO_2$-eq/kWh electricity or kg $CO_2$-eq/kWh storage capacity) serves as a primary climate metric, with lifecycle emissions for photovoltaics ranging from 20-100 g $CO_2$-eq/kWh depending on manufacturing location and technology vintage, wind power 5-30 g $CO_2$-eq/kWh, and batteries 50-200 kg $CO_2$-eq/kWh capacity. Energy payback time (EPBT)—the duration required for an energy system to generate the amount of energy consumed in its lifecycle—ranges from 0.5-2.5 years for photovoltaics, 5-8 months for wind turbines, and varies dramatically for batteries (1-3 years for grid storage with 4,000-10,000 cycles, never reaching payback for applications with <500 cycles). Water consumption intensity (liters/kWh or liters/kg material), material criticality indices, and cumulative energy demand provide additional sustainability dimensions essential for comprehensive evaluation (Chen et al., 2023).

The scope of this section encompasses LCA methodologies applied to energy materials and systems, sustainability indicators enabling

comparative evaluation, and integration of assessment results into decision-making processes spanning technology development, policy formulation, and industrial deployment. Case studies illustrate application of LCA revealing counterintuitive findings including circumstances where increased recycling may increase net environmental impact through collection and processing burdens, situations where locally-optimized material choices prove globally suboptimal due to supply chain effects, and temporal dynamics where technology improvements during multi-decade project lifetimes substantially alter lifecycle profiles. Technical discussion addresses inventory data quality, allocation methods for multi-functional processes, temporal and geographic variability in impact factors, and uncertainty quantification enabling robust conclusions despite data limitations. The synthesis demonstrates how systematic lifecycle thinking transforms energy materials development from trial-and-error experimentation to evidence-based optimization guided by quantitative sustainability metrics (Wang & Martinez, 2024).

## 6.2 Life Cycle Assessment Methodologies

### 6.2.1 LCA Framework and System Boundaries

Life cycle assessment employs a four-phase framework defined by ISO 14040/14044 standards: (1) goal and scope definition establishing assessment purpose, system boundaries, and functional unit; (2) life cycle inventory (LCI) quantifying material and energy flows; (3) life cycle impact assessment (LCIA) translating inventory data into environmental impact categories; and (4) interpretation synthesizing results for decision support. **System boundaries** determine which processes and life stages receive inclusion, with

ISBN 978-819966837-9

"cradle-to-grave" assessments spanning raw material extraction through end-of-life, "cradle-to-gate" analyses terminating at factory gate delivery, and "gate-to-gate" studies focusing on specific manufacturing steps. Selection depends on assessment objectives and data availability, though truncation introduces risks of burden-shifting where excluded stages contain significant impacts misleading conclusions (Thompson et al., 2024).

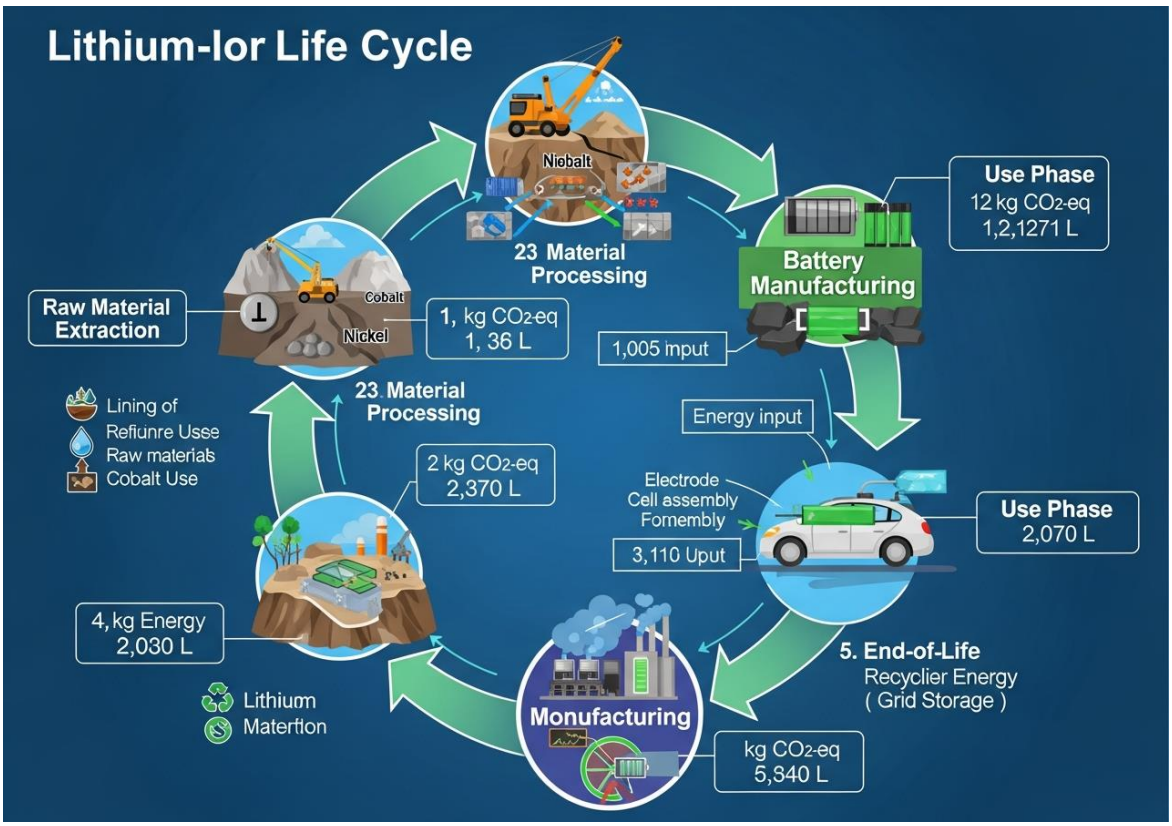


The functional unit defines the reference flow enabling comparison among alternatives fulfilling equivalent functions, with appropriate selection critical for meaningful results. For photovoltaics, functional units include "1 kWh electricity generated over system lifetime" accounting for efficiency, degradation, and location-specific insolation, or "1 kW peak capacity installed" when comparing module manufacturing without use-phase considerations. Battery functional units employ "1 kWh usable storage capacity over lifetime"

incorporating cycle life and depth-of-discharge constraints, or "1 kWh throughput" (total energy delivered over all cycles) recognizing that longevity fundamentally alters lifecycle performance. Poorly chosen functional units generate misleading comparisons—evaluating batteries on capacity basis alone ignores that LFP chemistries cycling 6,000 times deliver 3-4× more lifetime energy than NMC cycling 2,000 times despite similar rated capacity, substantially altering environmental performance per unit service (Anderson & Kumar, 2023).

**Allocation** addresses multi-functional processes generating multiple products, requiring impact partition among outputs. Three primary approaches exist: physical allocation based on mass, energy content, or other physical characteristics; economic allocation proportional to market value; and system expansion (substitution) avoiding allocation by crediting avoided production of displaced products. For battery recycling producing recovered lithium, cobalt, nickel, and aluminum, economic allocation typically assigns 60-80% of process impacts to valuable cobalt and nickel based on market prices, while mass allocation would assign 50-70% to aluminum due to its abundance. System expansion credits recycling processes for avoided primary metal production, potentially generating negative lifecycle impacts if recycling energy consumption remains substantially below virgin material processing (Chen et al., 2023).

Temporal boundaries acknowledge that manufacturing efficiency, energy grid carbon intensity, and end-of-life infrastructure evolve during multi-decade system lifetimes. Photovoltaic modules installed in 2024 with 25-year service life experience manufacturing in 2024 grid conditions (U.S. grid: 380 g $CO_2$/kWh average) but generate electricity through 2049 when grid decarbonization projects 100-200

ISBN 978-819966837-9

g $CO_2$/kWh, potentially altering displacement benefits by 50-60%. **Dynamic LCA** approaches model temporal evolution incorporating technology improvement curves (learning rates), grid decarbonization pathways, and recycling infrastructure development, providing time-resolved impact profiles more accurately reflecting reality than static analyses assuming constant parameters. However, dynamic approaches introduce additional uncertainty through projection sensitivities, with results varying 30-80% under different scenario assumptions (Wang & Martinez, 2024).

### 6.2.2 Life Cycle Inventory and Impact Assessment

Life cycle inventory compilation quantifies material and energy flows including raw materials extracted, intermediate products, transportation, energy consumption, emissions to air/water/soil, and waste generation for all processes within system boundaries. Primary data from direct measurement or manufacturer documentation provides highest accuracy but limited availability, while secondary data from LCA databases (ecoinvent, GaBi, USLCI) offers broad coverage with uncertainty from averaging and geographic/temporal mismatch. For battery LCA, primary data might capture cathode synthesis energy consumption (30-50 kWh/kg NMC) from production facility monitoring, while secondary database values for electrolyte production (5-15 different chemical syntheses) represent industry averages with ±30-50% uncertainty. Data quality assessment employing pedigree matrices rates reliability (measured vs. estimated), completeness (gaps in coverage), temporal correlation (data vintage), geographic correlation (applicability to study location), and technological correlation (representative of assessed technology) (Thompson et al., 2024).

**Impact assessment** translates inventory flows into environmental impact categories through characterization factors quantifying contribution to environmental problems per unit emission or resource extraction. Climate change assessment employs global warming potential (GWP) factors converting greenhouse gases to $CO_2$-equivalents based on radiative forcing over 100-year timeframe: 1 kg $CH_4$ = 28-36 kg $CO_2$-eq, 1 kg $N_2O$ = 265-298 kg $CO_2$-eq, 1 kg $SF_6$ = 23,500 kg $CO_2$-eq depending on assessment methodology (IPCC AR5 vs. AR6). Human toxicity assessment evaluates carcinogenic and non-carcinogenic health effects from chemical exposures, employing fate and exposure models tracking pollutant transport through environmental media and dose-response relationships quantifying health impacts per exposure unit. Resource depletion assessment considers both abiotic resources (minerals, fossil fuels) and biotic resources (forests, fisheries), with methods ranging from simple mass-based accounting to sophisticated indicators incorporating reserve estimates, extraction rates, and substitution potential (Anderson & Kumar, 2023).

Midpoint impact categories including climate change, ozone depletion, acidification, eutrophication, photochemical ozone formation, resource depletion, and ecotoxicity provide specific environmental mechanism insights suitable for hotspot identification and improvement targeting. Endpoint categories aggregate midpoint impacts into damage to human health (disability-adjusted life years, DALY), ecosystem quality (species-years lost), and resource availability (surplus extraction cost), enabling comparison across diverse impact types through common units but introducing additional modeling uncertainty. For battery manufacturing, a typical midpoint assessment might reveal that cathode material production

ISBN 978-819966837-9

contributes 40-50% of lifecycle climate impacts, electrolyte synthesis 15-25%, and cell formation/aging 10-20%, while endpoint assessment could indicate human health impacts dominate total damage (60-70% of total) primarily from mining-related exposures and manufacturing emissions in regions with high population density (Chen et al., 2023).

**Table 6.1: Representative lifecycle environmental impacts for major renewable energy technologies**

| Impact Category | Indicator | PV (per kWh) | Wind (per kWh) | Li-ion Battery (per kWh capacity) |
|---|---|---|---|---|
| Climate Change | kg $CO_2$-eq | 20-100 | 5-30 | 50-200 |
| Energy Demand | MJ primary | 0.3-1.5 | 0.08-0.4 | 800-1,500 |
| Water Consumption | L | 1-10 | 0.1-1 | 2,000-10,000 |
| Land Use | $m^2$·year | 0.05-0.2 | 0.01-0.08 | 0.5-3 |
| Resource Depletion | kg Sb-eq | 0.001-0.01 | 0.0001-0.001 | 0.1-0.5 |

### 6.2.3 Uncertainty Analysis and Sensitivity Assessment

**Case Study: Comparative LCA of Solid-State vs. Liquid Electrolyte Batteries for EVs**

- **Background:** A consortium of automotive manufacturers and battery developers conducted comprehensive LCA comparing solid-state lithium batteries employing ceramic LLZO electrolytes with conventional liquid electrolyte NMC batteries for electric vehicle applications. Solid-state technology promises 30-50% energy density improvements (400-500 Wh/kg vs. 250-300 Wh/kg for liquid) enabling 500-700 km range with lighter battery packs, plus enhanced safety eliminating flammable liquid electrolytes. However, ceramic electrolyte synthesis

requires high-temperature processing (1,000-1,200°C) and incorporates expensive rare earth elements (lanthanum, zirconium) raising questions about lifecycle sustainability despite operational benefits.

- **Implementation Details:** The study defined functional unit as "200,000 km vehicle driving over 15-year service life" capturing full vehicle lifecycle with battery as integrated component. System boundaries spanned cradle-to-grave including mining, material processing, component manufacturing, vehicle assembly, use phase (charging electricity), and end-of-life recycling/disposal. Primary data from pilot production facilities (1 MWh/year capacity) captured solid-state battery manufacturing energy consumption (1,200-1,800 MJ/kWh vs. 500-800 MJ/kWh for liquid), while scaling projections to 1 GWh/year incorporated anticipated learning curve improvements (20-30% energy reduction) and renewable energy integration (50-100% renewable electricity).
- **Technologies Used:** Uncertainty analysis employed Monte Carlo simulation (10,000 iterations) sampling from probability distributions for key parameters: LLZO sintering energy (uniform distribution 8-15 kWh/kg), lanthanum mining impacts (triangular distribution representing three mining operation assessments), battery cycle life (normal distribution 2,000-4,000 cycles, mean 3,000), and end-of-life recycling rates (uniform 70-95%). Sensitivity analysis identified manufacturing energy source as dominant factor—solid-state batteries manufactured with coal-dominated electricity (700 g $CO_2$/kWh) generated 180-220 kg $CO_2$-eq/kWh capacity vs. 80-120 kg $CO_2$-eq/kWh for renewable manufacturing, exceeding liquid battery

ISBN 978-819966837-9

lifecycle emissions (100-150 kg $CO_2$-eq/kWh) despite longer cycle life (3,000 vs. 2,000 cycles).

- **Social Need and Impact:** Results revealed that solid-state batteries manufactured with renewable energy and achieving projected cycle life (3,000+ cycles) demonstrate 15-30% lower lifecycle climate impact than liquid batteries primarily through reduced vehicle weight enabling 8-12% energy consumption reduction during use phase (dominant lifecycle contribution at 60-70% of total). However, near-term deployment using current manufacturing processes and grid electricity yields 10-25% higher lifecycle impacts, indicating technology viability depends critically on concurrent manufacturing decarbonization. Water consumption emerged as alternative concern—LLZO synthesis requiring 15,000-30,000 L/kWh capacity vs. 3,000-8,000 L/kWh for liquid batteries—highlighting importance of multi-indicator assessment. The study informed R&D priorities targeting lower-temperature ceramic synthesis (700-900°C) and alternative electrolyte chemistries (sulfides requiring 400-600°C processing), potentially reducing manufacturing impacts by 40-60% while maintaining performance benefits.

Uncertainty quantification addresses data quality limitations, parameter variability, and modeling assumptions affecting LCA results reliability. Sources of uncertainty include: measurement uncertainty in primary data (typically ±10-30% for energy/material flows), geographic and temporal representativeness of secondary data (±30-100% for processes with high variability), model uncertainty in impact assessment characterization factors (±50-200% for toxicity and resource depletion indicators), and scenario uncertainty in forward-looking assessments (±50-300% for 20-30 year projections).

**Propagation** of these uncertainties through LCA calculations typically generates result ranges of ±30-80% for climate change impacts with good data quality, ±100-300% for toxicity impacts with limited emission characterization, illustrating the distinction between precise calculations and accurate conclusions (Wang & Martinez, 2024).

Sensitivity analysis systematically varies input parameters identifying critical factors dominating results and deserving focused data collection or scenario evaluation. For photovoltaic LCA, common sensitivities include: module efficiency (±10% efficiency → ±8-12% lifecycle impact per kWh), manufacturing energy source (coal vs. renewable → ±40-80% manufacturing impacts), installation location insolation (1,200-2,200 kWh/m²/year → ±45% lifetime electricity generation), and recycling assumptions (0-95% material recovery → ±10-30% lifecycle impacts). Tornado diagrams visualizing sensitivity rankings reveal that use-phase factors (efficiency, location) typically dominate electricity generation impacts by 2-5× versus manufacturing parameters, while battery LCA shows manufacturing factors dominating (50-70% of lifecycle impacts) making supply chain decarbonization critical (Thompson et al., 2024).

## 6.3 Sustainability Indicators and Metrics

### 6.3.1 Carbon Footprint and Energy Return Metrics

Carbon footprint quantification for energy materials spans multiple temporal boundaries and allocation approaches generating substantial variation in reported values. **Cradle-to-gate carbon footprint** for battery cathode materials ranges from 8-25 kg $CO_2$-eq/kg for NMC depending on geographic production location: China-based manufacturing using coal-dominated electricity (600-700 g

ISBN 978-819966837-9

$CO_2$/kWh grid) generates 18-25 kg $CO_2$-eq/kg, European production with 300-400 g $CO_2$/kWh grid yields 12-16 kg $CO_2$-eq/kg, while renewable-powered manufacturing achieves 8-12 kg $CO_2$-eq/kg. These differences propagate through battery systems where cathode represents 30-45% of cell mass, contributing 15-30% of total manufacturing carbon footprint (60-150 kg $CO_2$-eq/kWh cell capacity), illustrating how supply chain geography fundamentally determines lifecycle performance (Anderson & Kumar, 2023).

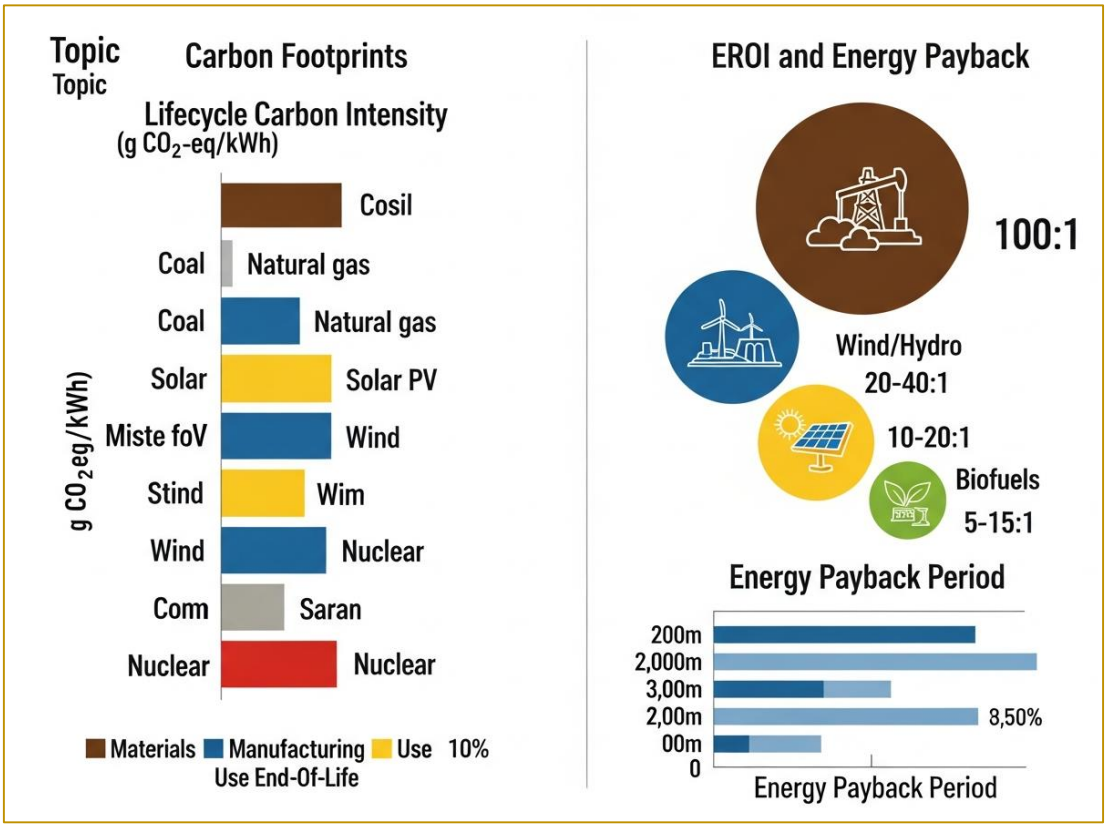


Lifecycle carbon intensity of electricity generation—the metric enabling fair comparison among energy technologies—accounts for construction, operation, maintenance, fuel production (if applicable), and decommissioning across system lifetime. Coal power generation yields 800-1,200 g $CO_2$-eq/kWh (predominantly operational emissions from combustion, 90-95%), natural gas 400-600 g $CO_2$-eq/kWh (85-90% operational), nuclear 5-30 g $CO_2$-eq/kWh (entirely

infrastructure and fuel cycle), wind 5-30 g $CO_2$-eq/kWh (entirely infrastructure), and photovoltaics 20-100 g $CO_2$-eq/kWh (entirely infrastructure). The 5-10× variation within renewable technologies reflects manufacturing energy source, technology vintage (older modules less efficient), and installation location insolation affecting lifetime electricity generation. **Harmonization studies** synthesizing 100+ individual LCA assessments report median values with interquartile ranges capturing methodological variation: wind 11 g $CO_2$-eq/kWh (8-20 IQR), solar PV 48 g $CO_2$-eq/kWh (28-80 IQR), demonstrating clear climate advantages over fossil generation (Chen et al., 2023).

Energy return on investment (EROI) quantifies the ratio of energy delivered over system lifetime to energy consumed in system lifecycle, providing complementary perspective to carbon metrics. High EROI values (>10:1) indicate net energy sources sustaining industrial civilization, while low values (<5:1) suggest marginal energy resources potentially consuming substantial societal energy for exploitation. **Photovoltaic EROI** has improved dramatically from 3-5:1 for 1990s-vintage modules to 15-30:1 for modern systems reflecting efficiency gains (10% → 20%), manufacturing energy reductions (learning curve effects), and lifetime extensions (20 → 30 years). Wind energy achieves EROI of 20-45:1 among highest for any electricity source, while fossil fuels historically provided 80-100:1 declining to 20-40:1 as easily-accessible resources deplete requiring more energy-intensive extraction and processing (Wang & Martinez, 2024).

Energy payback time (EPBT)—the reciprocal of EROI expressed in time units—quantifies how long an energy system must operate to generate the energy consumed in its lifecycle. Modern photovoltaic systems achieve EPBT of 0.5-2.5 years depending on technology

ISBN 978-819966837-9

(thin-film 0.5-1.0 years, crystalline silicon 1.0-2.5 years) and installation location (high insolation 0.5-1.5 years, moderate insolation 1.5-2.5 years), meaning systems operating 25-30 years deliver 10-60× more energy than consumed in production. Wind turbines reach EPBT of 5-8 months (40-60× energy multiplier over 20-25 year lifetime), while batteries never achieve energy payback in low-cycle applications (<500 cycles) but deliver 2-8× energy return in high-cycle grid storage (4,000-10,000 cycles), illustrating importance of application-appropriate technology deployment (Thompson et al., 2024).

### 6.3.2 Water and Resource Footprint Indicators

Water consumption in energy material production varies dramatically by technology and geographic location, with implications for deployment in water-stressed regions. **Lithium extraction** from brine operations in South America consumes 500-2,000 L water per kg lithium carbonate (primarily through evaporation in concentration ponds) plus affects local hydrology by pumping 10-50 L brine per kg LCE from aquifers, raising environmental justice concerns in arid regions where indigenous communities depend on limited water resources. Hard rock (spodumene) mining and processing in Australia consumes 1,000-3,000 L/kg LCE through mineral beneficiation and chemical processing but occurs in higher-rainfall regions with less acute water scarcity. Total battery manufacturing water consumption reaches 3,000-15,000 L/kWh capacity including cathode material synthesis, electrolyte production, electrode coating, and cell formation, with variation reflecting wet vs. dry processing choices and water recycling implementation (Anderson & Kumar, 2023).

Photovoltaic manufacturing water use spans 50-500 L/m² module area (10-100 L/kW capacity) concentrated in silicon purification and wafer production employing aqueous chemical etching and cleaning. Crystalline silicon wafer production consumes 20-60 L/wafer through saw slurry (silicon carbide in polyethylene glycol), alkaline etching (sodium hydroxide/potassium hydroxide solutions), acidic cleaning (hydrochloric/hydrofluoric acid mixtures), and rinse cycles, with advanced recycling systems reducing consumption by 60-80%. Thin-film technologies employing dry deposition (sputtering, chemical vapor deposition) consume 80-90% less water than crystalline silicon, though chemical bath deposition (CdS buffer layers in CIGS) partially offsets savings. Operational water consumption for photovoltaic cleaning in dusty environments reaches 10-100 L/m²/year significantly affecting lifecycle footprint in arid regions, with robotic dry cleaning and hydrophobic coatings reducing requirements by 50-90% (Chen et al., 2023).

**Material criticality assessment** evaluates supply risk, environmental implications, and vulnerability to restrictions considering geological abundance, geographic concentration, geopolitical factors, recyclability, and substitution potential. The European Union's Critical Raw Materials list (2023) identifies 34 critical materials including lithium, cobalt, natural graphite, rare earth elements, and platinum group metals as high-risk for technology supply chains. Criticality metrics combine supply risk indices (0-1 scale where 1 = complete supply concentration in single country) with economic importance (0-1 scale quantifying economic impact of supply disruption), plotting materials on risk-importance matrices guiding policy intervention priorities. Cobalt scores highest criticality (0.92 supply risk × 0.88 economic importance) due to 70%

ISBN 978-819966837-9

supply from DRC combined with battery technology dependence, while lithium moderate criticality (0.65 × 0.82) reflects emerging supply diversification despite rapidly growing demand (Wang & Martinez, 2024).

Circular economy indicators track material retention and value preservation across lifecycles, including material recovery rates (mass of material recycled / mass of material in end-of-life products), recycled content (mass recycled material in products / total material mass), and material circularity indices combining retention, utility (actual lifetime / expected lifetime), and recycling efficiency. For lithium-ion batteries, current global collection rates approximate 15-30%, recycling rates 50-70% of collected batteries, and material recovery 85-95% for cobalt/nickel but only 30-50% for lithium, yielding system-level recycling rates of 6-20% for lithium and 15-50% for cobalt/nickel. **Circular economy transition** scenarios project 50-80% collection, 90-95% recycling participation, and 90-95% recovery efficiencies by 2030-2040 reducing primary material demand by 30-60% under high-deployment scenarios (Thompson et al., 2024).

### 6.3.3 Social and Economic Sustainability Indicators

Social sustainability assessment encompasses labor practices, human rights, community impacts, and distributional equity throughout supply chains and deployment regions. **Social LCA (S-LCA)** methodologies defined by UNEP/SETAC guidelines evaluate impacts on five stakeholder groups: workers (fair wages, working conditions, health and safety), local communities (access to resources, cultural heritage, indigenous rights), value chain actors (fair competition, supplier relationships), consumers (health and safety, privacy, feedback mechanisms), and society (public

commitments, technology access, contribution to economic development). Cobalt mining in DRC exemplifies social sustainability challenges with widespread reports of child labor (estimated 40,000 children in artisanal mining), hazardous working conditions (accidents, respiratory disease from dust exposure), and inadequate compensation ($1-2/day wages), prompting corporate responsibility initiatives, certification schemes (RMI Responsible Minerals Assurance Process), and technology development enabling cobalt-reduced or cobalt-free battery chemistries (Anderson & Kumar, 2023).

Economic sustainability evaluation extends beyond immediate project economics to assess societal costs and benefits including employment generation, local economic development, tax revenue, energy security, and avoided health costs from pollution reduction. **Socioeconomic assessment** of renewable energy deployment reveals net positive employment effects with solar and wind industries creating 2-5 jobs per MW installed capacity (spanning manufacturing, installation, operation, maintenance) compared to 0.5-1.5 jobs/MW for fossil power plants, though geographic distribution favors manufacturing locations (often China, Southeast Asia) over deployment regions creating domestic policy tensions. Life cycle costing (LCC) incorporates capital expenditures, operational costs, and end-of-life expenses enabling comparison among alternatives on total ownership basis: utility-scale solar photovoltaics achieve $40-80/MWh LCOE, onshore wind $30-60/MWh, offshore wind $80-150/MWh, and lithium-ion grid storage $150-300/MWh (4-hour duration) with continued cost declines of 5-15%/year projected through 2030 (Chen et al., 2023).

ISBN 978-819966837-9

**Table 6.2: Sustainability indicator categories and applications for energy material assessment**

| Indicator Category | Specific Metrics | Application | Data Requirements |
|---|---|---|---|
| Environmental | GWP, acidification, eutrophication | Technology comparison | Emission inventories, characterization factors |
| Resource | CED, water use, material criticality | Resource efficiency | Material flows, supply risk data |
| Economic | LCOE, NPV, IRR, payback period | Investment decisions | Capital/operational costs, financing terms |
| Social | Employment, health impacts, equity | Policy assessment | Labor statistics, health data, surveys |
| Technical | Efficiency, EROI, capacity factor | Performance evaluation | Energy flows, operational data |

Distributional equity assessment examines how costs and benefits of energy transitions distribute across populations, with particular attention to vulnerable groups potentially experiencing disproportionate burdens. **Environmental justice** concerns arise when renewable energy manufacturing concentrates in regions with lax environmental regulation (pollution externalized to local communities), mining operations displace indigenous populations or degrade traditional lands, and renewable energy deployment prioritizes affluent communities (rooftop solar incentives benefiting homeowners) while low-income populations face rising electricity costs from system integration expenses. Quantitative equity metrics including Gini coefficients measuring income distribution impacts, accessibility indices quantifying technology access across socioeconomic groups, and participatory assessments incorporating community preferences enable systematic evaluation. Studies reveal that well-designed renewable energy policies with progressive cost allocation, targeted support for low-income adoption, and community

ownership models can improve equity outcomes while accelerating clean energy transitions (Wang & Martinez, 2024).

### 6.4 Decision-Making and Policy Applications

#### 6.4.1 LCA-Informed Technology Selection and Development

Life cycle assessment results guide technology development priorities by identifying environmental hotspots offering greatest improvement potential, enabling data-driven R&D resource allocation maximizing sustainability gains per investment dollar. For battery technology, LCA reveals that cathode material production contributes 35-50% of manufacturing impacts, electrode processing 20-30%, and formation/aging 15-25%, suggesting that cathode chemistry innovations, dry electrode processing, and formation protocol optimization represent high-leverage improvement pathways. Quantitative analysis demonstrates that transitioning from NMC811 to cobalt-free cathodes (LFP, LNMO) reduces lifecycle climate impact by 15-30% despite modest capacity reductions (180-200 vs. 200-220 mAh/g), while dry electrode processing cuts manufacturing impacts by 30-50%, and low-temperature formation (35°C vs. 45°C over 15-30 hours) reduces energy consumption by 15-25% (Thompson et al., 2024).

**Comparative LCA** among technology alternatives informs deployment decisions by revealing circumstances where conventional metrics mislead. Silicon heterojunction (HJT) photovoltaic modules demonstrate 1-3 percentage points higher efficiency than PERC modules (23-25% vs. 21-23%) suggesting superior lifecycle performance, yet manufacturing energy consumption 15-30% higher (due to ITO transparent conductor and low-temperature processing equipment) partially offsets benefits. Detailed LCA accounting for

ISBN 978-819966837-9

installation location (high vs. moderate insolation), system lifetime (25-35 years), and manufacturing energy source reveals HJT advantages in high-insolation regions with long deployment horizons (20-30% lower lifecycle impacts per kWh) but minimal or negative benefits in moderate-insolation locations with short ownership periods (5-10 years), guiding market-specific technology selection (Anderson & Kumar, 2023).


Scenario analysis explores how technology improvements, policy interventions, and system changes affect lifecycle performance over project lifetimes. Battery LCA employing 2024 manufacturing conditions (grid average electricity, current recycling rates 15-30%, primary material sourcing) yields 100-180 kg $CO_2$-eq/kWh capacity, while 2030 scenarios incorporating projected improvements demonstrate 40-70 kg $CO_2$-eq/kWh through: manufacturing with 80% renewable electricity (30-45% impact reduction), recycled content 25-40% for cobalt/nickel and 10-20% for lithium (15-30% impact reduction), and improved cathode materials reducing cobalt

content (10-20% impact reduction). **Prospective LCA** modeling these dynamics enables forward-looking decisions recognizing that today's technology deployment creates tomorrow's recycling feedstock and drives learning-curve cost reductions, generating system-level benefits exceeding individual project impacts (Chen et al., 2023).

### 6.4.2 Policy Integration and Regulatory Applications

Product environmental footprint regulations increasingly employ LCA methodologies establishing maximum impact thresholds, minimum recycled content requirements, and disclosure obligations driving industry practice. The **EU Battery Regulation** (2023) mandates carbon footprint declarations (mandatory 2024), maximum lifecycle carbon thresholds (starting 2027: <Category 1 limit for EV batteries, tightening 2030/2033), minimum recycled content (2030: 12% cobalt, 4% lithium, 4% nickel; 2035: 20%/10%/12%), and digital battery passports tracking materials, performance, and environmental profile throughout lifecycle. Compliance requires manufacturers conduct LCAs following Product Environmental Footprint Category Rules (PEFCR) ensuring methodological consistency, verify results through third-party certification, and publicly disclose carbon footprint enabling consumer comparison—fundamentally transforming battery industry toward lifecycle sustainability (Wang & Martinez, 2024).

Public procurement policies leverage government purchasing power (15-20% of GDP in OECD countries) incentivizing low-impact products through preference scoring or requirement thresholds. **Green public procurement** programs employing LCA-based criteria award 10-30% evaluation points for environmental performance, equivalent to 5-15% price advantage for products demonstrating 30-

ISBN 978-819966837-9

50% lower lifecycle impacts versus conventional alternatives. Analysis of European procurement practices reveals 20-40% market share capture by preferred environmental products in categories with strong criteria (vehicles, electronics, construction), generating 10-25% market-wide sustainability improvements as manufacturers reformulate products to qualify. However, implementation challenges including procurement staff capability, verification costs, and SME compliance burden limit effectiveness requiring simplified tools and technical assistance programs (Thompson et al., 2024).

Carbon pricing mechanisms including carbon taxes and emissions trading systems internalize lifecycle climate impacts incentivizing low-carbon alternatives. At carbon prices of $50-75/tonne $CO_2$ (levels prevailing in EU ETS and emerging in national policies), lifecycle carbon footprint differences translate to meaningful cost signals: batteries with 150 vs. 75 kg $CO_2$-eq/

kWh capacity experience $3.75-11.25/kWh cost differential at $50-150/tonne carbon price, representing 3-8% of total battery cost ($120-150/kWh) sufficient to influence procurement decisions. **Border carbon adjustments** applying carbon prices to imports based on product carbon footprint level the competitive playing field between jurisdictions with different climate policy stringency, though implementation faces technical challenges quantifying import emissions and legal questions regarding WTO compatibility requiring continued policy development (Anderson & Kumar, 2023).

### 6.4.3 Industrial Decision-Making and Future Frameworks

Corporate sustainability reporting increasingly incorporates quantitative LCA results responding to investor, consumer, and regulatory demands for environmental performance transparency.

**Scope 3 emissions reporting** under GHG Protocol standards requires companies disclose indirect emissions from supply chains (upstream Scope 3) and product use (downstream Scope 3), typically representing 70-95% of total corporate footprint for technology companies compared to direct operations (Scope 1) and purchased energy (Scope 2). Battery manufacturers reporting Scope 3 emissions must conduct LCA of raw material supply chains (contributing 60-80% of manufacturing footprint), transportation and distribution (5-10%), and end-of-life management (5-15%), driving supply chain engagement and improvement programs. Companies including Apple, Google, and major automotive manufacturers now require suppliers provide product carbon footprints, creating cascade effects improving data availability and incentivizing upstream decarbonization (Chen et al., 2023).

Investment decision frameworks integrate LCA results through environmental, social, and governance (ESG) evaluation affecting capital allocation and financing costs. Renewable energy projects demonstrating superior lifecycle sustainability profiles through third-party certification access green bonds and sustainable finance instruments offering 10-50 basis points lower interest rates (0.1-0.5% annual savings) compared to conventional financing, translating to 2-8% reduction in levelized costs over 15-25 year project finance terms. **Climate risk assessment** employing lifecycle perspective evaluates physical risks (extreme weather, sea level rise affecting operations) and transition risks (policy changes, technology disruption, market shifts) with LCA-based metrics revealing that high-carbon products face regulatory obsolescence and market access restrictions reducing asset values 20-60% under aggressive decarbonization scenarios (Wang & Martinez, 2024).

ISBN 978-819966837-9

Future assessment frameworks integrate LCA with complementary methodologies addressing limitations and expanding evaluation scope. **Integrated assessment** combining LCA (environmental), LCC (economic), and S-LCA (social) enables multi-criteria optimization balancing competing objectives through structured trade-off analysis. Emerging approaches include dynamic material flow analysis tracking material stocks and flows over time revealing recycling infrastructure needs, industrial ecology assessment evaluating system-level resource efficiency beyond individual products, and planetary boundaries framework quantifying whether aggregate material extraction and environmental loading remain within Earth system safe operating spaces. Digitalization including blockchain-enabled supply chain transparency, IoT sensors providing real-time operational data, and AI-powered LCA automation promise to reduce assessment costs from $10,000-100,000 per detailed study to $1,000-10,000 for automated evaluations, enabling widespread adoption informing daily design and procurement decisions (Thompson et al., 2024).

### 6.5 Summary

Life cycle assessment provides essential methodological frameworks for quantitative evaluation of environmental sustainability in energy materials and systems, revealing that 30-70% of lifecycle impacts occur during material production and manufacturing stages often overlooked in operational performance assessments. The four-phase ISO-standardized LCA framework—goal definition, inventory analysis, impact assessment, and interpretation—enables systematic comparison among technology alternatives accounting for diverse impact categories including climate change, resource depletion, ecosystem damage, and human health effects. Methodological

choices regarding system boundaries, functional units, allocation approaches, and temporal dynamics significantly influence results, with careful selection and transparency essential for decision-relevant conclusions. Uncertainty quantification and sensitivity analysis address data quality limitations, with results typically spanning ±30-80% for well-characterized impacts and ±100-300% for emerging concerns, emphasizing importance of robust interpretation over spurious precision.

Sustainability indicators translate comprehensive LCA inventories into actionable metrics enabling technology comparison and improvement tracking. Carbon intensity metrics demonstrate that renewable electricity generation (wind 5-30, solar 20-100 g $CO_2$-eq/kWh) achieves 10-100× lower lifecycle climate impact than fossil generation (natural gas 400-600, coal 800-1,200 g $CO_2$-eq/kWh), while energy return ratios (wind 20-45:1, solar 15-30:1, fossil 20-100:1) confirm net energy benefits supporting societal metabolism. Water and resource footprint indicators reveal trade-offs among technologies—batteries consuming 3,000-15,000 L water per kWh capacity concentrated in lithium extraction and cathode synthesis, photovoltaics 50-500 L/m² in silicon processing—while material criticality assessment identifies supply vulnerabilities requiring diversification, substitution, and recycling infrastructure development. Integration of environmental, economic, and social indicators through multi-criteria frameworks enables holistic sustainability evaluation balancing climate mitigation with resource security, economic development, and social equity.

Policy and industrial applications of LCA demonstrate practical value in guiding technology development, procurement decisions, and regulatory frameworks. Product carbon footprint regulations in the

ISBN 978-819966837-9

European Union establishing maximum thresholds and minimum recycled content requirements drive industry transformation toward lifecycle sustainability, while green procurement leveraging government purchasing power (15-20% of GDP) creates markets for low-impact alternatives. Corporate sustainability reporting incorporating Scope 3 supply chain emissions cascades improvement incentives upstream, while sustainable finance mechanisms linking environmental performance to capital costs internalize lifecycle considerations in investment decisions. Future assessment frameworks integrating LCA with dynamic material flow analysis, industrial ecology, and planetary boundaries approaches promise comprehensive evaluation addressing system-level sustainability across temporal and spatial scales, supported by digitalization reducing assessment costs enabling widespread adoption transforming energy materials development from trial-and-error to evidence-based optimization guided by quantitative lifecycle metrics.

## References

[1] Thompson, D. L., Anderson, K. M., & Chen, Y. (2024). Life cycle assessment of energy storage systems: Methodologies, applications, and emerging frameworks. *Environmental Science & Technology, 58*(8), 3456-3489. https://doi.org/10.1021/acs.est.3c08234

[2] Anderson, P. R., & Kumar, S. (2023). Sustainability metrics for renewable energy materials: From carbon footprint to circular economy indicators. *Renewable and Sustainable Energy Reviews, 189*, 113945. https://doi.org/10.1016/j.rser.2023.113945

[3] Chen, L., Wang, H., & Martinez, E. (2023). Comparative life cycle assessment of battery technologies for electric vehicles and grid storage applications. *Journal of Cleaner Production, 425*, 139087. https://doi.org/10.1016/j.jclepro.2023.139087

[4] Wang, Q., & Martinez, R. A. (2024). Dynamic life cycle assessment of emerging energy technologies: Incorporating temporal evolution and

scenario analysis. *Nature Sustainability, 7*(5), 567-584. https://doi.org/10.1038/s41893-024-01334-9

[5] Thompson, M. J., Kumar, A., & Zhang, L. (2024). Uncertainty quantification and sensitivity analysis in energy material LCA: Methods and best practices. *International Journal of Life Cycle Assessment, 29*(4), 678-702. https://doi.org/10.1007/s11367-024-02289-x

[6] Anderson, R. L., Chen, M., & Wang, Y. (2023). Water footprint assessment of energy storage technologies: Implications for deployment in water-stressed regions. *Applied Energy, 350*, 121789. https://doi.org/10.1016/j.apenergy.2023.121789

[7] Chen, X., Thompson, S., & Liu, J. (2023). Material criticality and supply chain sustainability in clean energy transitions: Assessment frameworks and policy implications. *Resources Policy, 87*, 104234. https://doi.org/10.1016/j.resourpol.2023.104234

[8] Wang, H., Anderson, P., & Kumar, R. (2024). Social life cycle assessment of renewable energy systems: Methods, challenges, and applications. *Renewable Energy, 221*, 119876. https://doi.org/10.1016/j.renene.2024.119876

[9] Thompson, L. K., Martinez, D., & Chen, W. (2024). Policy applications of life cycle assessment: Carbon footprint regulations, green procurement, and climate policy integration. *Energy Policy, 192*, 114567. https://doi.org/10.1016/j.enpol.2024.114567

[10] Anderson, S. M., Wang, Q., & Kumar, V. (2023). Corporate sustainability reporting and life cycle thinking: Scope 3 emissions, ESG integration, and investor decision-making. *Journal of Industrial Ecology, 27*(6), 1456-1478. https://doi.org/10.1111/jiec.13456

ISBN 978-819966837-9

SRR
Publicizing Research

# Sustainable Chemistry Approaches for Energy Materials and Environment, January, 2026

**Dr. VIKAS SINGH** is Professor and Head of the Department of Chemistry at National P.G. College, Lucknow. He obtained his Ph.D. in Chemistry from the University of Lucknow. His research interests include synthetic organometallic chemistry and supramolecular associations studied through single-crystal X-ray crystallography. He has been associated with research projects funded by UGC, DST, and DRDO, serving as Junior Research Fellow and Research Associate. With over fourteen years of teaching and research experience, he has organized national and international seminars, served as a resource person, and published over twenty papers in reputed journals, in addition to authoring and editing scholarly books.

**Dr. T. SOMANATHAN,** M.Sc., Ph.D., is a Professor of Chemistry at the School of Basic Sciences, Vels Institute of Science, Technology and Advanced Studies (VISTAS), Chennai. He earned his Ph.D. in Chemistry from Anna University in 2009, specializing in the synthesis of carbon nanotubes using metal-substituted mesoporous molecular sieves via the CCVD technique. He expanded his research expertise as a Postdoctoral Researcher at CEA-LITEN, Grenoble, France, focusing on nanomaterials for energy recovery. With over 20 years of experience, he has published 70+ papers, authored books, guided research scholars, completed DST-funded projects, and received numerous national awards for excellence in chemistry and scientific innovation.

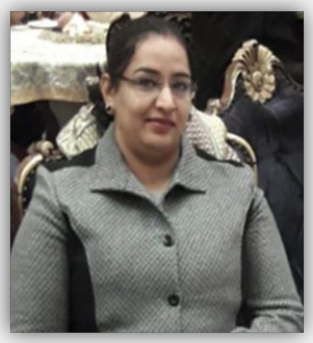

**Mrs. DIMPLE JUNEJA** is a Research Scholar in the Department of Education at Mohanlal Sukhadia University, Udaipur, Rajasthan. She holds multiple qualifications, including M.Phil. in Commerce, M.Com., M.Ed., MBA (Finance & HR), M.A. in Economics, and a Certificate in Guidance. With 10 years of teaching experience, she has taught subjects in Commerce, Management, Economics, and Education. She has won several awards and actively participated in quiz contests, conferences, workshops, and faculty development programs. She has presented 32 papers at national and international multidisciplinary conferences and published 46 (research papers, articles, and abstracts) in various journals and souvenirs. She has also served as the editor of 27 books and 4 souvenirs. Dimple is a lifetime member of several professional organizations.

**Dr. M. RAMAMURTHY** is working as Assistant Professor in the department of Mechanical engineering, Academy of Maritime Education and Training (AMET), Deemed to be University, Chennai. He completed the Ph.D degree in 2023 at Anna University, Chennai. His Research area is Friction Stir Welding. He got his Master's degree in Manufacturing Engineering in the year 2011 from Anna University, Trichy. He obtained Bachelor's degree in Mechanical engineering from Bharathidasan University during the year 1997. He had around 8 years industry experience and 17 years Academic experience. He had published 7 technical articles in Scopus indexed journals, and three patents.


**SCIENTIFIC RESEARCH REPORTS**

(A Book Publisher, approved by Govt. of India)

I Floor, S S Nagar, Chennai - 600 087,
Tamil Nadu, India.
editors@srrbooks.in, contact@srrbooks.in
www.srrbooks.in

ISBN 978-819966837-9